AN ABSTRACT OF THE DISSERTATION OF

Uyen Minh Le for the degree of Doctor of Philosophy in Pharmacy presented on September 5, 2008.

Titles:

1) Improving the Uptake and Retention of Gadolinium in Tumors for Potential Gadolinium-Neutron Capture Therapy.
2) Integration of Gemcitabine or Localized Irradiation into dsRNA Therapy Significantly Enhanced the Resultant Anti-tumor Activity.

Abstract approved:

Zhengrong Cui

Cancer is one of the leading causes of death in the U.S., and new approaches to control cancer are constantly sought. This dissertation is comprised of two parts: (i) improving the uptake and retention of gadolinium in tumors for potential gadolinium-neutron capture therapy (Gd-NCT) and (ii) integration of gemcitabine or localized irradiation into dsRNA therapy significantly enhanced the resultant anti-tumor activity.

One of the key factors for a successful Gd-NCT is to deliver and maintain a sufficient amount of Gd in tumor tissues (50-200 μg of Gd/g of wet tumor) during neutron irradiation, which has proven to be challenging to achieve. A gadolinium-encapsulated liposome (Gd-liposome) formulation was designed to address this need. The formulation was prepared by complexing diethylenetriaminepentaacetic acid (Gd-DTPA) with poly-L-lysine and then encapsulating the Gd-DTPA complexes into

pegylated liposomes. The Gd-liposome formulation delivered as high as 159 μg of pure Gd per g of wet tumor tissue into model tumors in mice. A liposome-in-thermo-sensitive gel system that significantly extended the retention of the Gd in model tumors in mice was also designed. These Gd delivery systems may be used to deliver Gd into solid tumors for NCT and tumor imaging.

Despite of the potent tumoricidal activity of polyinosine-cytosine (e.g. poly(I:C)), a synthetic dsRNA, in culture, its *in vivo* anti-tumor activity has proven to be limited. Gemcitabine, a chemotherapy agent, or localized x-ray radiation was successfully integrated into poly(I:C) therapy to improve the resultant anti-tumor activity in murine tumor models. Combining gemcitabine with poly(I:C) synergistically inhibited the growth of model tumors in mice and also generated a strong and durable tumor-specific immune response. Alternatively, integrating localized x-ray radiation into poly(I:C) therapy significantly delayed the tumor growth, but the combined activity was synergistic only in mice with highly immunogenic tumors, indicating that the T cell-mediated immunity was responsible for the synergy. The type I interferons (IFN-α/β) induced by poly(I:C) played a critical role in the resultant anti-tumor activity. These combination therapies may represent a promising approach to improve the clinical outcomes of poly(I:C) therapy.

1) Improving the Uptake and Retention of Gadolinium in Tumors for Potential Gadolinium-Neutron Capture Therapy.

2) Integration of Gemcitabine or Localized Irradiation into dsRNA Therapy Significantly Enhanced the Resultant Anti-tumor Activity.

by

Uyen Minh Le

A DISSERTATION

submitted to

Oregon State University

in partial fulfillment of
the requirements for the
degree of

Doctor of Philosophy

Presented September 5, 2008

Commencement June 2009

Doctor of Philosophy dissertation of Uyen Minh Le presented on September 5, 2008

APPROVED:

Major Professor, representing Pharmacy

Dean of the College of Pharmacy

Dean of the Graduate School

I understand that my dissertation will become part of the permanent collection of Oregon State University. My signature below authorizes release of my dissertation to any reader upon request.

Uyen Minh Le, Author

ACKNOWLEDGEMENTS

I would like to express my sincere gratitude to my advisor, Dr. Zhengrong Cui, for his extraordinary scientific guidance, encouragement, and financial support. I would like to thank Dr. J. Mark Christensen, Dr. Rosita Proteau, Dr. Lisa Madsen, and Dr. Douglas F. Markle for their willingness to be my dissertation committee members and for providing useful insights. I would like to thank Dr. Jean A. Hall for her valuable time as my graduate representative in the first committee meeting.

My appreciation also goes to Dr. Darryl G. L. Kaurin for his valuable help in radiation experiments, Dr. Christiane V. Löhr for her useful interpretation in histology, Ms. Kay A. Fischer for her helpful assistance in histology and apoptosis assays, and Mr. Andy Ungerer for his friendly assistance on the ICP-OES work.

Current students in Dr. Cui's lab, Mr. Brian Sloat and Ms. Nijaporn Yanasarn are wonderful lab-mates. I would especially like to acknowledge them for their help and friendship throughout the years. I would like to thank Dr. Qiu Fu and Dr. Dalia S. Shaker, former postdocs in Dr. Cui's lab, for their useful collaboration and advice. I also highly appreciate Ms. Brook Baker and Mr. Michael Sandoval for their help in lab work.

I am very grateful to my current and former colleagues in the Department of Pharmaceutical Sciences for their friendship throughout the years. I also would like to gratefully acknowledge the friendship of my Vietnamese friends in Oregon. They make me feel home and joyful during the time I have been here. I would especially like to thank my host family in Corvallis, Mr. and Mrs. Ray William for their kindness, hospitality, and friendship in the 3-day homestay and throughout the years.

I highly appreciate OSU College of Pharmacy for its partial financial support in 2005-2008, the Oregon Sports Lottery Scholarship for its partial financial support in 2007, Mr. George Baker and the ORCAL Inc. for their partial funding support in 2006-2008, and the James Ayres-OSU College of Pharmacy Award for the traveling award to a national conference in 2007.

I will never forget the encouragement and support of my aunt, uncles, and their families when I first came to the U.S. for my study. I also would like to thank my entire aunt and uncles' friends for their kindness, encouragement and friendship to me and my family throughout the years.

And last but most important, I would like to express my very special gratitude to my whole family. I would like to express my special thanks to my husband, Tuan Tran, for his love and support. He shared with me all happiness as well as difficulties. I also thank my will-be-born baby, Dua Hau, who encourages me to do my best all the time to accomplish my dissertation as soon as possible. I will also never forget the support and encouragement of my dear older brother, Hai Minh Le, and his family. They have constantly encouraged me and wonderfully taken care of my parents so that I could concentrate on my study through these challenging years. I would never have been able to defeat my timidness to go to study abroad and accomplish my degree without the love, support, and encouragement of my wonderful parents. I am forever indebted to them not only for their raising but also for their greatly helpful career orientation to me.

CONTRIBUTION OF AUTHORS

Dr. Dalia S. Shaker (College of Pharmacy, Oregon State University) assisted with some animal experiments in chapter 4.

Dr. Christiane V. Löhr (College of Veterinary Medicine, Oregon State University) involved with interpretation of the data of figure 5.4 in chapter 5.

Dr. Darryl G. L. Kaurin (Department of Radiation Oncology, Oregon Health and Science University) involved with radiation experiments in chapter 6.

Mr. Brian Sloat (College of Pharmacy, Oregon State University) assisted with some animal experiments in chapters 4 and 6.

Ms. Nijaporn Yanasarn (College of Pharmacy, Oregon State University) assisted with data collection of figure 5.2A in chapter 5 and some animal experiments in chapter 6.

Ms. Kay A. Fischer (College of Veterinary Medicine, Oregon State University) assisted with data collection of figures 5.3 and 5.4 in chapter 5.

TABLE OF CONTENTS

Page

TABLE OF CONTENTS (Continued)

Page

TABLE OF CONTENTS (Continued)

Page

TABLE OF CONTENTS (Continued)

Page

TABLE OF CONTENTS (Continued)

Page

TABLE OF CONTENTS (Continued)

Page

LIST OF FIGURES

LIST OF FIGURES (Continued)

Figure Page

LIST OF FIGURES (Continued)

Figure Page

LIST OF TABLES

1) IMPROVING THE UPTAKE AND RETENTION OF GADOLINIUM IN TUMORS FOR POTENTIAL GADOLINIUM-NEUTRON CAPTURE THERAPY.

2) INTEGRATION OF GEMCITABINE OR LOCALIZED IRRADIATION INTO dSRNA THERAPY SIGNIFICANTLY ENHANCED THE RESULTANT ANTI-TUMOR ACTIVITY.

Chapter 1

GENERAL INTRODUCTION

1.1 Background

Undesirable side effects of therapeutic agents due to the lack of specificity to the site of action are one of the major limitations for their clinical use in cancer treatments. It has been constantly sought to develop tumor-specific delivery systems to enhance the killing of tumors and to reduce the toxicity to normal tissues. From that regard, drug delivery systems play a central role in the achievement of selective cytotoxic effect on tumors while not influencing normal tissues. Neutron capture therapy (NCT), an experimental form of radiation therapy, is a potential cancer therapy that can enhance tumor selectivity with promising results. In NCT, a stable, non-toxic, and non-radioactive nuclide called a NCT agent is first delivered to tumor cells, and then a neutron beam is narrowly shined to the tumor sites. Based on the interaction of the nuclide and the neutron beam, localized cytotoxic radiations are emitted to kill the tumor cells (Barth et al., 1990;

Hawthorne, 1998; Matsumoto, 1992; Sauerwein, 1993). Although Boron^{10} has been utilized as a NCT agent for Boron-NCT (B-NCT) in many clinical trials since the beginning of NCT (Hatanaka, 1975; Hatanaka et al., 1978), a newer NCT agent, gadolinium (Gd) for Gd-NCT, demonstrated to be more advantageous because it can produce a larger thermal neutron capture cross-section (~ 66 times larger than that of Boron^{10}) and a longer range (> 100 μm) of γ-rays after neutron irradiation (Barth and Soloway, 1994; Brugger and Shih, 1989; Carlsson et al., 2002). Those properties of Gd-NCT can help to shorten the irradiation time and to kill tumor cells even when Gd is outside the tumor cells, thus eliminating the requirement of intracellular delivery of Gd (De Stasio et al., 2001; Hofmann et al., 1999). Furthermore, gadolinium diethylenetriaminepentaacetic acid (Gd-DTPA), a derivative of Gd, has been widely utilized as a contrast agent in Magnetic Resonance Imaging (MRI), which is a medical imaging technique used to visualize the structure and function of the body. Thus, using Gd-NCT has the potential to integrate both diagnosis and treatment of cancers. Although Gd-NCT is a very promising cancer modality, its clinical application has been rather limited because one of the key factors for the success of Gd-NCT is to deliver and retain a sufficient amount of Gd in tumors (50-200 μg of Gd/g wet tumor tissues) during the neutron irradiation (Shih and Brugger, 1992), which is challenging to achieve, if the Gd compounds have to be administered systematically (Jono et al., 1999; Khokhlov et al., 1995; Tokumitsu et al., 1999). Ideally, a Gd-delivery system should (i) contain a high concentration of Gd compound so that a large amount of

Gd can be delivered into tumors, (ii) have a slow and limited release of the Gd compound out of the delivery system to allow the Gd to both retain inside the delivery system prior to reaching tumors and remain inside tumors during the neutron irradiation, and (iii) have a long blood circulation time to achieve a greater efficiency of extravasations of the delivery system into tumors. Our research focused on developing stable and effective delivery systems for Gd that would be able to deliver a concentration of 50-100 μg of Gd per g of wet tumor tissue. A stable PEGylated liposome formulation (~ 100 nm) encapsulating a high concentration of Gd was engineered. Additional studies about blood circulation, biodistribution, and tumor-accumulation of Gd at various time points after the administration were carried out in model tumor-bearing mice. The correlation of the tumor uptake of Gd and the size of the tumors was also employed. Moreover, another Gd delivery system was engineered by dispersing the Gd-encapsulated liposomes into a thermo-sensitive polymeric gel system to further extend the retention of the Gd compound in tumors. The tumor uptake of Gd was also carried out in murine tumor models. The Gd-encapsulated liposomes or Gd-encapsulated liposomes dispersed in a thermo-sensitive polymeric gel as demonstrated in this research project hold great potential as effective Gd delivery systems for Gd-NCT.

Besides reducing the toxicities/adverse effects using effective and site-specific delivery systems of drugs, selecting appropriate therapeutic methods can also contribute greatly to the success of cancer treatments. Cancer is a class of diseases which has great diversity in causes and biology. Therefore, a single “cure

for cancer" seems unlikely to be effective. In fact, drug-resistance is a significant cause of failure of single therapy in a long-term treatment. In addition, severe toxicities due to high doses sufficient to eradicate tumors are also disadvantages of single therapy. Combination therapy for cancers to improve the therapeutic effects has been well documented since the 1950s (Caby and Tsevrenis, 1950; Ott, 1950; Podliashuk and Morgenstern, 1950; Sarasin and Dubois-Ferriere, 1951; Vesin, 1952). Generally, the combination therapy can activate various killing mechanisms simultaneously, thus it can enhance clinical responses (Gahr et al., 2007; Sandlund et al., 2008), reduce toxicity (Knobf, 1984; Lieu et al., 2008), and be more effective against the drug-resistance (Matei et al., 2008; Yadav et al., 2008) than the single therapy. A longtime development is the use of polyinosine-cytosine (e.g. poly(I:C)), a synthetic double-stranded ribonucleic acid (dsRNA), as a potential tumor therapy agent (Cui and Qiu, 2006; Degre and Elgjo, 1971; DuBuy, 1972; Ewel et al., 1992; Fisher et al., 1970; Larson et al., 1969; Nakamura et al., 1982; Sakurai et al., 2003). DsRNA possesses multiple mechanisms, including pro-apoptotic induction (Chawla-Sarkar et al., 2003; Meurs et al., 1993; Salaun et al., 2006), type I interferons (IFNs) induction (Absher and Stinebring, 1969), which are pro-apoptotic, anti-proliferative, and anti-angiogenic (Balkwill and Taylor-Papadimitriou, 1978; Chawla-Sarkar et al., 2001; Chawla-Sarkar et al., 2003; Sidky and Borden, 1987), and immunostimulatory (Le Bon et al., 2003; Salem et al., 2005; Schulz et al., 2005; Sivori et al., 2004; Yoneyama et al., 2004). Therefore, dsRNA itself can be a very promising candidate as a cancer

chemotherapy and immunotherapy agent. Although poly(I:C) was first tried in animals and clinical trials more than 30 years ago (Absher and Stinebring, 1969; Gazdar, 1972; Sakurai et al., 1990; Weinstein et al., 1971), its efficacy was inconsistent (Gazdar, 1972; Sakurai et al., 1990; Weinstein AJ, 1971), and adequate doses to induce anti-tumor activities were also associated with severe side effects (Cornell et al., 1976; De Clercq, 1972; Freeman et al., 1977; Levine and Levy, 1978; Okada et al., 2005), thus limiting its clinical application for cancer therapy. Recently, however, it has been shown that those obstacles can be overcome by using alternative approaches (Hirabayashi et al., 1999; Llopiz et al., 2008; Shakhar et al., 2007; Shir et al., 2006; Trumpfheller et al., 2008; Zhu et al., 2007), and interest in poly(I:C) applications for cancer treatment was revived. Our present research focused on designing new approaches to improve the anti-tumor activity of poly(I:C) by combining poly(I:C) therapy with gemcitabine, a chemotherapy agent, or with localized x-ray radiation, a type of radiation therapy. The poly(I:C) was delivered into tumor cells using a cationic liposome carrier system because it has been reported that poly(I:C) was more effective if internalized into the cells (Chawla-Sarkar et al., 2003; Meurs et al., 1993; Salaun et al., 2006). The outcome of the combination treatment was evaluated in cancer cells and in cancer models in mice. Possible mechanisms underlying the therapeutic effectiveness were also elucidated. The combination modalities demonstrated in our research may be promising to exploit the anti-tumor activity

of the synthetic dsRNA and to further improve the efficacy of chemotherapy and radiotherapy.

1.2 Cancer therapies

Cancer is one of the first leading causes of death in people under age 85 years in the United State (U.S.) (Jemal et al., 2007). It has been estimated that in 2007 in the U.S., there were more than 1.4 million new cancer cases and almost 560,000 deaths from cancers (Jemal et al., 2007). The costs for care during the initial phase of cancer was estimated to be approximately 2.3 billion dollars in 2005 (Yabroff et al., 2007), and the prices have the trend to rise every year (Warren et al., 2008). It has been reported that nearly 85% of cancers relate to solid tumors (Jain, 1996) which lead to approximately half of death from these patients. According to the U.S. National Cancer Institute, treatments for cancers, in general, include standard or conventional therapies (e.g. chemotherapy, radiation therapy, and surgery) and other new methods (e.g. angiogenesis inhibitor, biological therapy, gene therapy, bone marrow transplantation and peripheral blood stem cell transplantation, hyperthermia, lasers, photodynamic therapy, and targeted cancer therapies). The treatments for cancers can be the cure, control, or just palliative care. Although there have been an increasing number of new methods for cancer therapies, chemotherapy and radiotherapy remain dominant in clinical trials (Warren et al., 2008).

1.2.1 Cancer chemotherapy

It has been well known that cancer cells are characterized by cell division that lost the ability of checking and balancing the "contact inhibition", a process that helps to stop the cell division in normal cells. The hyper-proliferation of cancer cells can induce a mass of abnormal-growing cells forming tumors. The tumors can be benign (e.g. non-cancerous) or malignant (e.g. cancerous).

Chemotherapy has been applied for cancer treatments since the late 1940s (Cutting et al., 1949; Shapiro et al., 1949). In cancer chemotherapy, chemicals are used via an oral route, intravenous, intra-peritoneal, or intra-arterial injection to systemically destroy cancer cells. The actions of chemotherapy agents relate to the "cell cycle" in the body (Collins, 1997; Priestman, 2008). Cells are the structural units of living tissue, and the living cells constantly grow and reproduce to form new cells replacing dead or lost cells. There are, in general, 5 phases of the cell cycle in the mammalian living cells: G0, G1, S, G2, and M (Fig. 1.1). The G0 phase or resting phase is considered the starting point of the cycle in which cells do not divide. The rest of the actively reproducing phases (e.g. G1, S, G2, and M) are associated with ready division, synthesis, pre-mitosis, and mitosis, respectively (Priestman, 2008). Based on the cell cycle interferences, chemotherapy drugs have been categorized into two main groups: the cell-cycle specific agents that are able to work on particular phases of the cell cycle and not on the resting phase, and the cell-cycle nonspecific that can attack cells at any phase of the cycle (Collins, 1997; Priestman, 2008). Unfortunately, the growths of cancerous and normal cells

all involve the cell-cycle. Thus, they both can be affected by the chemicals, resulting in undesirable side effects in normal cells although the cancer cells proliferate uncontrollably and more rapidly which are primary targets of the chemotherapy agents. The fast-growing normal cells, such as blood cells in the bone marrow, red blood cells, cells in the digestive tract (e.g. mouth, stomach, intestines, and esophagus), hair follicles, and reproductive system are the most vulnerable, causing common side effects like bone-marrow depression, susceptibility to infections, anemia, vomiting, nausea, diarrhea, constipation, hair loss, low blood count, fertility change, and etc.

1.2.1.1 Gemcitabine as a chemotherapy agent

Gemcitabine belongs to the group of antimetabolites. In this family, the drugs' structures are very similar to those of normal substance in the cells. When incorporating into the cells, the drugs can interfere with the cellular metabolism and stop cell division. Antimetabolite drugs attack the cells at particular phases of the cell-cycle, so they are categorized as cell-cycle specific. Chemically, gemcitabine (or difluorodeoxycytidine, dFdCyd), having a molecular weight of 263.2, is an analogue of deoxycytidine nucleoside, in which fluorines replace the hydrogens on the 2'carbons of the deoxycytidine (Fig. 1.2). It has been reported that gemcitabine attacks the proliferative cells mainly in G1, M, and G2 phases, not the S phase (Cappella et al., 2001). As with other analogues of pyrimidines, such as 5-fluoruoracil, foxuridine, cytarabine, and capecitabine, it replaces deoxycytidine, one of the building blocks of nucleic acids, during DNA

replication, thus stopping the cell division, inhibiting DNA synthesis, and inducing programmed cell death or apoptosis (Bold et al., 1999; Cappella et al., 2001; Giroux et al., 2006; Santini et al., 1997).

Interestingly, not like most of chemotherapy agents which are immuno-suppressive, gemcitabine has certain favorable effects on the immune systems (Nowak et al., 2002; Plate et al., 2005; Suzuki et al., 2005; Suzuki et al., 2007). It enhanced the activity of tumor-specific CD8+ T cells and natural killer (NK) cells although selectively eliminating splenic myeloid suppressor cells in tumor-bearing animals (Suzuki et al., 2005). Its inhibition of lymphocyte proliferation was more than 2 times as potent on B cells than on T cells (Nowak et al., 2002). Furthermore, gemcitabine also displayed its immuno-modulatory activity in murine tumor models, independent of its cytotoxic effects (Suzuki et al., 2007), and promoted the activation of naïve T cells in patients with pancreatic cancer (Plate et al., 2005).

Gemcitabine, in the form of gemcitabine hydrochloride (Gemzar®), has been approved by the FDA firstly in 2004 for breast cancer and then in 2006 for ovarian cancer treatments (FDA, 2008). It has now also been applied in clinical trials for other types of cancers: non-small cell lung cancer, bladder cancer, and pancreatic cancer (Toschi et al., 2005). The treatment outcome of gemcitabine, however, is still weak and limited maybe due to its very short half-life in the plasma (8-17 min) (Abbruzzese et al., 1991) and its rapid metabolism (e.g. deamination) to the inactive product (2',2'-difluorodeoxyuridine) (Castelli et al.,

2007). It has been proposed to enhance the stability and half-life of gemcitabine in plasma to improve its anti-tumor activity by producing derivatives of gemcitabine which are more lipophilic (Castelli et al., 2007; Immordino et al., 2004) or encapsulating gemcitabine into nanoparticles like liposomes (Bornmann et al., 2008; Brusa et al., 2007; Castelli et al., 2006; Immordino et al., 2004; Moog et al., 2002) or polycyanoarcrylate (Stella et al., 2007). A more common alternative approach for gemcitabine is its combination with other cancer therapies. The combination has demonstrated the reduced toxicity due to low doses of gemcitabine and other therapy agents and the improved anti-tumor effects, especially in metastatic or advanced cancers. There have been more than 200 reports about that successful combination efficacy, for example, gemcitabine with other chemotherapy agents (Boeck et al., 2007; Leong et al., 2008; Loesch et al., 2008; Manzione et al., 2007; Sultana et al., 2008), with radiation therapy (Allendorf et al., 2008; Cengiz et al., 2007; Haddock et al., 2007; Morgan et al., 2008a; Morgan et al., 2008b), or with immunotherapy (Bauer et al., 2007; Milenic et al., 2007; Zustovich et al., 2007).

1.2.1.2 Poly(I:C) as a chemotherapy agent

Poly(I:C), pI:C or poly I poly C (e.g. polyinosine-polycytidine) is a polymer of synthetic dsRNA. The polymer is composed of two complementary strands, each of polyisosinic acid and polycytidylic acid (Fig. 1.3). Poly(I:C) was first introduced more than 30 years ago for its influence on Friend leukemia in mice (Larson et al., 1969), and since then it has been constantly studied for a

variety of purposes, including tumor therapy. Poly(I:C) can be considered a chemotherapy agent because it possesses properties of a dsRNA which can exert effects of a chemotherapy agent. DsRNA is commonly expressed in cells infected by viruses and activates several pro-apoptotic processes inside cells. In fact, dsRNA can indirectly kill tumor cells because it can induce the production of type I IFNs, which are anti-proliferative blocking G1 phase (Balkwill and Taylor-Papadimitriou, 1978), pro-apoptotic (Chawla-Sarkar et al., 2001) and anti-angiogenic (Balkwill and Taylor-Papadimitriou, 1978; Chawla-Sarkar et al., 2003). More interestingly, dsRNA can directly kill tumor cells (Hirabayashi et al., 1999a; Shir et al., 2006) because once delivered intracellularly, it has ability to promote apoptosis via the interaction with the intracellular dsRNA-dependent protein kinase (PKR) and the 2,5-oligo A synthetase (Chawla-Sarkar et al., 2003) which can terminate the protein synthesis and eventually lead to cell death (Farrell et al., 1978). Alternatively, dsRNA can also directly activate the Toll-like receptor-3 (TLR3) on some breast cancer cell surface (Salaun et al., 2006) and become cytotoxic to the cells. Although poly(I:C) can both indirectly and directly kill tumor cells, the latter seems to play a central role because the local injection of poly(I:C) has demonstrated more effectiveness in delaying tumor growth than systemic administration (DuBuy, 1972; Pimm et al., 1976; Shir et al., 2006).

1.2.2 Cancer radiation therapy

Cancer radiation therapy, or radiotherapy, was first used for cancer treatments more than 100 years ago and has become a major therapy applied in

nearly 50% of cancer patients (Landberg, 1995). In cancer radiation therapy, ionizing radiation of photon, electron, proton, neutron, or ion, is used to damage the DNA of cancer cells, making them unable to divide or grow, and so to control or kill them. There are, in general, two main types of radiation therapy: external and internal (NCI, 2008). In external radiation therapy, which is most commonly used, the radiation comes from a machine outside the body. In contrast, in internal radiation (or brachytherapy), the radiation is placed inside the body or released from unsealed radioactive materials that can go through the body, which is also called the systemic radiation therapy. The amount of radiation used in radiation therapy is measured in gray (Gy), and the total dose is fractionated (e.g. divided) over time to allow normal cells time to recover. Like chemotherapy, radiation therapy is also associated with common side effects in digestive tract, hair follicles, and reproductive system, and others, such as fatigue and skin problems. However, the side effects from radiation therapy are usually limited to the area under treatment and more dependently upon type of radiation, doses, and fractionation.

1.2.2.1 Localized x-ray radiation

Localized x-ray radiation therapy utilizes external beam of x-rays, a form of electromagnetic radiation, to shine locally to the target sites of tumors. Like other high-energy radiations, x-ray can be absorbed deeply into the dense material like tumor tissues and cause damage to the cells there. X-rays work on the cells by removing electrons from atoms and then breaking the bonds that hold DNA

compounds together in the nucleus, making the DNA broken and thus terminating the reproduction and viability of cells (Watters, 1999).

A disadvantage of x-ray therapy is the resistance of tumor cells, especially cells of solid tumors, to the radiation due to the hypoxia induction or low supplies of oxygen because of the enhancement of hypoxia-inducible factor 1 (HIF1) (Brown, 2007). Targeting to block HIF1 or using angiogenesis improvement factors (Coulter et al., 2008) can help to solve the problems. In another way, because the x-rays can act in either cancerous or healthy cells through which it passes, properly adjusting the size of radiation fields, treatment location, and treatment doses is a way used to maximize the treatment effects and minimize the destruction of x-ray to normal cells around the tumors. In practice, low doses of x-ray radiation were usually combined with surgery (al-Mefty and Borba, 1997; Hsu et al., 2002) and/or small doses of other cancer therapies, such as chemotherapy (Gatcombe et al., 2006; Gohongi et al., 2006) and immunotherapy (Chi et al., 2005; Smilowitz et al., 2002) to achieve the optimal results.

1.2.2.2 Gadolinium Neutron Capture Therapy (Gd-NCT)

Gd-NCT is an experimental form of radiation therapy, in which gadolinium (Gd) is used as a NCT agent to absorb the neutron. Gd is a rare earth element having atomic number of 64 and atomic mass of 157.25. Natural Gd consists of 7 stable isotopes including Gd^{154}, Gd^{155}, Gd^{156}, Gd^{157}, Gd^{158}, and Gd^{160}. Among them, Gd^{157} has the most excellent neutron capture properties with thermal neutron

capture cross-section of 255,000 barns (1 barn = 10^{-24} cm^2), which is approximately 66 times that of $Boron^{10}$, a NCT agent for the common NCT, B-NCT.

The procedure of Gd-NCT can be divided into two steps (Fig. 1.4) as follows: (Yanagie et al., 2002)

Step 1: ^{157}Gd is delivered to tumor sites and then

Step 2: neutron beam is narrowly shined to the target tumors

The reaction of Gd and the neutron beam (also called neutron capture reaction) can be expressed as:

$$^{157}Gd + neutron \rightarrow {}^{158}Gd + \gamma$$

The release of γ-rays is also followed by a succession of Auger electrons and low-energy conversion. It has been reported that the Auger electrons induced from γ-rays release can enhance remarkably the relative biological effectiveness and therapeutic index of Gd-NCT (Martin et al., 1988). In addition, each ^{157}Gd capture event can emit approximately 88% internal conversion electrons having a range of about 60 μm, which is approximately 6.7 times compared to that of Boron decay (Tamat et al., 1987). Another aspect of Gd-NCT's application that makes it more attractive than Boron-NCT's is that a Gd-based compound, e.g. Gd-DTPA, has been utilized in clinical trials as a contrast agent in MRI. Therefore, using Gd-NCT has the potential to integrate both diagnosis and treatment for cancer therapy.

Theoretically, Gd-NCT is an ideal modality for cancer therapy due to its safety. The ^{157}Gd nuclide used as a NCT agent is non-toxic and the neutron beam ideally applied in NCT itself has a very low energy (between 1 eV and 10 KeV) which is not harmful to tissues. More importantly, the cytotoxic emission is elicited only when the Gd compounds interact with the neutron beam at the desired sites. In practice, for the success of Gd-NCT, besides the quality of neutron beam and other parameters necessary for the appropriate beam-shining to the targeted locations, sufficient concentration of Gd at the tumor sites before and during the neutron irradiation is one of critical factors that is, however, rather difficult to achieve. The optimal ^{157}Gd concentration in tumors adequate for the capture of neutron beam to emit enough cytotoxic photons was proposed to be between 50 and 200 μg per g of wet tumor (Shih and Brugger, 1992). The usage of Gd chelates, such as Gd-DTPA, instead of free Gd has demonstrated a higher safety profile (Barnhart et al., 1987). However, the application of Gd-DTPA in Gd-NCT is limited because it rapidly diffuses out of tumors due to its highly hydrophilic properties (Akine et al., 1992). There have been many approaches attempting to meet the requirement of delivery and retention of sufficient amount of Gd at the tumor sites, such as direct intratumoral injection of gadopentetic acid/chitosan complexes and Gd containing emulsions and microspheres (Miyamoto et al., 1999; Tokumitsu et al., 2000; Tokumitsu et al., 1999); arterial administration of Gd-microcapsules (Akine et al., 1992); or systemic injection of tumor-targeted Gd (Watanabe et al., 2002). Nevertheless, the previous studies still contain a number

of limitations: low concentrations of Gd in tumors or infeasible for tumors deep inside the body which are difficult to reached or localized by directly injection.

1.2.3 Cancer immunotherapy

Cancer immunotherapy, belonging to biological therapies, is the method using the immune system of the body to combat cancers. It was first reported more than 100 years ago when Dr. Coley used the Coley's toxin, a mixture of streptococcal and staphylococcal bacteria, to control the tumor growth in sarcoma patients after surgery (Coley, 1991). The interest in cancer immunotherapy has been augmented since the last decades of the 20^{th} century thanks to the development of molecular biology and specific targeting technology for loading cytotoxic agents as well as the findings of cytokines involved in cancer fighting. These treatments can be classified into three types (Schuster et al., 2006): active cancer immunotherapy (cancer vaccines), cytokine therapies, and passive cancer immunotherapy. Our work focused on the first two types with emphasis on T cell-based therapy and cytokines therapies.

1.2.3.1 T cell-based therapy

Immunotherapy for cancers is established based on stimulation of the immune system to fight against the cancer cells, in which the host's own immune system is recruited to recognize and destroy abnormal cells (e.g. stimulation of the immune surveillance or immunostimulants), or therapeutic antibodies are administered to attack the tumor cells. The immune system is generally composed

of white blood cells responsible for the adaptive immune responses, including B cells (B lymphocytes) and T cells (T lymphocytes), and others for the innate immune responses, such as natural killer cells (NK cells), monocytes, eosinophils, and basophils (Janeway, 2005). T cells, which are mature in the thymus and have a special receptor on the surface called T cell receptor (TCR), play a key role in cell-mediated immunity. T cells are comprised of helper T cells (T_h), cytotoxic T cells (T_c), memory T cells, regulatory T cells (T_{reg}), natural killer T cells (NKT cells), and γδ T cells. Cytotoxic T lymphocytes (also known as CTLs, cytotoxic T cells (T_c), or CD8+ T cells), a subset of T cells which express the CD8+ glycoprotein on their membrane, have the important function of destroying "target cells" including infected cells, damaged or dysfunctional cells, and tumor cells. Mechanisms of action of CTLs have been known to involve in perforin/granzyme killing and FasL/Fas killing (Wajant, 2002). In one way, when exposed to infected/target cells, CTLs bind to the cells and release the perforin to form pores in the plasma membrane of the target cells, allowing granzymes, which are serine proteases, to enter the target cells and then activate the caspase cascade that ultimately leads to the programmed cell death or apoptosis. Another way to induce apoptosis by CTLs is via the interactions between the cell surface of CTLs and that of the target cells. CTLs express on their surface proteins called Fas ligand (or FasL) which can recognize and bind to their receptors called Fas molecules expressed on the surface of the target cells. This binding also leads to the lysis of the target cells. The activation of CTLs plays an important role in the specific tumor-cell killing. It is

dependent on the interactions between molecules expressed on the surface of the T cells and those of the antigen presenting cells (APCs), (e.g. dendritic cells (DCs) that displays foreign antigen complexed with major histocompatibility complex (MHC) on its surface). When receiving appropriate signals, the CTLs are activated and proliferate with the help of interleukin-2 (IL-2) cytokine. The activated CTLs then circulate throughout the body searching for antigen-positive somatic cells and destroying them.

It has been known that the cancer cells have genetic instability and usually express on their surface abnormal proteins called tumor-associated antigens (TAAs) which are potentially immunogenic and usually absent or limited on the normal cells (Kawakami et al., 1994; Keogh et al., 2001). The TAAs are supposed to be recognized by the host's immune system or by CTLs in particular, and the tumor cells will be attacked. However, this endogenous immune response against the tumor cells in practice only has trivial effects (Maecker et al., 2005; Ward et al., 1999). The tumor cells escape from the immune surveillance's detection and destruction maybe due to the down-regulation of factors essential for the invasion of T cells and APCs and the production of immunosuppressive cytokines, such as interleukin-10 (IL-10) and transforming growth factor (TGF) (Kiessling et al., 1999; Platsoucas et al., 2003; Salih and Nussler, 2001). Therefore, providing signals necessary for the activation of CTLs and APCs is one of approaches in immune intervention that have been developed with efforts to lead to effective therapy in a number of cancers. Using an appropriate activator of CTLs has been

known to be able to inhibit the tumor growth in human colon carcinomas growing in severe combined immune deficiency (SCID) mice (Dohlsten et al., 1995), in humanized SCID mice carrying Daudi lymphoma cells (Gidlof et al., 1997), or in patients with advanced colorectal or pancreatic carcinoma (Nielsen et al., 2000). Induction of specific T cell responses for cancers is also one of the major factors for an ideal cancer vaccine (Schuster et al., 2006), and its long-lasting over months or even years is both challenge and interest of recent cancer immunologists.

1.2.3.2 Cytokine therapies

Cytokines are small proteins and glycoproteins involved in cellular communication. They play important roles in the functions of both innate and adaptive immune responses. When the immune cells confront a pathogen, they usually secret cytokines that bind to surface membranes of the pathogen and then lead to a chain of reactions that terminate certain types of responses in the targeted cell (Pardoll, 1995). In cancer therapy, cytokines are in general utilized to enhance immunity. Cytokine-based cancer therapy was reported with severe side effects, such as high fever, swelling and redness, fatigue, and nausea (Kammula et al., 1998; Panelli et al., 2004) when used individually because an adequate dose of cytokines can be associated with the hyperactive immune reaction called “storm cytokines” that can be potentially fatal. In fact, cytokines act in cascades in the immune system. Therefore, various cytokines rather than single ones may be applied in clinical trials to achieve optimal results. More importantly, the

combination of cytokines at low and appropriate doses can also induce synergistic effects and minimize the side effects (Kircheis et al., 1998).

IL-2 and IFN-α-2b are two cytokines approved by the FDA (Hurley and Chapman, 2005; Yang et al., 2003) for the treatment of some type of carcinoma, leukemia, lymphoma, or Kaposi's sarcoma. In our research projects, we have roughly examined the roles of interferon alpha, a major cytokine currently in use, for the evaluation in cancer therapy.

Interferon alpha (IFN-α) is one of the three types of IFNs, including IFN-α, IFN-β, and IFN-γ. Structurally, it is a protein composed of about 150 amino acids and binds to some receptors on the surface of immune cells. IFN-α has multiple functions for anti-tumor activity, such as pro-apoptotic, anti-proliferative, and anti-angiogenic (Balkwill and Taylor-Papadimitriou, 1978; Chawla-Sarkar et al., 2001; Chawla-Sarkar et al., 2003; Sidky and Borden, 1987). Interestingly, it is also strongly immunostimulatory (Le Bon et al., 2003). IFN-α has been applied in treatment for a number of cancers like renal cell carcinoma (Obara et al., 2008; Tatsugami et al., 2008), metastatic melanoma (Green et al., 2008; Hauschild et al., 2008), hairy cell leukemia (Rosenberg et al., 1986), chronic myelogenous leukemia (Topalian et al., 1989), hematologic cancers (Karmaniolas et al., 2005; Nara, 1995), and solid tumors (Currie et al., 2008; Fuxius et al., 2002).

1.2.3.3 Poly(I:C) as an immunotherapy agent

As described above (Chapter 1, section 1.2.1.2), poly(I:C) possesses properties of dsRNA which can act as a chemotherapy agent via an indirect way, e.g. type I IFNs induction, and a direct way, e.g. interaction with PKR, 2,5-oligo A synthetase, and TLR3. Similarly, poly(I:C) can also work as an immunotherapy agent through indirect and direct mechanisms. In the first mechanism, the type I IFNs induced by dsRNA are also immunostimulatory (Chawla-Sarkar et al., 2003; Le Bon et al., 2003; Liu et al., 2001). They have been demonstrated to augment CTLs, NK cells, and DCs and promote the cross-priming of CD8+ T cells (e.g. CTLs) by stimulating the maturation of DCs (Le Bon et al., 2003). In the latter mechanism, it has been reported that dsRNA can interact with TLR3 and intracellular retinoid acid-inducible gene-1 protein (RIG1) that can activate not only the innate but also the adaptive immune responses (Alexopoulou et al., 2001; Yoneyama et al., 2004).

1.2.4 Combination therapies for cancers

Combination therapy has been nowadays the best approach for various cancers because it can overcome three critical obstacles in cancer treatment: low therapeutic effects, drug resistance, and high toxicity (Gahr et al., 2007; Knobf, 1984; Lieu et al., 2008; Matei et al., 2008; Sandlund et al., 2008; Yadav et al., 2008). The improved outcome may account from the different mechanisms of drugs that help to attack multiple targets, escape from the tumor resistance, and decrease the therapeutic doses with acceptable clinical toxicity. Standard therapies,

e.g. surgery, chemotherapy, and radiation therapy, have been widely applied in combination in clinical trials. The number and order of treatments are dependent on the tumor size, cancer stage and the patient's health state. Sometimes, low-dose chemotherapy and/or radiation therapy after surgery can help to destroy any remaining cancer cells. Another time, they were given before surgery to shrink the tumors, thus providing greater ease in tumor removal. Frequently, radiation and chemotherapy or many chemotherapy agents were also incorporated together for the treatment of advanced and metatastic cancers. We are more interested here in exploiting the combination therapy using the less conventional immunotherapy with two most common modalities: chemotherapy or radiation therapy.

1.2.4.1 Combination of chemotherapy and immunotherapy

Combination of chemotherapy and immunotherapy may help to improve the therapeutic effects due to different mechanisms of action. However, most chemotherapy agents are strongly immunosuppressive with the common side effect of lymphopaenia. Therefore, the combination seems to be unrelated in theory. In practice, successful integration of some chemotherapy agents and immunotherapy agents has been well documented in animal models (Bauer et al., 2007; Kim et al., 2007; Ko et al., 2007; Samanta et al., 2007; Zhong et al., 2007) and in clinical trials (Fujimoto et al., 2006; Holmberg et al., 2006; Masucci et al., 2006; Oka et al., 2007; Recchia et al., 2007; Ruttinger et al., 2007; Ryan et al., 2007; Weide et al., 2007; Yamanaka et al., 2007). One critical interaction between chemotherapy and immunotherapy for cancers that could boost endogenous

immune responses via cross-presented tumor antigens can be briefly described as follows. A majority of chemotherapy drugs kill tumor cells via the process of apoptosis induction, and dead-tumor cells are a good source of antigens. They can be phagocytosed by APCs and presented to T cells to induce anti-tumor immune responses (Lake and Robinson, 2005). It has been well known that in the absence of inflammatory signals, apoptotic remnants are phagocytosed by the macrophages (Savill and Fadok, 2000), and apoptotic cells becomes non-immunogenic (Kerr et al., 1972), thus nearly no immune response is generated. Therefore, it is essential to have the presence of certain "danger" signals that can activate APCs, so that the tumor-cell death from chemotherapy can "set the stage" for an effective anti-tumor immune response (Lake and Robinson, 2005). Our research using gemcitabine in combination with poly(I:C) potentially applies the above mechanism to specifically kill tumor cells. In fact, the effects of gemcitabine on the immune system are well-documented (Bauer et al., 2007; Milenic et al., 2007; Nowak et al., 2002; Plate et al., 2005; Suzuki et al., 2005; Suzuki et al., 2007; Zustovich et al., 2007), and the poly(I:C) is strongly immunostimulatory and is a potent "danger" signal because it is a ligand of TLR3, a pathogen associated molecular pattern molecule (Alexopoulou et al., 2001; Le Bon et al., 2003; Schulz et al., 2005). Moreover, poly(I:C) also pocesses functions of a chemotherapy agent (e.g. direct killing of tumor cells) besides the immuno-stimulation and IFN type I induction. Therefore, the combination may be a very promising modality of chemo^2-

immunotherapy for cancers to both synergistically control the tumor growth and to induce innate and specific tumor-killing immune responses.

1.2.4.2 Combination of radiation therapy and immunotherapy

Similarly to the integration of chemotherapy and immunotherapy as mentioned above, the collaboration of radiation and immunotherapy can be favorable with appropriate doses and regimens. Radiation can improve the immune system activity to tumor cells or vice-versa. For example, radiation therapy prior to adoptively transferring of prostate-specific CD4 T cells improved the immune response to prostate cancer in transgenic mice to control tumor growth (Harris et al., 2008). In another way, adoptively transferred CTLs improved the antitumor effects of radiation in human squamous cell carcinoma (Krause et al., 2007). Administration of a prostate cancer tissue vaccine prior to radiation treatment augmented the effects of radiation and inhibited the tumor growth in rats (Suckow et al., 2008). IFN-α as an adjuvant after the pretreatment of chemoradiotherapy increased the apoptosis in pancreatic carcinoma (Schmidt et al., 2006).

Our research of combining radiation therapy and poly(I:C) was expected to potentially improve the resultant anti-tumor activity due to different mechanisms of killing tumors. The hypothesis of the combination treatment was also based on the theory of cross-priming of CD8+ T cells. Ionizing radiation has been well documented to induce apoptosis to kill tumor cells (Watters, 1999). This effect may not only eradicate radio-sensitive tumor cells, but also can generate other

responses (Chakraborty et al., 2003; Chakraborty et al., 2004; Garnett et al., 2004; Kudo-Saito et al., 2005). In fact, radiation was also considered immunosuppressive, dependent on doses, and there is not any direct evidence demonstrating that the radiation itself can enhance tumor immunity (Koski and Czerniecki, 2005). The dead tumor cells after irradiation can be a good source of tumor antigens, taken up by APCs, and introduced to T cells inducing specific anti-tumor immune response to inhibit the tumor growth (Demaria et al., 2004; Salio and Cerundolo, 2005). However, this process cannot occur as expected without the presence of "danger" signals to activate the APCs, which can be provided with the administration of poly(I:C). Therefore, the combination of radiation therapy and poly(I:C), which can act as both a chemotherapy and immunotherapy agent, may generate a new modality for cancer of radio-chemo-immunotherapy to improve the application of poly(I:C) therapy in clinical trials.

1.3 Liposomes as a drug delivery system in tumor therapy

1.3.1 Properties of liposomes

Liposomes are vesicles having membranes made of double layers of phospholipids. They were first mentioned in literature more than 40 years ago by British hematologist A. D. Bangham at the Babraham Institute, Cambridge (Bangham et al., 1965), and since then their functions, as well as applications, have been explored in various fields of research including drug delivery. Liposomes have a hydrophilic core, but the unique characteristic of liposomes lies in their membrane structure composed of phosphohlipids similar to cell

membranes that make them biocompatible and biodegradable. Liposomes prepared from natural phospholipids are biologically inert and non-immunogenic with low intrinsic toxicity (Immordino et al., 2006). The phospholipids contain a water-soluble head (e.g. polar region) and two oil-soluble tails (e.g. non-polar region). When placing them together in an aqueous environment, they will orientate themselves spontaneously to make the non-polar region away from the aqueous phase with which the polar contact. Liposomes can encapsulate hydrophilic compounds in their core and incorporate hydrophobic substances in their membranes, thus enabling them to be a very versatile delivery system of both hydrophilic and hydrophobic drugs.

Liposomes can be generally classified based on the structure of lipid bilayers (Table 1.1), on the basis of their preparation, or on the surface charges of vesicles (e.g. neutral, anionic, or cationic).

1.3.2 Long-circulating liposomes for tumor therapy

Liposomes can work as a carrier to encapsulate/incorporate drugs, protect them from degradation, and bring them to the tissues or organs having discontinuous endothelium by passive penetration. Under tumor condition, the endothelial lining in the tumor vasculature is discontinuous which facilitates extravasation of liposomes into the interstitial space (Fig. 1.5). From there, liposomes can act as a sustained drug-release system to release drugs, and then the drugs diffuse into tumor cells. In another way, liposomes can continue to penetrate

into the tumor cells and release drugs inside the cells. These processes are known as enhanced permeation and retention effect (EPR). In order to undergo all steps necessary for the EPR, it is required that liposomes have the ability to carry drugs stably in them, deliver a sufficient amount of drug to the tumor regions, and retain drugs there long enough to efficiently exert the anti-tumor activity. Therefore, liposomes need to be stable and have a long blood circulation time so that they have more opportunities to extravasate into tumor regions. The physicochemical properties of liposomes have strong effects on their fate in the body, and the success of long-circulating liposomes for drug delivery is dependent on numerous factors.

The size of liposomes is one of several factors that determine their stability and application. Multilamellar vesicles can trap a large amount of lipid-soluble drugs because of their high content of lipid in the membrane. Besides, for encapsulating of water-soluble drugs, they can increase the retention time of drugs inside them since the multilayers are obstacles for drugs to release out of the vesicles. However, the unilamellar vesicles with diameter size of less than 100 nm composed of only one layer of phospholipids are more preferred in drug delivery for the systemic administration because the small sizes can enhance the ability of liposomes to penetrate into the cells and to avoid entrapment by macrophages and the reticuloendothelial system (RES) (Harashima et al., 1994; Senior and Gregoriadis, 1982), which prevent drugs from reaching their targets.

The appropriate fluidity of the vesicles' membrane also plays an important role in the stability of liposomes. According to Damen et al. (Damen et al., 1981), incorporating cholesterol can help to increase the rigidity of the bilayer and decrease the interaction of liposomes with high density lipoprotein (HDL) which causes fast release of encapsulated drugs into the plasma. Furthermore, liposomes prepared from phospholipids with unsaturated fatty acyl chains are less stable in the blood than those with saturated fatty acyl chains because the latter can increase the critical transition temperature (Tc) of vesicles (Senior and Gregoriadis, 1982).

The modification of vesicles' membrane has been a critical approach for liposome technology to improve the stability and longevity of liposomes in the body. It has been well documented that the conventional liposomes in which their membrane consists of only phospholipids are removed quickly from the blood circulation and are not optimal for systemic drug delivery (Scherphof et al., 1985). "Stealth" liposomes have surfaces coated with a hydrophilic polymer polyethylene glycol (PEG) to form a spatial barrier that makes liposome surface hinder from the plasma proteins (Blume and Cevc, 1993; Vert and Domurado, 2000), thus reducing the interaction of liposomes to the RES. Furthermore, the PEG chains provide the surface of liposomes with a strong interbilayer repulsion to prevent vesicle aggregation and improve the stability of liposomes (Needham et al., 1992). The benefits of PEG grafted on the liposome surface have been demonstrated as increasing drugs solubility and stability, reducing immunogenicity and clearance, limiting RES uptake, and strongly prolonging blood half-life (Caliceti and

Veronese, 2003). The appropriate amount of PEG in liposomes has been recommended to be in the range of 5-10% (molar ratio) of phospholipids (Manojlovic et al., 2008; Maruyama et al., 1992) to enable the vesicles to avoid the effects of the RES. In addition, the molecular weight (MW) of PEG of at least 2000 Da has shown to be effective in prolonging the blood circulation time of carriers (Gaur et al., 2000; Maruyama et al., 1992).

1.3.3 Cationic liposomes for tumor therapy

Cationic liposomes, as named, are prepared by including positively charged phospholipids in the formulation. Cationic liposomes (CLs) can have various applications in gene delivery and drug delivery areas. They are more advantageous than viral vectors, a well-developed gene delivery mode, due to their formulated simplicity, weak hazard, and easy adaptation for particular applications. CLs have been studied for more than a decade for delivery of DNA (Hofland and Huang, 1995; U'Ren et al., 2006), nucleic acid (Tana et al., 1997; Whitmore et al., 2001), polyinosinic:polycytidilic acid (Bucur et al., 1998), and paclitaxel (Campbell et al., 2001; Manojlovic et al., 2008) for tumor therapy *in vitro* and *in vivo*. This type of liposome was utilized to deliver compounds by forming complexes with the compounds mainly based on electrostatic attraction between the positive charge on the surface of the cationic liposomes and the negative charge on the surface of the compounds (Fig. 1.6), or based on hydrophobic interaction between them. For example, the complexes of cationic liposomes and DNA, called lipoplexes, are made by the attraction of positively-charged liposomes and negatively-charged

nucleic acids. The lipoplexes have been demonstrated to deliver DNA to the nucleus of cells via clathrin-involved endocytosis (Cao et al., 2000). The net surface charge of the complexes is dependent on the charge ratio of positive cationic liposomes to negative compounds. A highly charged ratio can have a stronger ability of killing tumor cells *in vitro*, but it can also be associated with more toxicity *in vivo*, of course dependent on the administered doses (Dass et al., 2002; Manojlovic et al., 2008). Cationic liposomes, together with other cationic polymers, have been remarkably developed and studied for drug delivery applied in tumor therapy, especially for the purposes of enhancement immune responses, because the complexes can provoke the production of pro-inflammatory cytokines like TNF-α, IFN-γ, and IL-12 (Freimark et al., 1998; Scheule et al., 1997).

1.3.4 Preparation of liposomes

The bilayer components, which basically are phosphotidylcholine (PC), phosphatidylenolamine (PE), and phosphatidylserine (PS), play the central role in preparation of liposomes. Cholesterol and PEG can be included to increase the rigidity and hindrance effects, respectively, of the formulation. Liposomes can be prepared in general by various methods: film hydration, ultrasonication, reverse-phase evaporation, ether vaporization, freeze-thaw extrusion, and dehydration-rehydration. In our research projects, we utilized the thin film hydration method followed by sonication, freeze-thaw, and extrusion because it is easy to handle, widely applied (de Almeida Silva et al., 2006; Dipali et al., 1996; Joshi and Misra, 2001; Kallinteri et al., 2004; Koromila et al., 2006; Ohsawa et al., 1985; Sezer et

al., 2004; Tilcock et al., 1989), and can also produce liposomes appropriate for our purposes. The process can be briefly described as follows.

Chloroform solutions of lipids including phospholipids, cholesterol, and PEG were placed together into a glass vial and then evaporated under nitrogen gas to form a thin lipid film on the vial wall. The closed vesicles were formulated and the research compounds were trapped in their core (only in case of preparation of drug-encapsulated liposomes) by hydrating the thin film with a solution of compounds at temperature above the transition temperature (Tc) of the phospholipids followed by vigorous vortex until the entire film was suspended. In this stage, heterogeneous sized MLVs with a diameter greater than 1 μm were achieved. The MLVs then underwent 6 cycles of freezing in nitrogen liquid and thawing in a warm water bath to achieve a larger internal core so that the vesicles can contain higher concentrations of research compounds. The resulting vesicles were a mixture of MLVs and LUVs with heterogenous sizes. Further short bath sonications were employed to yield a population of smaller sizes SLVs and facilitate the following sequential extrusion through polycarbonate membranes starting from 1 μm, to 0.4 μm and 0.1 μm to get homogenous SLVs having diameters approximately of 0.1 μm. The formed liposomes were composed of both encapsulated and unencapsulated research compounds. Therefore, they need to undergo further steps of purification to remove the unencapsulated components. Methods of gel permeation chromatography (GPC) (Bakouche and Gerlier, 1985;

Manojlovic et al., 2008; Patel and Misra, 1999) or dialysis (Liang et al., 2004) can be commonly used for this purpose.

In the case of preparation of cationic liposomes, the vesicles were formed by hydration with an appropriate buffer solution before sonication and extrusion.

1.3.5 Application of drug-encapsulated/incorporated liposomes for tumor therapy

With properties as mentioned above, liposomes have been a very versatile delivery system of various drugs for either small or large molecules. One of the most common applications of liposomes in drug delivery for tumor therapy is their carriage of hydrophilic small molecules of chemotherapy agents. Normally, those agents are well water-soluble and can be eliminated quickly after administration, not producing enough effects for cancer treatment. Therefore, it is required to increase the doses or frequency of doses of the drugs, which is also associated with toxicity. Liposomes can encapsulate these agents and improve their pharmacokinetic profile to induce a more stable and longer-lasting exposure of the agents to tumor cells, thus enhancing their opportunities to enter the tumors. In fact, liposome-entrapped daunorubicin (a well-known chemotherapy agent) showed a “superior” therapeutic effect of lymphoma cell killing in mice compared to the free drug, even with a single or multi- intravenous injection, by a factor up to 100 times (Gabizon et al., 1985). Daunorubicin-associated liposomes enhanced the concentration of the drug in blood but lowered it in the heart, leading to lower cardiotoxicity in nude mice, as compared to the free drug (Kojima et al., 1986).

There have been at least 500 reports up to now about the improved anti-tumor activity and minimized-toxicity of daunorubicine-encapsulated liposomes, as compared to the free drug, in various tumor models. Eventually, DaunoXome® has been approved in the U.S and distributed in the market as products of daunorubicin-associated liposomes (FDA, 1996). Similarly, Doxil®, Caelyx®, Myocet® (doxorubicin-encapsulated liposomes) has been well-known for the treatment of AIDS-related Kaposi's sarcoma, breast cancer, ovarian cancer, and other solid tumors (Campos et al., 2001; Gabizon et al., 1994; Halford et al., 2001; James, 1995; Ranson et al., 1997; Simpson et al., 1993; Sparano et al., 2001; Vaage et al., 1993). Various other chemotherapy agents, either hydrophilic or hydrophobic, such as arsenic trioxide (Zhao et al., 2008), curcumin (Thangapazham et al., 2008), camptothecin (Watanabe et al., 2008), methotrexate (Vodovozova et al., 2007), 5-fluorouracil (Fanciullino et al., 2007), vinorelbine (Webb et al., 2007), combretastatin (Nallamothu et al., 2006), cisplatin (Ramachandran et al., 2006), and many more, have been formulated with liposomes and also displayed very promising results as compared to the free drugs.

Another aspect of liposomes's application is their ability to carry large molecules, such as poly(I:C), cytokines, antibodies, and plasmid DNA for tumor therapy. Cationic liposomes complexed with poly(I:C) can inhibit the progression of murine melanoma (Fujimura et al., 2006) and metastiatic carcinomas (Hirabayashi et al., 1999b). Kedar et al. (Kedar et al., 2000) have proved that IL-2-encapsulated liposomes (Lip-IL-2) were much more efficiently immunodulatory in

mice than free IL-2 thanks to their prolonged blood half-life although the route of administration and type of liposomes can influence their pharmacokinetic profiles. In a nude mouse breast cancer metastasis model, a cationic immunolipolex sytem incorporating anti-transferrin receptor single-chain antibody (TfRscFv) and docetaxel demonstrated remarkably enhanced anti-tumor efficacy with prolonged survival (Xu et al., 2001). In another research study, liposomes have shown to improve the effectiveness of plasmid DNA for cancer vaccines (U'Ren et al., 2006). It has been reported in a very current study that liposomes conjugated with bio-nanocapsules (BNCs) containing hepatitis B virus surface antigen (HBsAg) can incorporate large materials of fluorescence-labeled polystyrene beads and plasmids to form a complex producing significantly higher transfection efficiency than the BNC, increasing possibilities for both drug delivery and bio-imaging systems (Jung et al., 2008).

Apart from the above advantages, liposomes still express certain limitations. They seem to be less effective in retaining highly hydrophilic small molecule compounds inside them, resulting in rapid elimination of compounds out of the body (Unger et al., 1990), unless the drugs encapsulated were gelated (Lasic et al., 1992) or precipitated inside liposomes (Lasic et al., 1995), or a further modification of the compounds' structure was employed (Brusa et al., 2007; Castelli et al., 2007; Immordino et al., 2004). Another limitation of liposomes is the lack of "active triggers" causing weak anti-tumor activity (Andresen et al., 2005; Kong et al., 2000; Needham et al., 2000). Stable and rigid formulations of

stealth liposomes provide drugs with long circulation time, but also make certain compounds which are membrane impermeable, such as ciplastin, release slowly only after liposomes are degraded, consequently leading to the low efficacy *in vivo* (Bandak et al., 1999; Harrington et al., 2001; Zamboni et al., 2004). Also, DNA-loaded liposomes can have a decreased capacity of DNA transfection due to their interaction with serum proteins (Cullis et al., 1998; Li et al., 1998; Sakurai et al., 2001). Anionic molecules in the serum can aggregate with the lipoplexes or release DNA from them, restricting their application via intravenous administration. Nevertheless, due to their versatile functions and safe profile, liposomes are still a promising drug delivery system. Alternative approaches and further modification in the formulations have been constantly developed to improve their functions and applications as well as minimize their limitations.

Table 1.1 Types of liposomes based on the structure of lipid bilayers. (Adapted from Rongen et al., 1997).

Vesicle Types	Diameter Size	Number of lipid bilayers
Small unilamellar vesicles (SUV)	20-100nm.	1
Large unilamellar vesicles (LUV)	>100nm.	1
Oligolamellar vesicles (OLV)	0.1-1μm.	~ 5
Multilamellar vesicles (MLV)	>0.5μm.	5-20
Multivesicular vesicles (MMV)	>1μm.	Multicompartmental structure

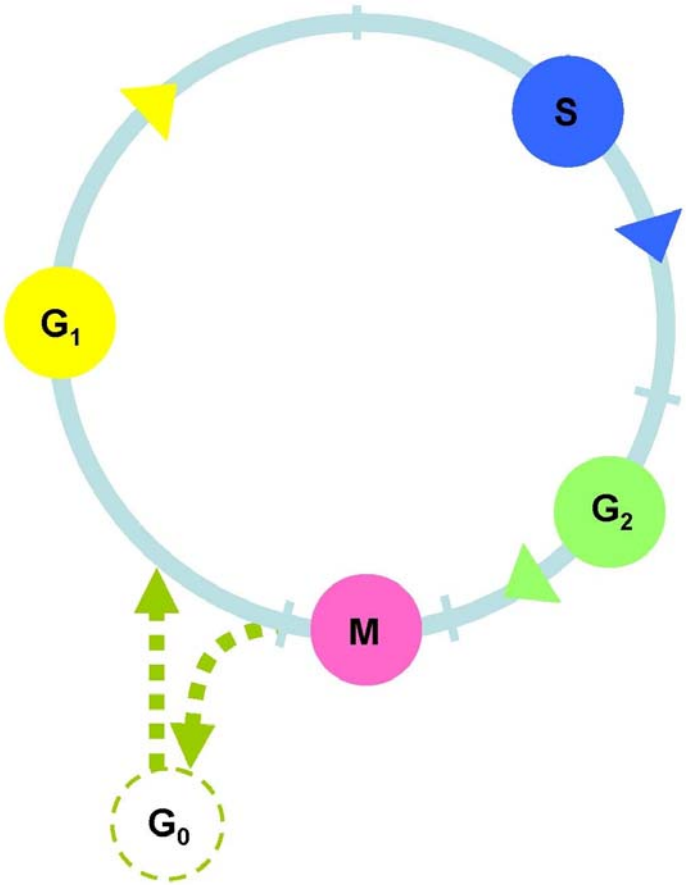

Figure 1.1 Scheme of the mammalian cell cycle. (Adapted from Priestman, 2008).

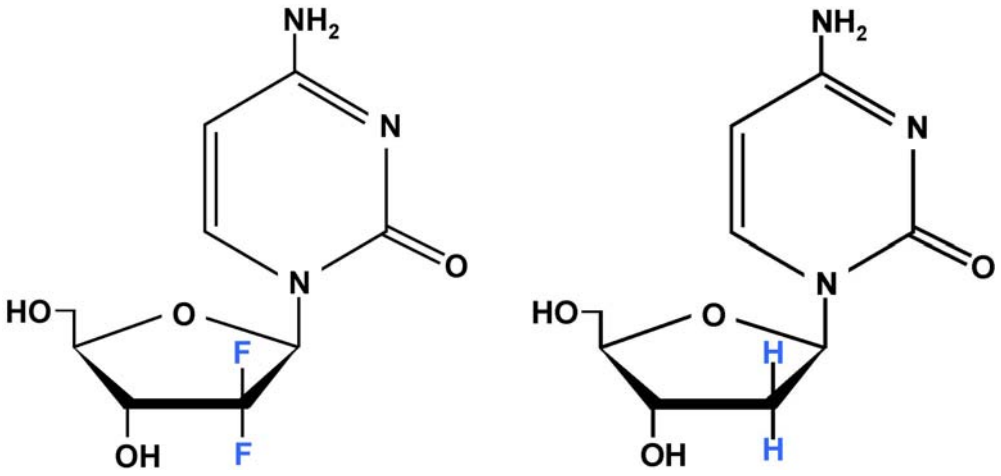

Gemcitabine **Deoxycytidine**

Figure 1.2 The structures of Gemcitabine and Deoxycytidine

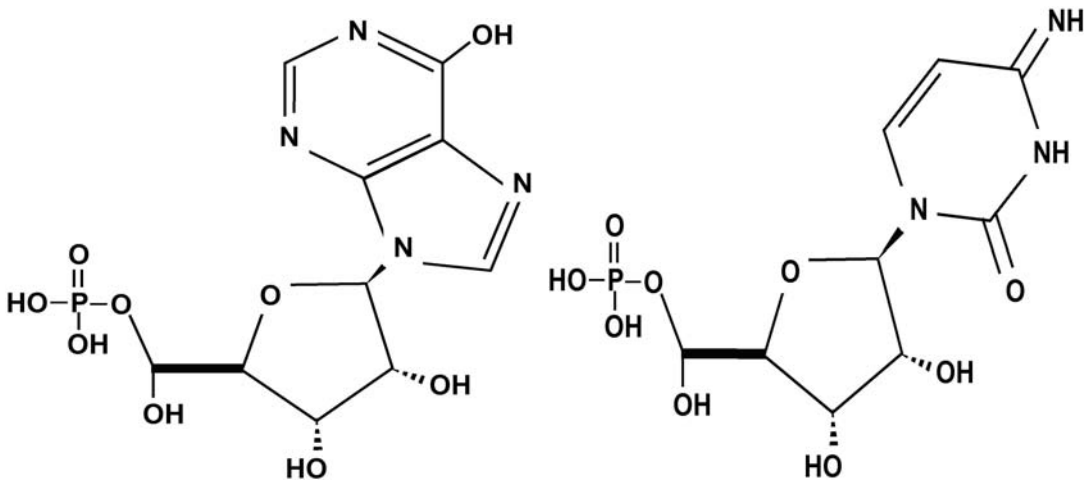

Inosinic acid **Cytidylic acid**

Figure 1.3 The structures of inosinic acid and cytidylic acid.

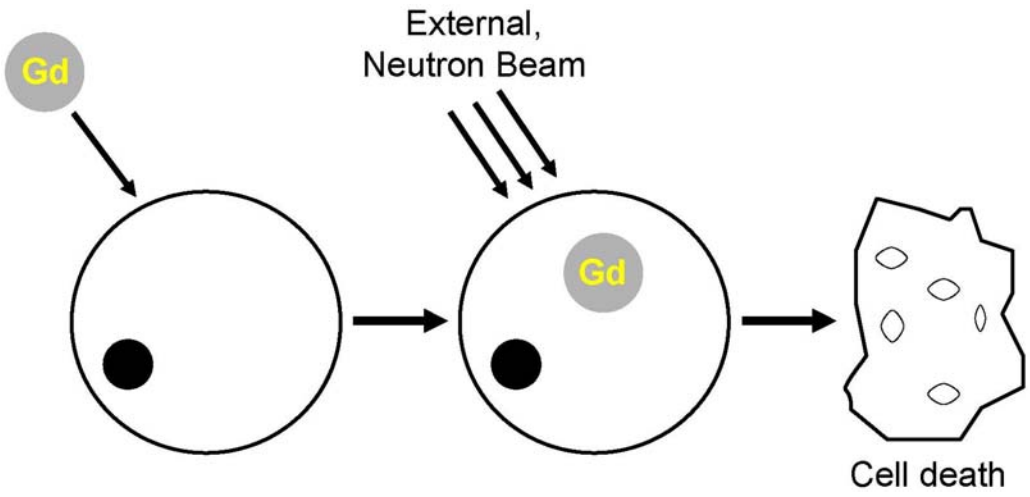

Figure 1.4 A schematic illustration of two steps in Gd-NCT. (Adapted from Yanagie et al., 2002).

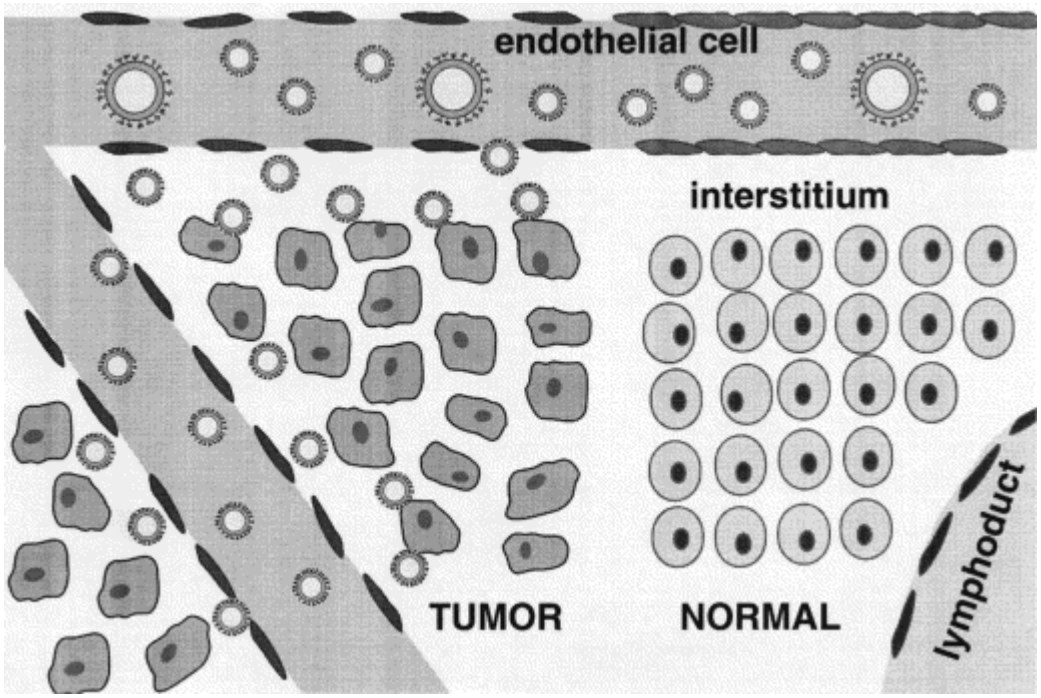

Figure 1.5 Scheme of "anatomical barriers of solid tumor tissue and extravasation of liposomes through capillaries from blood circulation". (Based on Maruyama et al., 1999).

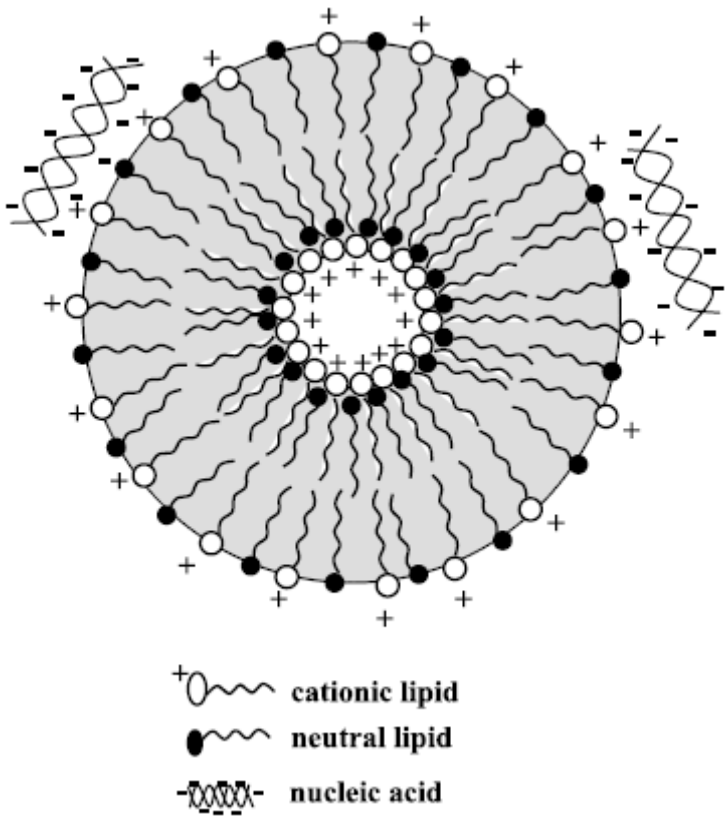

Figure 1.6 Formation of lipoplexes. (Based on Dass, 2002).

Chapter 2

LONG-CIRCULATING GADOLINIUM-ENCAPSULATED LIPOSOMES FOR POTENTIAL APPLICATION IN TUMOR NEUTRON CAPTURE THERAPY

Uyen M. Le and Zhengrong Cui

International Journal of Pharmaceutics, 2006; 312(1-2): 105-12.

2.1 Abstract

Gadolinium neutron capture therapy (Gd-NCT) is a promising cancer therapy modality. One of the key factors for a successful Gd-NCT is to deliver and maintain a sufficient amount of Gd in tumor tissues during neutron irradiation. We proposed to prepare a Gd delivery system by complexing a Gd-containing compound, diethylenetriaminepentaacetic acid (Gd-DTPA), with a polycationic peptide, poly-L-lysine (pLL), and then encapsulate the complexed Gd-DTPA into pegulated liposomes. Complexation of Gd-DTPA with pLL not only enhanced the encapsulation efficiency of Gd-DTPA in liposomes, but also significantly limited the release of Gd-DTPA from the liposomes. A Gd-DTPA-encapsulated liposome formulation that contained 6.8 ± 0.3 mg/mL of pure encapsulated Gd was prepared. The blood half-life of the Gd encapsulated into the liposome formulation was estimated to be about 24 hours in healthy tumor-free mice. Twelve hours after the Gd-encapsulated liposomes were intravenously injected into mice with pre-established model tumors, the Gd content in the tumors reached an average of 159 μg/g of wet tumor tissue. This Gd-DTPA encapsulated liposome may be used to deliver Gd into solid tumors for NCT and tumor imaging.

2.2 Introduction

Neutron capture therapy (NCT) is a promising cancer therapeutic approach. In NCT, stable and non-radioactive nuclides are delivered to target tumors. The nuclides then produce localized cytotoxic radiations upon irradiation by thermal or

epithermal neutrons (Barth and Soloway, 1994; Carlsson et al., 2002). Earlier studies were mainly focused on using boron-10 (^{10}B) as a nuclide for the treatment of melanoma and brain glioma. Gadolinium neutron-capture therapy (Gd-NCT) is a potential cancer therapy using the γ-rays and auger electrons emitted from the ^{157}Gd (n,γ) ^{158}Gd reaction to kill tumor cells. Gd-NCT is generally considered to be advantageous over B-NCT due to the 66 times larger thermal neutron capture cross section (Martin et al., 1989) and the long range (> 100 μm) of γ-rays released by the Gd after neutron irradiation (Brugger and Shih, 1989).

One of the key factors for the success in Gd-NCT is to deliver and maintain a sufficient amount of Gd in tumor tissues during the neutron irradiation (Shikata et al., 2002). The optimal ^{157}Gd concentration in tumors for Gd-NCT was reported to be 50 to 200 μg/g tumor tissues (Shih and Brugger, 1992). Many drug delivery systems, such as calcium carbonate microparticles (Miyamoto et al., 1997), lecithin microcapsules (Jono et al., 1999), lipid emulsions (Miyamoto et al., 1999), gadopentetic acid-chitosan complexed nanoparticles (Tokumitsu et al., 1999), chitosan nanoparticles (Shikata et al., 2002), and lipid or emulsifying wax-based solid nanoparticles (Oyewumi and Mumper, 2003; Oyewumi et al., 2004; Watanabe et al., 2002), have been prepared to enhance the delivery and retention of Gd in tumors. In order to deliver a sufficient amount of Gd into tumors, several of these Gd-systems were directly injected into tumors. However, direct intratumor injection is not practical for tumors that may not be easily located and injected.

Ideally, Gd should be injected intravenously (i.v.), and then, allowed to accumulate into tumors. To achieve this, an appropriate delivery system is needed. An optimal Gd-delivery system should at first contain a large amount of Gd so that more Gd could be delivered into tumors. Some Gd-delivery systems that carried a high concentration of Gd were prepared in earlier studies. These included the Gd-chitosan nanoparticles (430 nm) containing 9.3% (w/w) of Gd (Tokumitsu et al., 1999), the distearylamide gadopentetic acid microcapsules (106-149 μm) containing 5.13% (w/w) of Gd (Jono et al., 1999), the gadolinium hexanedione (GdH) nanoparticles containing 2.5 mg/mL of GdH (Oyewumi and Mumper, 2002), and the Gd-incorporated lipid-nanoemulsions (100 nm) containing 3 mg/mL of Gd (Watanabe et al., 2002). Secondly, the release of Gd from the delivery system should be slow and limited, which will allow the Gd to remain inside the delivery system prior to reaching tumors. A slow and limited release should also slow down the diffusion of the Gd out of the tumors before and during the neutron irradiation. Another key requirement for an ideal Gd delivery system is that its particle size should be less than 150 nm in order to efficiently target tumors (Desai et al., 1997; Hobbs et al., 1998; Wu et al., 1993). Small size particles (about 100 nm) were reported to be ideal to avoid the uptake by liver macrophages and the reticuloendothelial system (RES) (Harashima et al., 1995; Litzinger et al., 1994) and to deliver molecules to specific tissues of interest (Kreuter, 1995). Finally, having a prolonged circulation time in blood is also critical because it has been shown that there was a strong correlation between the residence time of a

drug delivery system in the blood and its uptake by implanted tumors in mice (Gabizon and Papahadjopoulos, 1988). It was reasoned that drug delivery systems have extravasations in tumors due to the passive convective transport through the leaky endothelium of tumors (Gabizon, 2001). A longer blood circulation time is associated with repeated passages of a high concentration of the delivery system through the tumor microvascular bed, and thus, a greater efficiency of extravasations per unit volume of convective transport. Coating of particles with polyethylene glycol (PEG) has been shown to have a pronounced effect on the distribution the particle in that it can lead to a prolongation of the circulation time of the particles in blood, a decrease in uptake of the particles by liver and spleen, and a corresponding increased accumulation of the particles in implanted tumors (Gabizon et al., 1990). It was believed that PEG reduced the coating (opsonisation) of delivery systems by plasma protein, and thus, enabled them to escape recognitions by liver and spleen (Allen, 1994).

Our strategy is to utilize liposomes as a delivery system to deliver Gd into tumors. Liposomes have been studied for decades as a drug delivery system. They theoretically fulfill the key requirements to retain, target, and release drugs and have been evaluated clinically for drug delivery in a variety of diseases (Cagnoni, 2002; Muggia and Hamilton, 2001; Sparano and Winer, 2001). The unique characteristic of liposomes lies in their membrane structure composed of double phospholipid layers similar to biological membranes. They can encapsulate a large variety of both hydrophilic and hydrophobic compounds without the use of

surfactants or other emulsifiers and can be introduced into the body without triggering immune rejection reactions. In fact, there are liposomally delivered drugs currently available on the market (e.g., Daunoxome® and Doxil®) (Massing and Fuxius, 2000). Gd-DTPA, a nontoxic, hydrophilic, and stable chemical commonly used as a magnetic resonance imaging (MRI) diagnostic agent, which can potentially be useful for assessing tumors or metastases (Unger et al., 1990), was used as the source of Gd. The utilization of this MRI diagnostic agent promises the potential of coordinating MRI diagnosis with Gd-NCT using a single functional Gd compound in the future.

Our objective in this study was to design a long-circulating, small (100 nm) liposome preparation that encapsulates a high concentration of, but slowly releasing, Gd. Moreover, the biodistributions of the encapsulated Gd in both healthy and model tumor-bearing mice were also evaluated.

2.3 Materials and Methods

2.3.1 Materials

Magnevist® was from Berlex Laboratories (Wayre, NJ). Soy phosphatidylcholine (Soy PC), soy hydrogenated phosphatidylcholine (Soy HPC), 1,2-distearoyl-sn-glycero-3-phosphocholine (DSPC), and 1,2-distearoyl-sn-glycero-3-phosphoethanolamine-N-[methoxy (polyethylene glycol)-2000] (PEG 2000) were purchased from Avanti Polar Lipids, Inc (Alabaster, AL). Cholesterol (Chol), diethylenetriaminepentaacetic acid (Gd-DTPA), poly-L-lysine (pLL, MW 5,600), Sephadex-G75, and phosphate buffered saline (PBS, pH 7.4) were

purchased from Sigma-Aldrich (St. Louis, MO). Cellulose dialysis tubes (MWC 10,000 and 50,000) were from Spectrum Chemicals & Laboratory Products (New Brunswick, NJ).

2.3.2 Methods

2.3.2.1 Preparation of liposomes

Liposomes were prepared by the thin film hydration method followed by 6 cycles of freeze-thaw. Briefly, a thin film of phospholipids and cholesterol with PEG 2000 (10% molar ratio of the phospholipid) was formed in the bottom of a glass tube by chloroform evaporation. The lipid thin film was suspended in a Gd-DTPA aqueous solution or the aqueous solution of Gd-DTPA-pLL complex (Gd-DTPA:pLL = 1:0.25, w/w) by vigorous mixing at room temperature. For some preparations, the liposome was frozen and thawed for 6 cycles, sonicated for 5-6 min. One hundred nm-range liposomes were prepared by extruding the preparation 11 times sequentially through 1000, 400, and then 100 nm-polycarbonate membranes (Avanti Polar Lipids). Unencapsulated Gd-DTPA was removed by gel permeation chromatography using a Sephadex G-75 column or by dialyzing against 0.9% NaCl solution through a cellulose dialysis membrane (MWC 50,000) for at least 15 hours.

2.3.2.2 Gel Permeation Chromatography (GPC)

The unencapsulated Gd-DTPA was removed by GPC. One hundred μL of liposomes were eluted with water through a Sephadex-G75 column (6 mm x 30

cm). Each elution fraction of 1 mL was collected, and the amount of Gd in each elution fraction was measured using an Inductively Coupled Plasma Optical Emission Spectrometer (ICP-OES, Teledyne Leeman Labs, Hudson, NH) at 342.247 nm. Based on the turbidity (OD655) of each elution fraction, liposomes were determined to be mainly in the third 1-mL fraction, which was the most turbid fraction.

The encapsulation efficiency of Gd in liposomes was calculated as following: Encapsulation efficiency (%) = [Gd encapsulated/(Gd encapsulated + Gd unencapsulated)] x 100.

2.3.2.3 Dialysis

Gd-encapsulated liposomes were dialyzed against 4 L of physiological NaCl solution (0.9%, w/v) through a cellulose dialysis membrane (MWC 50,000) at room temperature for at least 15 hours.

2.3.2.4 *In vitro* release of Gd-DTPA from liposomes

GPC-purified, Gd-DTPA-encapsulated liposomes (100 μg of pure Gd) were dispersed into PBS (10 mM, pH 7.4) and placed into a 1-mL cellulose ester dialysis tube. The tube was then placed into 12 mL of PBS (10 mM, pH 7.4) and incubated in a 37 ± 2^{o}C shaker incubator. At predetermined time points, the dialysis tube was taken out and re-placed into another 12 mL of fresh medium. The amount of Gd in the release medium was determined using ICP-OES.

In order to evaluate the feasibility of using the dialysis tube to measure the release of Gd-DTPA, the diffusion of pure Gd-DTPA through the membrane of the tube in PBS (10 mM, pH 7.4) was also measured.

Moreover, the release of Gd from liposomes in PBS buffer (10 mM, pH 7.4) containing fetal bovine serum (FBS, Invitrogen, Carlsbad, CA) was also measured using the same procedure as mentioned above, except that the PBS medium was replaced by FBS in PBS (FBS/PBS, 10%, v/v).

2.3.2.5 Biodistribution

The biodistribution of Gd-DTPA-encapsulated liposomes was carried out in 6-8-week-old female Balb/C mice or model tumor-bearing C57BL/6 mice (Charles River Laboratories, Wilmington, MA). All experiments were completed following the National Institutes of Health guidelines for care and use of laboratory animals. To evaluate the distribution of Gd encapsulated into liposomes in healthy, tumor-free mice, Balb/C mice were injected (i.v.) with a dose of liposomes equivalent to 20 mg Gd per kg body weight, and euthanized 6, 10 or 24 hours later after the injection. The blood, liver, spleen, heart, lung, and kidney were collected, desiccated at 60^{o}C overnight, and then incinerated with nitric acid (6.6 N) at 60^{o}C for 15 hours. The samples were filtrated through a 0.45 μm filter. Gd concentration was determined using ICP-OES. To estimate the concentration of Gd in blood, the total blood volume of a mouse was assumed to be 7.5% (v/w) of its total body weight (Davies and Morris, 1993; Mosqueira et al., 2001).

The distribution of Gd in tumor-bearing mice was evaluated similarly. The tumor cells used were the TC-1 tumor cell line, which was engineered by Dr. T. C. Wu at the Johns Hopkins University (Baltimore, MD) from C57BL/6 mouse lung endothelial cells. Cells were grown in Roswell Park Memorial Institute (RPMI) 1640 medium (Invitrogen) supplemented with 10% FBS (Invitrogen), 100 U/mL of penicillin (Sigma), and 100 μg/mL of streptomycin (Sigma) and cultured at 37°C in a humidified incubator containing 5% CO_2. Mice (n = 7) were subcutaneously implanted with TC-1 cells (5 x 10^5/mouse) on day 0. The tumors reached around 4-7 mm in diameter in about 10 days. On day 10, the mice were injected via the tail vein with Gd-DTPA encapsulated in one of the liposome formulations (formulation VI). The total Gd amount injected with 414 μg pure Gd/mouse (~20 mg Gd/kg body weight). As a control, TC-1 tumor-bearing mice (n = 4) were also injected via the tail vein with Gd-DTPA dissolved in PBS (10 mM, pH 7.4). Twelve hours later, mice were euthanized; organs and tissues were harvested; Gd content in them was measured.

2.3.2.6 Statistical analysis

The student t-test assuming equal variances was used if two groups were to be compared. If more than two groups were involved, the one way analysis of variance (ANOVA), followed by pair-wise comparisons with Fisher's protected least significant difference (PLSD) procedure, was used. A p value of ≤ 0.05 (two-tail) was considered to be statistically significant.

2.4 Results and Discussions

2.4.1 *In vitro* release of Gd-DTPA from liposomes

In order to deposit a large amount of Gd into tumors, the encapsulated Gd should not significantly leak out from the liposomes. In addition, a slow and limited release may keep the Gd that are delivered into tumors remaining inside the tumors prior to the neutron irradiation (Hobbs et al., 1998). Due to the high water solubility of Gd-DTPA, we expect that the release of Gd-DTPA from liposomes will be very rapid and extensive. It has been reported that the covalent conjugate of Gd-DTPA and pLL substantially slowed down the blood clearance of Gd-DTPA (Vexler et al., 1994). Moreover, Gd-DTPA and pLL conjugate has been used to enhance tissue signals in MRI (Bock et al., 1997; Curtet et al., 1998; Su et al., 1998; Uzgiris, 2004). However, the effect of complexing pLL with Gd-DTPA on the release of Gd-DTPA from liposomes has not been evaluated. We hypothesized that complexation of Gd-DTPA with pLL will decrease the release of Gd-DTPA from liposomes because the Gd-DTPA/pLL complex has a relatively larger molecular size than Gd-DTPA alone. To test this hypothesis, four liposome formulations (Soy PC:Chol = 3:2, molar ratio) with or without PEG 2000 (10%, m/m) coating were prepared using the thin film hydration method without multiple freeze-thaw cycles. The liposomes were: (I) liposome encapsulated with Gd-DTPA (LP-Gd-DTPA); (II) liposome encapsulated with Gd-DTPA complexed with pLL (LP-Gd-DTPA-pLL); (III) PEG-coated liposome encapsulated with Gd-

DTPA (PEG-LP-Gd-DTPA); and (IV) PEG-coated liposome encapsulated with Gd-DTPA complexed with pLL (PEG-LP-Gd-DTPA-pLL).

We have found that complexation of Gd-DTPA with pLL enhanced the encapsulation efficiency of the Gd-DTPA in liposomes and that a Gd-DTPA: pLL ratio of 1:0.25 (w/w) led to the highest Gd-DTPA encapsulation efficiency. Further increasing the amount of pLL did not lead a significantly higher Gd-DTPA encapsulation. Thus, this ratio was chosen to complex Gd-DTPA with pLL in further studies.

Data from Figure 2.1A clearly supported our hypothesis. The release of Gd-DTPA from formulation I (LP-Gd-DTPA) was very fast, with approximately 30% being released within 4 hours. Complexation of Gd-DTPA with pLL (formulation II) significantly slowed down the release. Only about 5% of Gd-DTPA was released within the same period of time (4 h). Interestingly, coating of PEG on the surface of the liposomes also helped to reduce the release of Gd-DTPA from the liposomes (Figure 2.1A, formulation III). It is possible that the saturated phospholipids (DSPE), to which the PEG molecule was attached, helped to enhance the rigidity of liposome membrane, and thus, decreased the leakage of the Gd-DTPA from the liposomes. The release of Gd-DTPA from formulation IV was the slowest. Only less than 4% of Gd-DTPA was released within 22 hours, demonstrated the existence of a synergistic effect by complexing Gd-DTPA with pLL and coating the liposomes with PEG 2000.

In order to simulate the release of Gd-DTPA from liposomes in a more biologically relevant medium, the release of the Gd-DTPA was also evaluated in FBS/PBS (10%, v/v). Because formulation IV had the lowest release rate, the release of Gd-DTPA from it was measured. The release of Gd-DTPA was slightly slower in the FBS/PBS medium than in the PBS (Fig. 2.1B), promising a slow and limited release *in vivo*.

In this release study, we have placed the Gd-DTPA-encapsulated liposomes in a cellulose membrane dialysis tube to prevent the liposomes from entering the release medium. Data in Figure 2.1A also showed that the cellulose dialysis membrane was feasible for studying the release of Gd-DTPA from the liposomes because the rate for the diffusion of pure Gd-DTPA through the dialysis membrane was much greater than that for the release of Gd-DTPA from any of liposome formulations. Pure Gd-DTPA has a molecular weight of 547.58. It diffused through the dialysis membrane (MWC 10,000 Daltons) very rapidly. In fact, nearly all of the free Gd-DTPA (99%) was diffused out of the dialysis membrane within 30 minutes.

2.4.2 Optimization of the Gd-encapsulated liposome formulation

A key factor for the success of Gd-NCT is to develop a delivery system that can efficiently deliver and retain a sufficient amount of Gd into tumors prior to the neutron irradiation. Although the release of Gd-DTPA for formulation IV was slow and limited, in a preliminary biodistribution study, we found that this

formulation IV (Soy PC:Chol:PEG = 60:40:6, molar ratio) was quickly cleared from the blood when injected (i.v.) into mice. Only about 14% of injected dose was recovered in the blood 4 hours after the injection. It was believed that the low level of Chol and the use of Soy PC, an unsaturated phospholipid with a low transition temperature (less than 37^{o}C), were responsible for the short blood circulation time. In order to prolong the circulation time of Gd in blood, saturated phospholipids with a high transition temperature, such as Soy HPC and DSPC, were combined with a higher concentration of Chol to increase the rigidity of the membrane of the liposomes. Three different liposome formulations were prepared with PC, Chol, and PEG 2000 at a molar ratio of 50:35:5 and an aqueous solution of Gd-DTPA (10%, w/v) complexed with pLL (Gd-DTPA:pLL = 1:0.25, w/w). They were formulation V, liposomes prepared with Soy PC as phospholipid (LP-Soy PC); formulation VI, liposomes prepared with Soy HPC (LP-Soy HPC); and formulation VII, liposomes prepared with DSPC (LP-DSPC).

Figure 2.2 shows the GPC profiles of these three liposome formulations. The encapsulation efficiencies of Gd-DTPA in formulations V, VI, and VII were presented in Table 2.1. Formulation VI had the highest encapsulation efficiency, and thus, the highest amount of Gd-DTPA encapsulated, with an estimated encapsulated Gd-DTPA concentration of 23.6 ± 1.1 mg/mL, which corresponded to 6.8 ± 0.3 mg/mL of pure Gd. Although there were reports of Gd-delivery systems with a higher Gd concentration in earlier studies (Jono et al., 1999; Tokumitsu et al., 1999), the previously reported systems were either too big (i.e.,

the 100-μm particles) (Jono et al., 1999) or may not be stable in a biological medium (i.e., chitosan-gadopentetic acid complex, 400 nm) (Tokumitsu et al., 1999), and thus, may only be suitable for direct intratumoral injection. Torchilin (2000) and Weissig et al. (2000) prepared a liposome encapsulated with 31% (w/w) of Gd for MRI (Torchilin, 2000; Weissig et al., 2000). However, the concentration was expressed in term of the weight of Gd over the weight of the Gd-liposomes, and the solubility of the Gd-liposomes was not reported. To our knowledge, the value of 6.8 ± 0.3 mg/mL represents a high amount of pure Gd that had been encapsulated into a Gd delivery system with small particle size (< 150 nm) (Devoisselle et al., 1988; Grunder et al., 1998; McDannold et al., 2004; Oyewumi and Mumper, 2002; Tilcock et al., 1991; Unger et al., 1990; Watanabe et al., 2002). As predicted, the release of Gd-DTPA from these three formulations was also very slow and limited (Table 2.1). These liposomes, with small size, high concentration of Gd, and low Gd release rate, were expected to be a suitable delivery system for targeting Gd into tumors.

Although GPC efficiently removed free Gd-DTPA from liposomes, Gd-DTPA was significantly diluted after this step. Thus, the liposomes were dialyzed against physiological NaCl solution for at least 15 hours to remove free Gd-DTPA. As shown in Figure 2.3, almost all of the unencapsulated Gd-DTPA was removed using this dialysis procedure.

2.4.3 Biodistribution of Gd-DTPA-encapsulated liposomes in mice

The distribution of Gd in healthy, tumor-free mice was initially determined 6 hours after i.v injection. As shown in Figure 2.4, increasing the ratio of Chol in the liposome (i.e. from Soy PC:Chol = 3:2 to 50:35, molar ratio) significantly enhanced the blood circulation time of Gd. For formulation V (Soy PC:Chol = 50:35), about 40% of the Gd injected was still in the blood 6 hours after the injection, compared to only 14% for formulation IV (Soy PC:Chol = 3:2) 4 hours after the injection (Fig. 2.4). Furthermore, liposomes prepared with saturated phospholipids with a high transition temperature, such as Soy HPC and DSPC, had a longer blood circulation time when compared to liposomes prepared with unsaturated Soy PC (Fig. 2.4). Also, it needs to be pointed out that, when pure Gd-DTPA alone (Magnevist) was dosed similarly, it was quickly cleared, with only a recovery rate of 0.58 ± 0.15% 6 hours after the injection. Because the percent of Gd remained in the blood for formulation VI (LP-Soy HPC) tended to be slightly higher than that for formulation VII (LP-DSPC), and formulation VI encapsulated a higher amount of Gd, it was used to further evaluate its blood circulation and biodistribution in tumor-free and tumor-bearing mice.

Figure 2.5 shows the percent of Gd recovered in the blood, liver, and spleen of tumor-free mice 6, 10 and 24 hours after the i.v injection of formulation VI. The percent of Gd remained in the blood was 71 ± 20%, 63 ± 7%, and 42 ± 5% (mean ± S.D.) of the total injected Gd dose 6, 10, and 24 hours after the injection, respectively. The half-life of the Gd in the blood was calculated to be 24 hours,

higher than the 19-hour blood half-life for a previously reported Gd-liposome formulation composed of the gadopentetate dimeglumine lipid and ditricosadiynoyl tricosadinynayl phosphatidylcholine in rats (Storrs et al., 1995). This value was also in sharp contrast to the blood $t_{1/2}$ of other previously reported Gd-liposome preparations, which ranged from 2 h (Bertini et al., 2004) to 4 h (Unger et al., 1990) to complete clearance within 12 hours (Tilcock et al., 1989). Finally, the uptake of the Gd by the liver increased from 10% (at 6 h) to 19% (at 24 h) of the injected dose. Similarly, the uptake by the spleen was also increased from 3% (at 6 h) to 8% (at 24 h) of the injected dose, clearly showing the uptake by the RES was limited.

With its long blood half-life in mice, we expected that a sufficient amount of Gd will be delivered into tumors using our formulation VI for Gd-NCT. As shown in Table 2.2, an average of 158.8 ± 115.6 μg of Gd per gram of tumor tissue was accumulated into the tumor tissues 12 hours after the Gd-encapsulated liposome formulation VI was injected into tumor-bearing mice via the tail vein. Of the seven mice evaluated, only one had a Gd content of less than 50 μg/g tumor tissues (34.7 μg/g). The large variation in the tumor uptake may be caused by the variation in tumor size (Harrington et al., 2000). In contrast, the Gd recovered in tumors when a Gd-DTPA solution was injected (i.v.) into similar TC-1 tumor-bearing mice was only 1.43 ± 0.14 μg of Gd/g of tumors, which was about 260-fold less than when the Gd-DTPA-encapsulated liposomes were injected. As mentioned earlier, the optimal Gd concentration in tumors for a successful Gd-

NCT was estimated to be 50 to 200 μg/g tumor tissue (Shih and Brugger, 1992). More Gd is expected to be delivered to tumors if more formulation VI is dosed by multiple injections. The tumor uptake of Gd may also be enhanced by coupling appropriate monoclonal antibodies onto the surface of liposomes to further target tumors (Blanco et al., 2005; Desormeaux and Bergeron, 2005; Laginha et al., 2005). Therefore, it is believed that this Gd encapsulated liposome formulation VI can be used to deliver a sufficient amount of Gd in tumors for Gd-NCT. Of course, a ^{157}Gd-enriched Gd compound has to be used when performing NCT because natural Gd only contains 15.56% of ^{157}Gd. Finally, it needs to be mentioned that, in the tumor-bearing mice, the uptake of the Gd by the liver and the spleen after the Gd-encapsulated liposomes were injected tended to be high, although it was unlikely to be caused by the species of the mice or the tumor per se. Nevertheless, this RES uptake may be further decreased in future studies by decreasing the size of the liposomes, by increasing the content of the PEG 2000 in the liposomes, or by using PEG with a longer chain, such as the PEG 7000 (Drummond et al., 1999).

Another advantage for our Gd-liposome is its potential application in MRI. The MRI technique has been used to examine brain and other parts of the central nervous system, blood vessel, and tumors. In MRI, contrast agents increase the difference in the intensity of signals from tissues with and without them. Gd-DTPA-encapsulated liposomes had been shown to be effective for MRI due to its high relaxavity (Curtet et al., 1998; Torchilin, 2000; Weissig et al., 2000). Therefore, our Gd-DTPA-pLL-encapsulated liposome preparation has the potential

for integrating MRI diagnosis and Gd-NCT, which is advantageous over some previously reported Gd-delivery systems utilizing hydrophobic Gd-compounds, such as distearylamide of gadopentetic acid (Jono et al., 1999), gadolinium hexanedione (Oyewumi and Mumper, 2002), and gadolinium acetylacetonate (Dierling et al., 2005), as the source of Gd.

In conclusion, we prepared a Gd-DTPA-encapsulated liposome formulation that had 6.8 ± 0.3 mg/mL of pure Gd encapsulated in the liposomes. The complexation of Gd-DTPA with pLL significantly slowed down the release of Gd-DTPA from the liposomes. This encapsulated Gd-DTPA had a half-life of about 24 hours in mouse blood. Moreover, an average of 158.8 ± 115.6 of Gd per gram of tumor tissues was delivered into tumors 12 hours after the Gd-encapsulated liposomes were injected (i.v.) into mice pre-implanted with model tumors. This Gd-encapsulated liposome formulation is expected to be promising for delivering Gd into tumors for future Gd-NCT and/or MRI.

Table 2.1 The encapsulation efficiency and release of Gd-DTPA from liposome formulations V, VI, and VII.

	Phospholipids		
	Soy PC	**Soy HPC**	**DSPC**
Encapsulation efficiency (%)	19.2 ± 0.6	25.7 ± 1.4 *	21.0 ± 0.3
% release	1.83 ± 0.57	1.13 ± 0.05	1.14 ± 0.15

The encapsulation efficiency of Gd-DTPA and the percent of Gd-DTPA released from liposomes (Phospholipid:Chol:PEG = 50:35:5, m/m/m, Gd-DTPA:pLL = 1:0.25, w/w) after 24 h of incubation at 37^{o}C in PBS were determined. Data reported are mean ± S.D. (n = 3).

* indicates that the encapsulation efficiency for Soy HPC was significantly higher than those for Soy PC ($p = 0.002$) and DSPC ($p = 0.005$). The releases of Gd-DTPA from those three liposome formulations were comparable.

Table 2.2 Biodistribution of Gd encapsulated into liposome formulation VI in tumor tissues and other organs of model tumor-bearing mice.

	Pure Gd content (Injected dose, 414 μg Gd)
Tumor (μg/g tissue)*	158.8 ± 115.6 (34.7-365.6)
Blood (% injected Gd)	57.8 ± 11.6 (%)
Liver (μg/g)	121 ± 7.0
Spleen (μg/g)	577 ± 81.8
Heart (μg/g)	44.7 ± 3.1
Lung (μg/g)	74.2 ± 3.3
Kidney (μg/g)	31.6 ± 1.6

C57BL/6 mice (n = 7) were implanted with TC-1 tumor cells (5 x 10^5) on day 0. Ten days later, mice were injected (i.v.) with Gd encapsulated in liposome formulation VI (~20 mg Gd/Kg body weight). Mice were euthanized 12 h after the injection; their tumor, blood, liver, spleen, heart, lung, and kidney were harvested. Gd content in them was determined using ICP-OES. Data shown are mean ± S.D. (n = 7). The Gd content in the blood was reported as the % of total injected Gd that remained in the blood. The Gd contents in other tissues and organs were reported as final pure Gd amount (μg) per gram of wet tissue. * The range of Gd content in tumors was shown in parenthesis. Only one out of seven mice had a Gd content of less than 50 μg/g tumor tissue in its tumor.

(A)

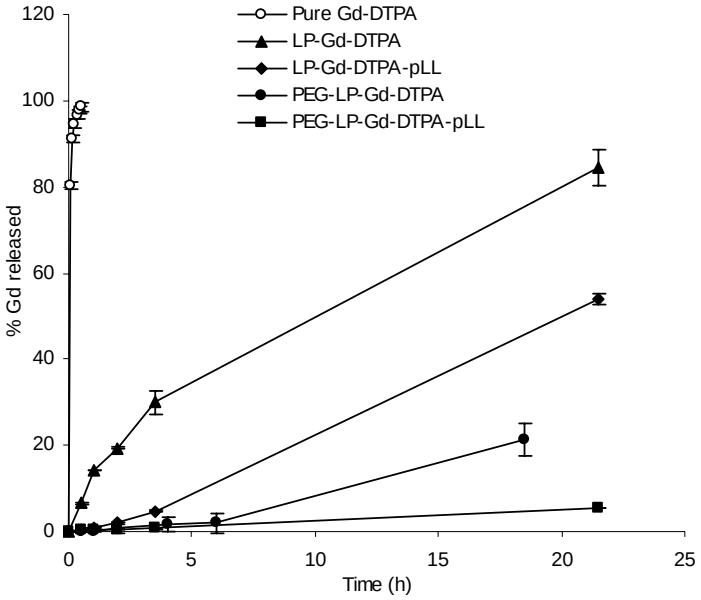
Pure Gd-DTPA
LP-Gd-DTPA
LP-Gd-DTPA-pLL
PEG-LP-Gd-DTPA
PEG-LP-Gd-DTPA-pLL
% Gd released
Time (h)
0
20
40
60
80
100
120
0
5
10
15
20
25

(B)

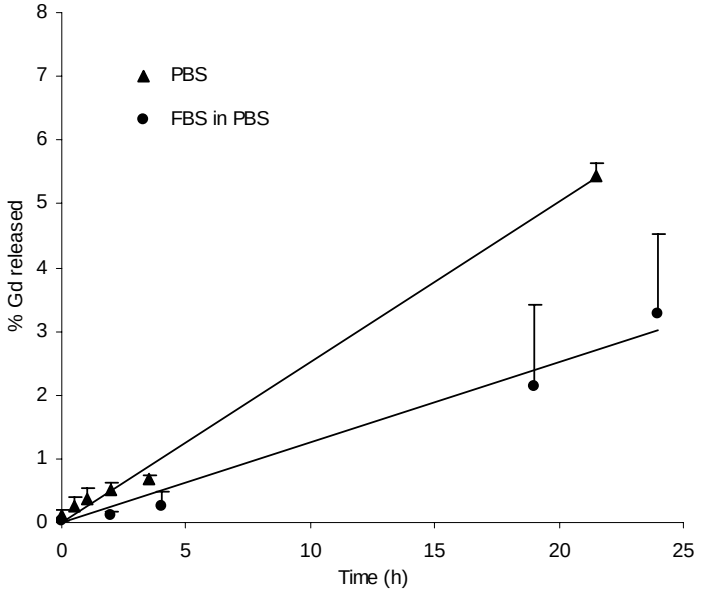
PBS
FBS in PBS
% Gd released
Time (h)
0
1
2
3
4
5
6
7
8
0
5
10
15
20
25

Figure 2.1

Figure 2.1 The release of Gd-DTPA from liposomes. (**A).** The diffusion of Gd-DTPA through the dialysis membrane and the release of Gd-DTPA from liposome formulation I through IV were determined at 37^{o}C in PBS medium. Pure Gd-DTPA solution or GPC-purified, Gd-DTPA-encapsulated liposomes, each containing 100 µg of pure Gd, was placed into a cellulose ester dialysis tube (MWC 10,000). The dialysis tube was placed into 12 mL of PBS (pH 7.4, 10 mM). The amount of Gd released was determined using ICP-OES at 342.247 nm. Data shown are mean ± S.D. (n = 3). The liposomes were comprised of soy PC and Chol at a molar ratio of 3:2. Formulation I: LP-Gd-DTPA: liposome encapsulated with Gd-DTPA. Formulation II: LP-Gd-DTPA-pLL: liposome encapsulated with Gd-DTPA-pLL. Formulation III: PEG-LP-Gd-DTPA: PEG-coated-liposome encapsulated with Gd-DTPA. Formulation IV: PEG-LP-Gd-DTPA-pLL: PEG-coated liposome encapsulated with Gd-DTPA-pLL. (**B).** The release of Gd-DTPA from liposome formulation IV in PBS or FBS/PBS (10%, v/v) medium.

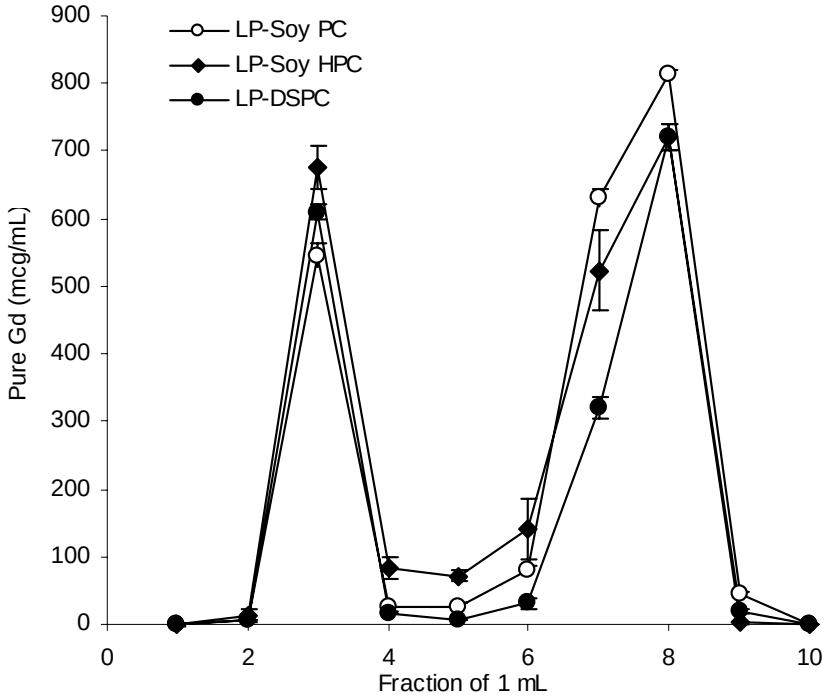

Figure 2.2 The separation of the unencapsulated Gd-DTPA from Gd-DTPA-encapsulated liposomes by gel permeation chromatography (GPC). Pegulated liposomes prepared with different PCs (soy PC, Soy HPC, and DSPC) and PEG 2000 (PC:Chol:PEG 2000 = 50:35:5, molar ratio, Gd-DTPA:pLL = 1:0.25, w/w) were applied into a sephadex G75 column (diameter = 0.6 cm, length = 30 cm) and eluted with de-ionized water. The concentration of Gd in each elution fraction of 1 mL was measured using ICP-OES at 342.247 nm. Data reported are mean ± S.D. (n = 3). Formulation V: LP-Soy PC: liposome prepared with Soy PC as phospholipid. Formulation VI: LP-Soy HPC: liposome prepared with Soy HPC as phospholipid. Formulation VII: LP-DSPC: liposome prepared with DSPC as phospholipid.

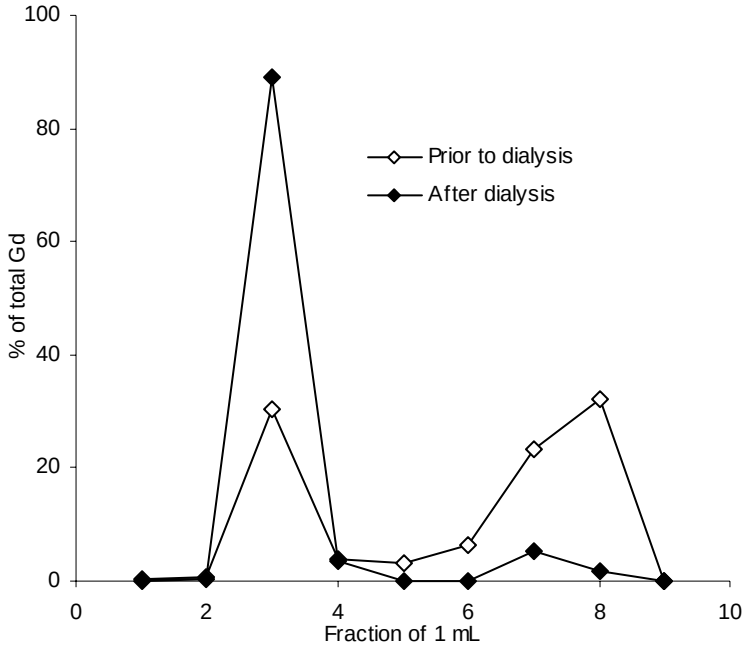

Figure 2.3 The GPC profiles of Gd-DTPA-pLL-encapsulated liposomes prior to and after dialysis. One hundred μL of Gd-DTPA-pLL-encapsulated liposomes (Soy HPC:Chol:PEG = 50:35:5, molar ratio; Gd-DTPA:pLL = 1:0.25, w/w) was applied into a sephadex G75 column (diameter = 0.6 cm, length = 30 cm) and eluted with de-ionized water. The Gd concentration in each 1 mL of elution fraction was measured using ICP-OES at 342.247 nm. Data shown were the percent of the total Gd that were applied into the column in every 1 mL fraction. Prior to dialysis: Freshly prepared liposome formulation VI was applied directly to a GPC column. After dialysis: Formulation VI was dialyzed against NaCl (0.9%, w/v) for 15 h at room temperature and then applied to the same GPC column.

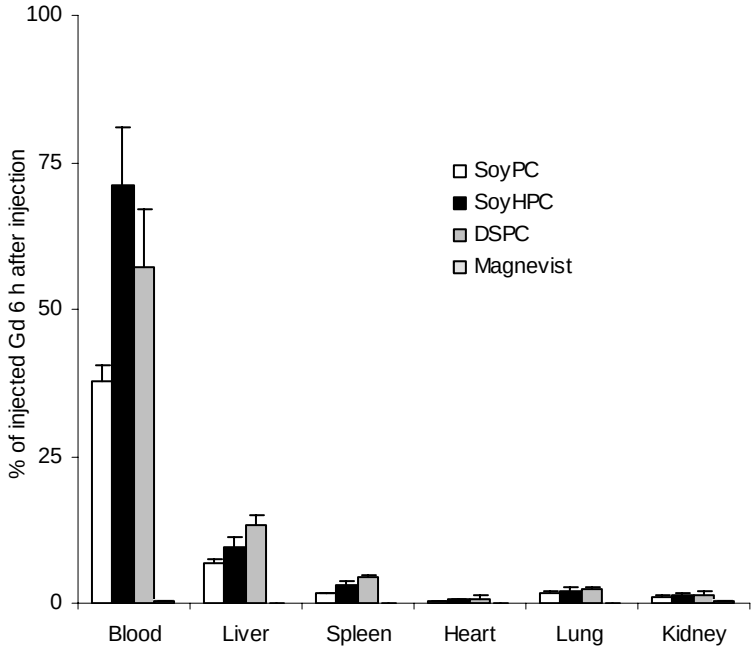

Figure 2.4 The biodistribution of Gd-DTPA encapsulated into liposomes in healthy mice. Balb/C mice (n = 5) were injected via the tail vein with a single dose (20 mg of pure Gd/kg of body weight) of Magnevist® solution or Gd-DTPA-pLL-encapsulated liposomes. Six hours after the injection, mice were sacrificed, and their blood, liver, spleen, heart, lung, and kidney were harvested. The concentration of Gd in them was determined using ICP-OES at 342.247 nm. Data shown are mean ± S.E.M. (n = 5). Formulation V: LP-Soy PC: liposome prepared with Soy PC as phospholipid. Formulation VI: LP-Soy HPC: liposome prepared with Soy HPC as phospholipid. Formulation VII: LP-DSPC: liposome prepared with DSPC as phospholipid. The concentrations of Gd in the blood for formulations VI and VII were comparable, but significantly higher than that for formulation V ($p = 0.006$ and $p = 0.04$, respectively). ANOVA analyses revealed that there were significant differences among the concentrations of Gd in the liver ($p < 0.0001$) and the spleen ($p < 0.00001$) of mice injected with formulations V, VI, and VII.

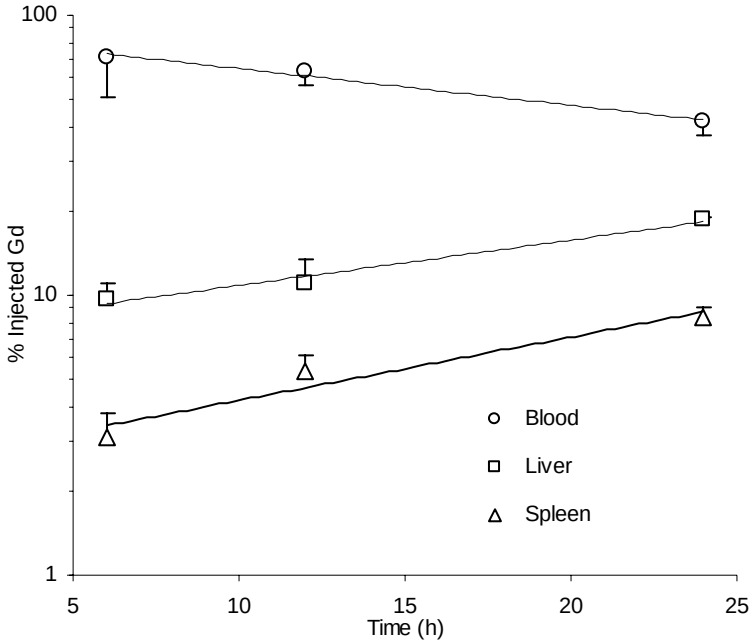

Figure 2.5 The distribution kinetics of Gd encapsulated into liposome formulation VI in healthy mice. Balb/C mice were injected via the tail vein with a single dose (20 mg of pure Gd/kg of body weight) of liposome formulation VI. Six, 10, and 24 hours after the injection, mice (n = 5) were sacrificed, and their blood, liver, and spleen were harvested. The concentration of Gd in them was determined using ICP-OES. Data shown are mean ± S.E.M. (n = 5).

Chapter 3

BIODISTRIBUTION AND TUMOR-ACCUMULATION OF GADOLINIUM (Gd) ENCAPSULATED IN LONG-CIRCULATING LIPOSOMES IN TUMOR-BEARING MICE FOR POTENTIAL NEUTRON CAPTURE THERAPY

Uyen M. Le and Zhengrong Cui

International Journal of Pharmaceutics, 2006; 320(1-2): 96-103.

3.1 Abstract

To deliver and maintain a sufficient amount of Gd into tumors is required for a successful Gd neutron capture therapy (Gd-NCT), but it has been proven to be rather challenging to achieve. Previously, we have reported a Gd-encapsulated liposome formulation that has the potential to overcome this challenge. In the present study, we sought to systemically evaluate the biodistribution and the tumor-accumulation of the Gd in model tumor-bearing mice. The Gd-encapsulated liposomes were injected into mice pre-grafted with two different model tumors. The Gd content in the tumors and other organs were determined at various time after the injection. A sufficient amount of Gd was readily delivered into two different model tumors. Increasing the dose of Gd by injecting the Gd-encapsulated liposomes multiple times tended to increase the uptake of the Gd by the tumors. Finally, the uptake of Gd by tumors was inversely correlated with the size of the tumors. The Gd-encapsulated liposomes hold great potential as a Gd delivery system for NCT of small- and medium-size tumors. Alternative strategies may have to be adopted in order to use NCT to treat large, advanced solid tumors, although for which, Gd-NCT might be advantageous over boron-NCT.

3.2 Introduction

NCT is a cancer therapeutic modality with promising potentials. In NCT, stable, non-radioactive nuclides are delivered into the target tumors. Upon irradiation by thermal or epithermal neutrons, the nuclides then produce localized cytotoxic radiations (Barth and Soloway, 1994b; Carlsson et al., 2002a). Earlier

studies were mainly focused on using boron-10 (^{10}B) as the nuclide for the treatment of melanoma and brain glioma (Barth et al., 2005). Gd-NCT is a new NCT approach using the γ-rays and auger electrons emitted from the ^{157}Gd (n,γ) ^{158}Gd reaction to kill tumor cells (Shih and Brugger, 1992b). Gd-NCT is generally considered to be advantageous over B-NCT due to the 66 times larger thermal neutron capture cross-section of the Gd nuclide (Martin et al., 1989) and the longer range (> 100 μm) of the γ-rays released by the Gd after a neutron irradiation (Brugger and Shih, 1989a). The γ-rays are expected to kill tumor cells even when the Gd is outside the tumor cells, which eliminates the requirement for the delivery of the Gd into tumor cells (De Stasio et al., 2001; Hofmann et al., 1999a). In addition, because many Gd compounds, such as the Gd-DTPA (diethylenetriaminepentaacetic acid), are used clinically as a contrast agent in magnetic resonance imaging (MRI) (Caravan et al., 1999), using Gd as the nuclide provides an opportunity to integrate MRI diagnosis with NCT.

One of the key criteria for the Gd-NCT to be successful is to deliver and maintain a sufficient amount of Gd into tumors during the neutron irradiation (Shikata et al., 2002). The optimal Gd concentration in tumors for Gd-NCT was estimated to be 50 to 200 μg/g wet tumor tissues (Shih and Brugger, 1992b), which had proven to be rather challenging to achieve, if the Gd compounds are to be injected systemically. Thus, many Gd delivery systems, such as calcium carbonate microparticles (Miyamoto et al., 1997), lecithin microcapsules (Jono et al., 1999a), lipid emulsions (Dierling et al., 2005; Miyamoto et al., 1999),

gadopentetic acid-chitosan complex nanoparticles (Tokumitsu et al., 1999a), chitosan nanoparticles (Shikata et al., 2002), and lipid or emulsifying wax-based solid nanoparticles (Oyewumi and Mumper, 2003; Oyewumi et al., 2004; Watanabe et al., 2002), had been prepared to enhance the delivery and the retention of Gd in tumors. Unfortunately, only a couple of those systems were able deliver the required amount of Gd into tumors when they were intravenously (i.v.) injected into tumor-bearing murine models (Miyamoto et al., 1999). In order to deliver a sufficient amount of Gd into tumors, several of these Gd-systems were directly injected into tumors (Akine et al., 1992; Hofmann et al., 1999a; Khokhlov et al., 1995a; Matsumura et al., 2003; Tokumitsu et al., 2000; Tokumitsu et al., 1999a). However, direct intra-tumor injection is not preferred for tumors that may not be easily located.

Ideally, Gd compounds or delivery systems should be intravenously injected to allow the Gd to spontaneously accumulate into tumors. To achieve this, we have developed a Gd-DTPA-encapsulated, PEGylated liposome formulation that encapsulated as high as 6.8 mg of Gd per mL of liposomes (Le and Cui., 2006a). Due to the PEGylation and the high content of cholesterol in the lipid composition, the liposomes exhibited a prolonged blood circulation time (i.e., the $t_{1/2}$ in mouse blood was > 24 h), which was expected to lead to repeated passages of the Gd-encapsulated liposomes through the tumor microvascular bed, and thus, a greater efficiency of extravasations per unit volume of convective transport time (Gabizon and Papahadjopoulos, 1988; Gabizon, 2001). In addition, because the

Gd-DTPA was complexed with a cationic polymer, poly-L-lysine (pLL), prior to being encapsulated into the liposomes, the "leakage" of Gd from the liposomes was found to be very limited (Le and Cui, 2006a). The pLL could be readily replaced with a USP material protamine sulfate to decrease any potential toxicity from pLL. More importantly, in a preliminary study, we have found that a tumor Gd concentration of more than 100 μg per gram of wet tumor tissues was readily achieved when the Gd-encapsulated liposomes were injected (i.v.) into mice pre-established with a model tumor. These findings warrant further exploration of this Gd-encapsulated liposome formulation for Gd-NCT.

In the present study, we sought (i) to define the distribution and tumor uptake kinetics of the Gd encapsulated into the liposomes in model tumor-bearing mice, (ii) to evaluate the effect of multiple dosing and the type of tumors on the distribution and tumor uptake of Gd, and (iii) to identify the relationship between the size of tumors and the amount of Gd that can accumulate in the tumors. The results from this study have clinically relevant implications.

3.3 Materials and Methods

3.3.1 Materials

Soy hydrogenated phosphatidylcholine (Soy HPC) and 1,2-distearoyl-sn-glycero-3-phosphoethanolamine-N-[methoxy (polyethylene glycol)-2000] (PEG 2000) were purchased from Avanti Polar Lipids, Inc (Alabaster, AL). Cholesterol (Chol), Gd-DTPA, pLL (MW 5,600), sephadex-G75, and phosphate buffered

saline (PBS, pH 7.4) were purchased from Sigma-Aldrich (St. Louis, MO). Cellulose dialysis membranes (MWC 50,000) were from Spectrum Chemicals & Laboratory Products (New Brunswick, NJ). TC-1 cells were from Dr. T. C. Wu at the Johns Hopkins University. TC-1 cells were C57BL/6 mouse lung endothelial cells transformed with the HPV 16 E6 and E7 oncogenes and an activated H-ras (Lin et al., 1996). The 24JK tumor cell line, a tumor cell line derived from the MCA102 fibrosarcoma generated from C57BL/6 mice, was generated by Dr. P. Hwu in the National Cancer Institute (Hwu et al., 1995). Cells were grown in Roswell Park Memorial Institute (RPMI) 1640 medium (Invitrogen, Carlsbad, CA) supplemented with 10% fetal bovine serum (FBS, Invitrogen), 100 U/mL of penicillin (Invitrogen), and 100 μg/mL of streptomycin (Invitrogen).

3.3.2 Methods

3.3.2.1 Preparation of Gd-DTPA-encapsulated liposomes

Gd-encapsulated liposomes were prepared by the thin film hydration method with subsequent freeze-thaw as previously described (Le and Cui, 2006a). Briefly, a thin film of soy HPC:Chol:PEG 2000 (50:35:5, molar ratio) was formed in the bottom of a glass tube by chloroform evaporation. The lipid thin film was suspended in an aqueous solution with Gd-DTPA/pLL complexes (1:0.25, w/w) by vigorous mixing at room temperature. The suspension was frozen and thawed for 6 cycles and sonicated for 15 minutes. The concentrations of Soy HPC, Chol, and PEG 2000 were 33 mg/mL, 12.73 mg/mL, and 12.15 mg/mL, respectively. One-hundred (100) nm-range liposomes were prepared by extruding the suspension 11

times through 400 nm- and 100 nm-polycarbonate membranes sequentially (Avanti Polar Lipids). Free Gd-DTPA was removed by dialyzing against 0.9% NaCl solution through a cellulose dialysis membrane (MWC 50,000) for 15 hours. The amount of Gd encapsulated in the liposomes was measured using an Inductively-Coupled Plasma Optical Emission Spectrometer (ICP-OES, Teledyne Leeman Labs, Hudson, NH) at 342.247 nm. The Gd content in the Gd-encapsulated liposomes was estimated to be 6.8 ± 0.3 mg pure Gd/mL. The encapsulation efficiency (%) of the Gd-DTPA in liposomes was 25.7 ± 1.4%. The Gd-DTPA solution used to hydrate the lipids was 10% (w/v).

3.3.2.2 Biodistribution and tumor uptake study

Female C57BL/6 mice, 6-8 weeks old, were purchased from the Simenson Lab (Gilroy, CA). All experiments were completed following the National Institutes of Health guidelines for care and use of laboratory animals. To establish tumors in mice, TC-1 cells (5×10^5) were subcutaneously (s.c) injected in the flank of mice on day 0. On days 10-15, mice were injected (i.v) with the Gd-encapsulated liposomes via the tail vein. The volume of the liposomes was adjusted to 200 μL per mouse (~20 μg Gd/g of body weight). Mice were euthanized at predetermined time points. Their tumor, blood, liver, spleen, heart, lung, and kidney were collected, weighed, desiccated at 60^{o}C for 12 hours, and then incinerated with nitric acid (6.6 N) at 60^{o}C for 15 hours. The samples were filtrated through a 0.45-μm filter. Gd content in the samples was then determined using ICP-OES. To estimate the total amount of Gd in the blood, the total blood

volume of a mouse was assumed to be 7.5% (v/w) of the mouse total body weight (Davies and Morris, 1993).

In the multiple-dosing experiment, tumor-bearing mice were injected (i.v.) three times with the Gd-encapsulated liposomes at hours 0, 8, and 14, each time with a dose of 20 μg Gd per g of body weight. Twelve hours after the last injection, mice were euthanized with CO_2. The organs were harvested, and Gd concentrations in them were determined as mentioned above.

To evaluate the biodistribution and tumor uptake of Gd by a different tumor, a similar experiment was completed in mice pre-grafted with 24JK tumors. Briefly, mice were seeded with 24JK cells (5×10^5) on day 0 in their flank. On day 15, mice were injected (i.v.) with a single dose of the Gd-encapsulated liposomes. About 12-13 h later, mice were euthanized; tumor and other organs were collected and processed as mentioned above.

3.3.2.3 Statistical analysis

The student t-test assuming equal variances was used if two groups were to be compared. If more than two groups were involved, ANOVA followed by pair-wise comparisons with Fisher's protected least significant difference (PLSD) procedure was used. Linear regressions were completed using the S-Plus 7.0 software from the Insightful Corporation (Seattle, WA). A p value of ≤ 0.05 (two-tail) was considered to be statistically significant.

3.4 Results and Discussions

Gd-NCT is a promising therapeutic modality for solid tumors. One of the key factors for the success of Gd-NCT is to deliver and maintain a sufficient amount of Gd in tumor tissues during neutron irradiation (Shikata et al., 2002). We have previously reported a Gd-encapsulated liposome formulation, which (i) had a blood half-life of more than 24 hours in mice, (ii) was encapsulated with 6.8 mg of Gd per mL of liposomes, and (iii) readily led to an average tumor Gd concentration of more than 100 μg Gd per g of wet tumors when intravenously injected into mice pre-grafted with model tumors (Le and Cui, 2006a)**.** These findings were encouraging because it was estimated that the optimal Gd concentration in tumors for Gd-NCT should be 50 to 200 μg/g tumor tissues (Shih and Brugger, 1992b). In the present study, we systemically evaluated the biodistribution and tumor-uptake of Gd in mice pre-established with two different model tumors and investigated the effect of tumor size on the tumor uptake of Gd encapsulated into the liposomes.

3.4.1 The biodistribution and tumor uptake of Gd in TC-1 tumor-bearing mice

In order to identify the time it takes for the content of Gd in tumors to reach the maximum, the kinetics of the Gd accumulation in tumor tissues was evaluated. The TC-1 tumor in C57BL/6 mice is a murine model of human lung cancer (Lin et al., 1996). TC-1 cells grow rapidly in mice. Subcutaneously injected TC-1 cells (5×10^5 per mouse) generally kill the host mice in about 25-30 days, if

left untreated (Cui and Huang, 2005). Thus, the TC-1 model tumors were used to evaluate the biodistribution and tumor uptake of Gd, not necessarily indicating to use the Gd-encapsulated liposomes to treat cervical cancers in the future, although it could be a possibility. As shown in Fig. 3.1A, the Gd encapsulated into the liposomes quickly reached tumor tissues and resulted in a pure Gd content of 33.9 ± 4.6 μg/g tumor tissues 30 min after the injection. The concentration of Gd in tumors then increased gradually and reached a maximal average value of 158.9 ± 48.7 μg/g tumor tissues 12 hours after the injection (Fig. 3.1A). When measured 24 hours after the injection, the concentration of Gd that remained in tumors was 103.1 ± 23.5 μg Gd/ g wet tumor tissues, although this value was not significantly different from that in the 12 hour time point ($p = 0.45$, two-tail) due to the large variations in the Gd content in tumors. Thus, in future studies, at least 12 hours should be given to allow a sufficient amount of the i.v. injected liposome-encapsulated Gd to accumulate into tumor tissues. Finally, it should be pointed out that the amount of Gd in tumors achieved in this study not only surpassed the estimated concentration of Gd required for a successful NCT (Shih and Brugger, 1992b), but also represent one of the highest Gd contents reported in tumor tissues when a Gd compound or delivery system was i.v. injected into a tumor-bearing animal model. Other high tumor Gd concentrations previously reported included the 101 μg Gd per g wet tumor tissues when a high-Gd-nanoemulsion formulation (high-Gd-nanoLE) was injected (i.v.) twice into tumor-bearing hamsters (Shikata et al., 2002) and the 107 μg Gd per g wet tumor tissues when an emulsion

containing a distearylamide-Gd-DTPA was intraperitoneally injected into Greene's melanoma-bearing hamsters at a dose of 2.0 mL (6.0 mg Gd) per hamster (Miyamoto et al., 1999). Of course, a ^{157}Gd-enriched Gd compound has to be used when performing NCT because natural Gd only contains 15.56% of ^{157}Gd; commercially available Gd-enriched compounds may contain as high as 99.5% of ^{157}Gd.

The biodistribution of the Gd encapsulated into liposomes in other organs of the tumor-bearing mice was also evaluated. Similar to the $t_{1/2}$ value previously reported in tumor-free Balb/C mice (Le and Cui, 2006b), the $t_{1/2}$ of the liposome-encapsulated Gd in the blood of the TC-1 tumor-bearing mice was more than 24 hours (Fig. 3.1B), suggesting that mouse species and their health condition did not significantly influence the behavior of the Gd-encapsulated liposomes in the blood. The content of Gd in the liver and spleen increased gradually and reached 24.1 ± 5.0% and 8.9 ± 1.9% (both are mean ± S.E.M.), respectively, of the total injected Gd, 24 hours after the injection (Fig. 3.1B). The contents of Gd in other organs, including heart, lung, and kidney, were all gradually decreased as a function of time, as shown in Fig. 3.1C.

For comparison, the contents of Gd in the tumor, blood, liver, and spleen were also measured when free Gd-DTPA was injected (i.v.) into TC-1 tumor-bearing mice. As expected, the free Gd-DTPA was quickly cleared from the blood. Only 0.14 ± 0.01% of the total injected Gd-DTPA were remaining in the blood circulation 12 hours after the injection. The Gd taken up by the tumors when the

free Gd-DTPA in solution was injected was over 260-fold lower than that when the Gd encapsulated into liposomes was injected (Fig. 3.2). These findings clearly demonstrated the advantage of delivering the Gd-DTPA using the liposomes.

Shown in Fig. 3.3 were the tumor-to-normal tissue ratios (T/N) of the Gd contents. Except in the spleen, the T/N ratios of the Gd content in blood and other organs (i.e., liver, heart, lung, and kidney) were all above one, 12 hours after the injection (Fig. 3.3A). Similar to previous reports about the splenic liposome uptake (Gabizon, 2001; Harrington et al., 2001), the liposome-encapsulated Gd was more concentrated in the spleen than in other organs that were examined. Thus, more modifications may have to be introduced into the Gd-liposome formulation to further reduce its uptake by the spleen. Otherwise, the spleen will have to be properly avoided when neutrons are to be applied in a NCT. In addition, the T/N ratios of the Gd in the tumor tissues over that in the rest of the non-tumor tissues (i.e., total body weight less tumor weight) were significantly higher than 1 in all the time points evaluated (i.e., ranged from 154 to 783) (Fig. 3.3B). These findings are important because they indicated a preferred accumulation of the Gd encapsulated into the liposomes in tumor tissues, which is expected to allow a selective targeting of neutrons to tumor tissues.

3.4.2 The biodistribution and tumor uptake of Gd in tumor-bearing mice after three injections of Gd-encapsulated liposomes

A single injection of our Gd-encapsulated liposomes had resulted in a sufficiently high concentration of Gd in tumors in the mouse model, although, as

mentioned earlier, the Gd has to be ^{157}Gd-enriched. Thus, we evaluated the feasibility of further enhancing the amount of Gd that can be taken up by the tumors by dosing more Gd-encapsulated liposomes via multiple injections. The distribution and tumor uptake of Gd in TC-1 tumor-bearing mice after they were injected (i.v.) three times with the Gd encapsulated into the liposome were determined and compared to that after a single injection. The triple injections did not significantly change the relative distribution of Gd in all organs and tissues examined, except the tumor (Table 3.2). The % of the Gd injected that accumulated into tumors after the triple injections was more than doubled, when compared to that after a single injection (from 1.9 ± 0.4% to 3.9 ± 0.6%, $p = 0.007$). In fact, the actual amount of Gd accumulated into the tumors after the triple injections was 45.1 ± 13.0 μg, which was about 5.3-fold higher than that after the single injection (8.5 ± 4.8 μg). These data clearly demonstrated that increasing the dose of the Gd by multiple injections can further increase the uptake of the Gd incorporated into the liposomes by tumors, although it needs to be pointed out that the final Gd concentration accumulated in tumors after the triple injections was not significantly different from that after the single injection (158.9 ± 43.7 vs. 233.9 ± 81.2 μg Gd / g tumor). This might be attributed to the relatively larger size of tumors in mice injected three times. Tending to be significantly different ($p = 0.08$, two-tail), the average weight of tumors in mice who were injected three times (360 ± 340 mg) was 3.75-fold larger than that in mice who were injected only once (96 ± 86 mg). As we will discuss in details later in section

3.4.4, the tumor size could have a significant effect on the final concentration of Gd accumulated in the tumors.

3.4.3 The uptake of Gd by 24JK tumors in mice

To evaluate the effect of tumor type on the tumor uptake of Gd, the biodistribution and tumor uptake of Gd in 24JK tumor-bearing mice were examined. The 24JK cells were a B6 sarcoma cell line and can grow into tumors when injected into C57BL/6 mice (Hwu et al., 1995), although the growth tended to be much slower than that of the TC-1 tumors. Again, an average Gd content of 58.8 ± 12.9 μg per g of wet tumor tissues was achieved 13 hours after the Gd-encapsulated liposomes were injected (i.v.) into the 24JK tumor-bearing mice (Table 3.2). Thus, we expect that our Gd-encapsulated liposomes can be used to deliver a sufficient amount of Gd into solid tumors of other different origins for potential NCT, although it needs to be pointed out that, the differences in the extent of the vascularity in different tumors could have significant effects on the Gd that can accumulate in tumors because it had been shown that a tumor that is poorly-vascularized tended to take less liposomes (Gillies et al., 1999; Harrington et al., 2000). As will be discussed in details in the following section, the extent of the vascularity of the 24JK tumors was quite different from that of the TC-1 tumors.

3.4.4 The effect of tumor size on the uptake of Gd encapsulated into the liposomes by tumors

Data from our preliminary studies have suggested that the size of the tumors tended to influence the uptake of Gd by tumors *in vivo*. A higher percent of the total injected Gd tended to be recovered in large tumors than in small ones. However, the Gd content reported as μg of Gd per g of wet tumor tissues tended to be smaller in larger tumors. These observations agreed well with previous reports showing that tumor size influenced the uptake of PEGylated liposomes by tumors in patients and in mice grafted with model tumors (Harrington et al., 2001; Harrington et al., 2000). This prompted us to identify the relationship between TC-1 tumor size and the *in vivo* uptake of the Gd encapsulated into the liposomes by the tumors, whose size ranged from less than 1 mg to more than 2 g. By looking at the scatter plot (Fig. 3.4A), it can be seen that the Gd concentration in the TC-1 tumors shown as μg of Gd in tumors per g of tumors per g of total Gd injected (μg Gd/g tumor/g Gd injected) and the tumor weight (g) had a close relationship that can be reasonably represented by a straight line. Simple linear regression found a straight line that best fits the data with p-value < 0.0001 for the slope of the line. So, there was a strong inverse correlation between the Gd concentration in the TC-1 tumors and the tumor weight. Doubling the weight (g) was associated with a decrease of approximately 38% in median of Gd uptake/g tumor/g Gd injected. The correlation can be described using the following equation: Gd [(μg)/g tumor/g Gd injected] = 29.746 * (tumor weight)$^{-0.7267}$. A similar equation can also be

derived for the uptake of Gd by 24JK tumors: Gd = 32.132 * (tumor weight)$^{-0.4502}$ (R^2 = 0.54) (Fig. 3.4A). These equations indicated that increasing tumor size will lead to a decrease in the concentration of Gd that can be delivered into tumors. This relationship can be explained by the poor or heterogeneous vascularization of larger tumors (Acker et al., 1990; Gillies et al., 1999; Harrington et al., 2000; Sevick and Jain, 1989; Su et al., 1996). Thus, from the two equations shown for the TC-1 and the 24JK tumors, it is clear that the extents of the vascularity in these two tumors were different from each other. Also, for TC-1 tumors, the effect of tumor size on the Gd uptake tended to be more dramatic than that for 24JK tumors. This tumor size dependence of liposome-encapsulated Gd uptake is clinically relevant. Similar to the delivery of anti-tumor chemicals using long-circulating liposomes or other particulates, for small and medium size solid tumors, a sufficient amount of Gd is expected to be readily delivered into the tumors for successful NCT. However, for those very small, non-vascularized or very large, poorly-vascularized solid tumors, the advantage of using the liposome as a delivery system for Gd might be limited. Thus, alternative strategies might have to be applied to treat the very small, non-vascularized tumors and the very large, poorly-vascularized, and locally advanced tumors. Increasing the dose of the Gd-encapsulated liposomes by injecting more frequently and/or using more liposomes might increase the Gd-uptake by large tumors as shown in Table 3.1. However, the extent to which this strategy of increasing dose can help might be limited. In chemotherapy, one of the strategies is to deliver multiple cycles of cytotoxic

chemicals over a period of many weeks in an attempt to reduce the tumor mass and its interstitial pressure and increase tumor blood flow (Harrington et al., 2000). This strategy might be adopted in future Gd-NCT. Finally, there was an association of tumor weight and the percent of the total injected Gd that was recovered in the tumor tissues ($p = 0.002$, linear regression). Doubling the weight (g) was associated with an increase of approximately 23% in median of the percent Gd uptake/g tumor.

It needs to be pointed out that the relationships between tumor Gd uptake and tumor size might indicate another advantage of Gd-NCT over B-NCT because the long-range γ-rays emitted from the Gd can kill cells without being taken up by the cells; while, in the case of B-NCT, the B has to be delivered inside tumor cells for the short-range α particles emitted by the boron to kill the tumor cells. Thus, Gd-NCT may have an improved efficiency in killing tumors in the less- or non-vascularized tissues in large tumors than B-NCT, although experiments have to be carried out to confirm it.

The composition of the liposome is similar to that of some commercial liposomally-delivered anti-cancer drugs, such as Doxil® and Daunoxome® (Massing and Fuxius, 2000). Gd-DTPA is essentially an inert complex (Caravan et al., 1999). Although the pLL component in the Gd-encapsulated liposomes may be potentially toxic, it can be easily replaced by a USP material such as the protamine sulfate. Both pLL and protamine are polycations and can provide positively

charged groups to complex with the Gd-DTPA. Thus, it is expected that this Gd-encapsulated liposome formulation will have a good safety profile.

In conclusion, we reported that a Gd concentration of above 50 μg per g of wet tumor tissues can be readily achieved by injecting (i.v.) our Gd-encapsulated liposomes into mice. It took about 12 hours for the Gd concentration in tumors to reach its maximum. Finally, a strong inverse correlation between tumor size and the final amount of Gd that accumulated into the tumors was identified, suggesting that alternative strategies might have to be adopted for Gd-NCT to be effective in large, poorly vascularized, advanced solid tumors or very small, non-vascularized tumors.

Table 3.1 Comparison of the biodistribution and tumor uptake of Gd in TC-1 tumor-bearing mice when mice were injected once or three times with the Gd encapsulated into liposomes.

	Single dose (414 μg/mouse)	**Triple dose (1187 μg/mouse)**
Gd concentration in tumors (μg Gd/g tumor)	158.9 ± 43.7 (34.7-365.6)	233.9 ± 81.2 (63.1-430.5)
Gd amount in tumor (μg)	8.5 ± 4.8	45.1 ± 13.0
Tumor (% injected)	1.9 ± 0.4	3.9 ± 0.6
Blood (% injected)	61.2 ± 5.9	60.6 ± 5.9
Liver (% injected)	24.4 ± 1.9	21.6 ± 4.6
Spleen (% injected)	4.4 ± 0.8	4.1 ± 1.7
Heart (% injected)	0.9 ± 0.1	1.1 ± 0.7
Lung (% injected)	2.5 ± 0.5	2.5 ± 0.4
Kidney (% injected)	1.8 ± 0.2	2.0 ± 0.2

TC-1 tumor-bearing C57BL/6 mice were injected (i.v.) with Gd-encapsulated liposomes either once or three times (8 and 6 hours apart). Twelve hours later, tumors, blood, and other organs were collected, and the amount of Gd in them was determined. Data reported are mean ± S.D. (n = 4 or 7).

Table 3.2 The biodistribution and tumor uptake of Gd in 24JK tumor-bearing mice.

	Gd content
Tumor (μg/g tissue)	58.8 ± 12.9
Tumor (% injected)	1.0 ± 0.6
Blood (% injected)	57.8 ± 4.1
Liver (% injected)	13.6 ± 1.3
Spleen (% injected)	6.8 ± 1.2
Heart (% injected)	1.1 ± 0.6
Lung (% injected)	1.2 ± 0.2
Kidney (% injected)	1.8 ± 0.4

C57BL/6 mice with 24JK tumors were injected (i.v.) with the Gd-encapsulated liposomes (Gd, 30 μg/g body weight in 0.2 mL) when the tumors were about 5-7 mm in diameter. Mice were euthanized 13 hours later to determine Gd distribution. Data were reported as the percentages of the total injected dose (% injected dose). Data in tumors were also reported as μg of Gd per g of tumors. In only one mouse, the Gd content was below 50 μg/g tumor. Data reported are mean ± S.D. (n = 5). This experiment was repeated twice, and similar results were obtained.

(A)

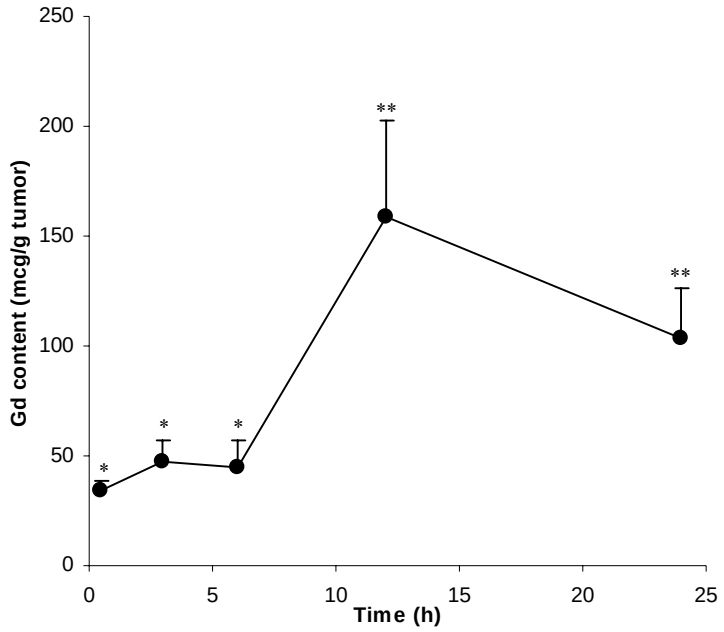
Gd content (mcg/g tumor)
Time (h)
0
50
100
150
200
250
0
5
10
15
20
25
*
*
*
**
**

(B)

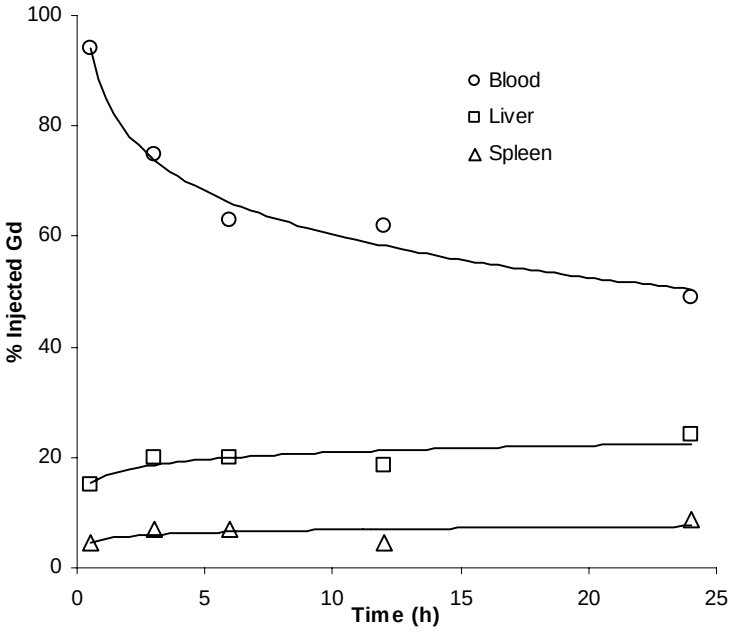
% Injected Gd
Time (h)
Blood
Liver
Spleen
0
20
40
60
80
100
0
5
10
15
20
25

Figure 3.1

(C)

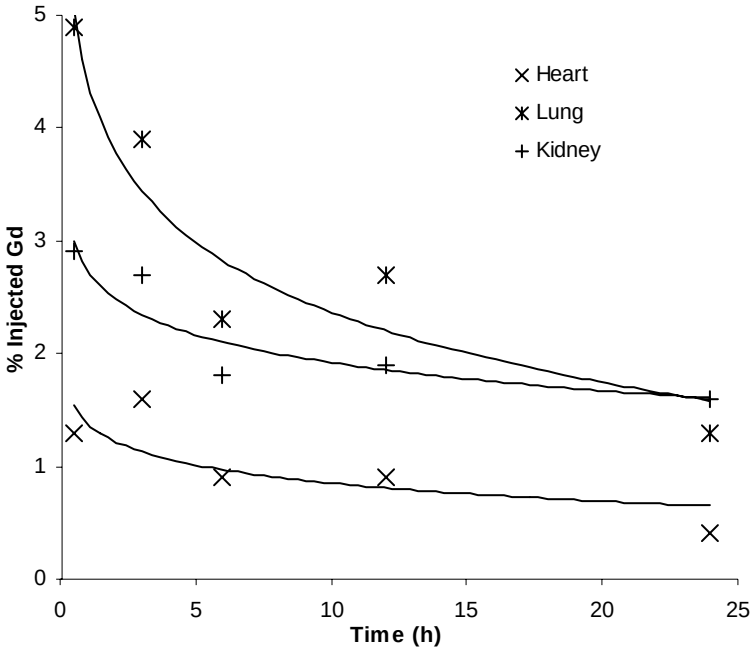

Figure 3.1 The biodistribution of Gd encapsulated into the liposomes in TC-1 tumor-bearing mice. (**A**): The content of Gd in tumor tissues (μg Gd per g of tumors). ANOVA analysis revealed that there were significant differences among the values at the five different time points ($p = 0.02$). * indicates that the values at 0.5, 3, and 6 hours were not different from one another ($p = 0.66$, AVONA). ** indicates that the values at 12 and 24 hours were comparable ($p = 0.29$, t-test). (**B** and **C**): The percent of the total injected Gd that was recovered in the blood and other organs. Data shown are mean ± S.E.M. ($n = 4$-7).

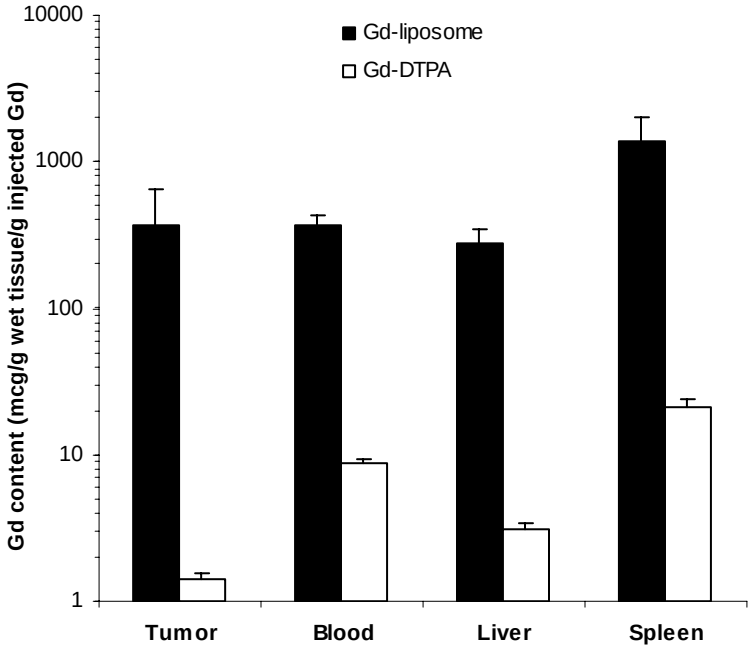

Figure 3.2 The distribution of free Gd-DTPA and Gd-DTPA encapsulated into liposomes in TC-1 tumor-bearing mice. Data reported (mean ± S.D.) were the content of Gd normalized by the weight of the tissues and the total Gd injected (μg Gd per g of tissues per g of Gd injected). Statistical analyses (t-test) revealed that the values between the Gd-liposome and free Gd-DTPA were different from each other in all the organs tested (p values were 0.03, << 0.05, << 0.05, and 0.002 for tumor, blood, liver, and spleen, respectively).

(A)

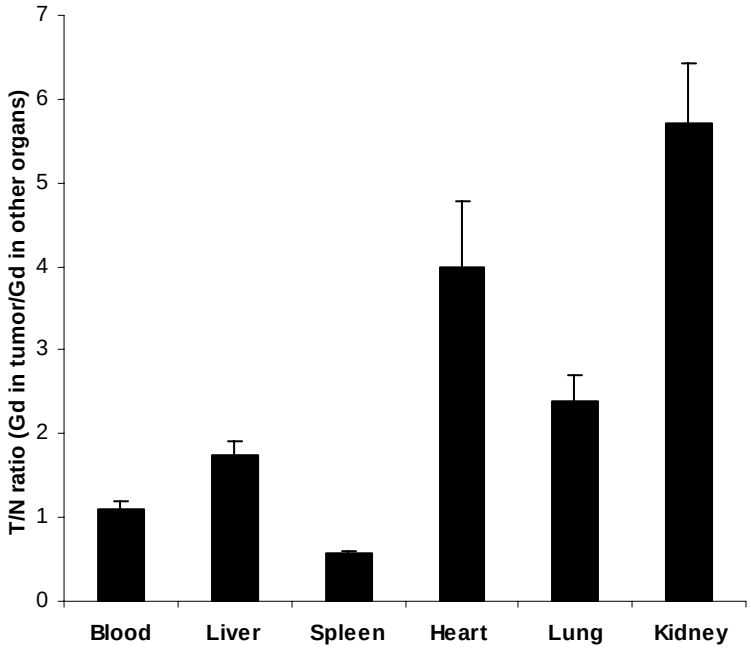
T/N ratio (Gd in tumor/Gd in other organs)
0
1
2
3
4
5
6
7
Blood
Liver
Spleen
Heart
Lung
Kidney

(B)

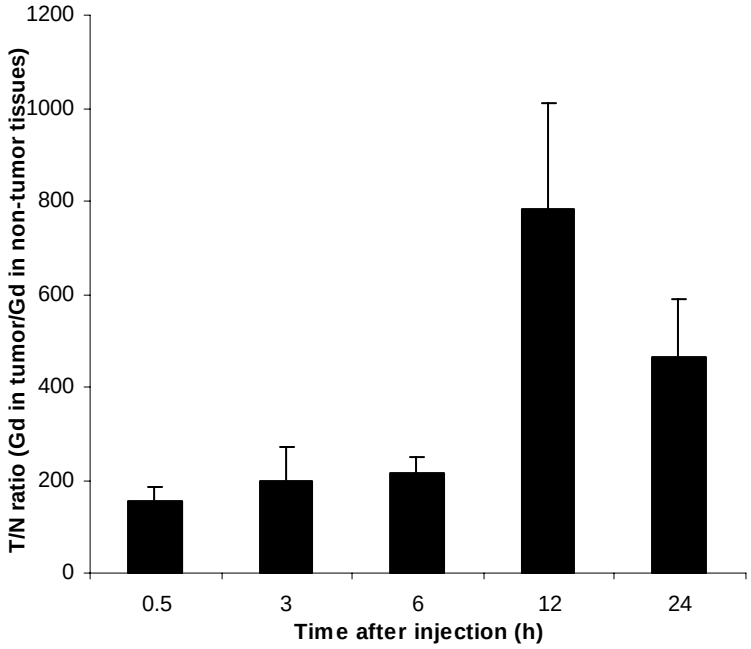
T/N ratio (Gd in tumor/Gd in non-tumor tissues)
0
200
400
600
800
1000
1200
0.5
3
6
12
24
Time after injection (h)

Figure 3.3

Figure 3.3 The ratios of the concentration of Gd in tumors over that in other organs. Tumor-bearing C57BL/6 mice were injected via the tail vein with a single dose of the Gd-encapsulated liposomes (20 μg Gd/g of body weight). In (**A**), twelve hours after the injection, mice were euthanized to determine Gd distribution. The ratios shown in Y-axis were the concentration of Gd in tumors (μg Gd/g tissue) over that in other organs (μg Gd/g tissue) [i.e., T/N ratio, Gd_{tumor} (μg/g)/$Gd_{non\text{-}tumor\ tissues}$ (μg/g)]. Data shown were the mean from 7 mice. Shown in (**B**) were the T/N ratios of the concentration of Gd in tumors (μg Gd/g tumor) over that in the non-tumor tissues (i.e., body weight minus tumor weight) as a function of time (hours after the Gd-liposomes injection). Data shown were mean ± S.E.M. (n = 3-7).

(A)

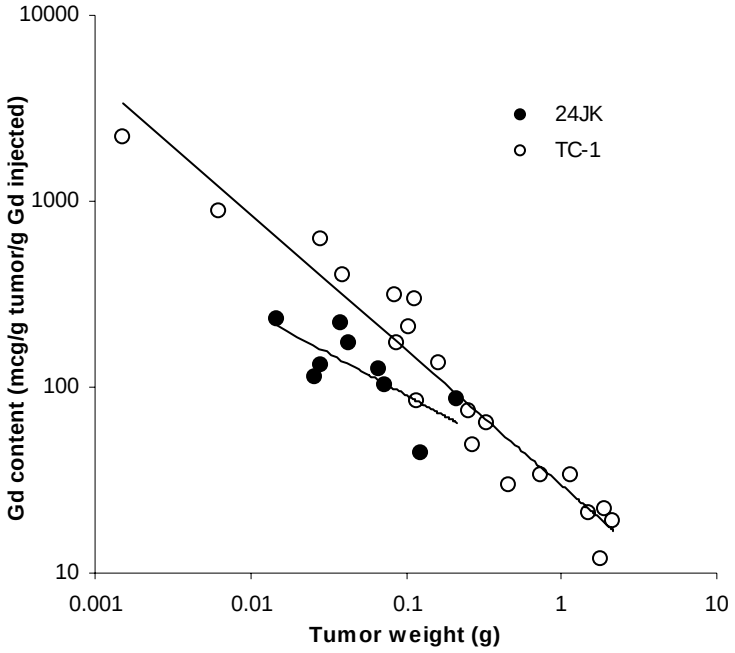
10000
1000
100
10
Gd content (mcg/g tumor/g Gd injected)
24JK
TC-1
0.001
0.01
0.1
1
10
Tumor weight (g)

(B)

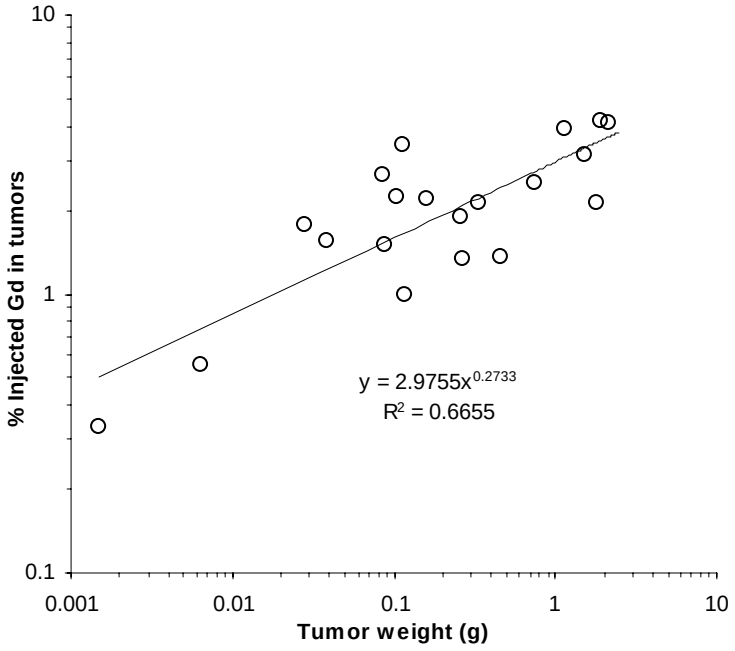
10
1
0.1
% Injected Gd in tumors
y = 2.9755x^0.2733
R² = 0.6655
0.001
0.01
0.1
1
10
Tumor weight (g)

Figure 3.4

Figure 3.4 The effect of tumor size on the uptake of Gd by tumors. TC-1 tumor-bearing C57BL/6 mice (n = 20) or 24JK tumor-bearing mice (n = 9) were i.v. injected with the Gd-encapsulated liposomes. Mice were sacrificed 12-13 hours later. Shown in (**A**) was the relationship between the final Gd concentration in tumors (TC-1 = ○, 24JK = ●, unit in μg Gd per g of wet tumor tissues per g of injected Gd) as a function of the tumor weight (g). A linear regression analysis using the S-plus software revealed p values of << 0.05. Shown in (**B**) was the relationship between the percent of the total injected Gd recovered in the TC-1 tumors (% ID) as a function of the tumor weight (g). A linear regression analysis revealed a p value of 0.002.

Chapter 4

A THERMO-SENSITIVE POLYMERIC GEL CONTAINING A GADOLINIUM (Gd) COMPOUND ENCAPSULATED INTO LIPOSOMES SIGNIFICANTLY EXTENDED THE RETENTION OF THE Gd IN TUMORS

Uyen M. Le, Dalia S. Shaker, Brian R. Sloat, and Zhengrong Cui

Drug Development & Industrial Pharmacy, 2008; 34(4): 413-8

4.1 Abstract

Gadolinium neutron capture therapy (Gd-NCT) is a promising approach to fight cancer. One key factor for the success of Gd-NCT is to deliver and maintain a sufficient amount of Gd inside tumors. A large amount of Gd can be readily introduced into tumors by direct intratumor injection. However, an innovative approach is needed to maintain the Gd in the tumors. We encapsulated a Gd compound into a liposome formulation and then dispersed the liposomes into a thermo-sensitive polymeric gel. In murine tumor models, we showed that this liposome-in- thermo-sensitive gel system significantly extended the retention of the Gd compound in tumors. This similar concept may be applied to prolong the retention of other cytotoxic chemicals in tumors, and thus, improve their anti-tumor efficacy.

4.2 Introduction

Gd-NCT is a promising tumor therapeutic modality (Akine et al., 1993; Khokhlov et al., 1995b). During a Gd-NCT, a stable and non-radioactive Gd compound is delivered into tumors. Upon irradiation by thermal or epithermal neutrons, the Gd emits cytotoxic γ-rays and auger electrons (Shih and Brugger, 1992a). Gd-NCT is generally considered to be advantageous over boron-NCT due to the larger thermal neutron capture cross-section of the ^{157}Gd (255,000 barns, 66 times larger than that of the ^{10}B) and the longer range (> 100 μm) γ-rays generated after a neutron irradiation (Barth and Soloway, 1994a; Brugger and Shih, 1989b;

Carlsson et al., 2002b). Thus, in Gd-NCT, the short range auger electrons with high linear energy transfer will extensively destroy DNA in tumor cells, and the long range γ-rays are expected to kill tumor cells even when the Gd is outside of the tumor cells, eliminating the requirement for the intracellular delivery of the Gd (De Stasio et al., 2001; Hofmann et al., 1999b).

One of the key factors for the success of Gd-NCT is to deliver and maintain a sufficient amount of Gd in tumors (50-200 μg of Gd/g wet tumor tissues) during the neutron irradiation (Shih and Brugger, 1992a). Although it is quite easy to deliver a high concentration of Gd in tumors by direct intratumor (i.t.) injection (Hofmann et al., 1999b; Khokhlov et al., 1995b), it is rather challenging to maintain the Gd in tumors in order to complete the NCT (Jono et al., 1999b; Khokhlov et al., 1995b; Tokumitsu et al., 1999b). This is largely due to the rapid diffusion of the Gd compound out of the tumors after the injection. Therefore, there is a need for a delivery system to prevent or slow down the diffusion of the Gd compounds out of the tumors. To address this need, we proposed to encapsulate a Gd compound into liposomes and then disperse the Gd-encapsulated liposomes into a thermo-sensitive polymeric gel.

We hypothesized that the liposomes would slow down the diffusion of the Gd and that the polymeric gel would slow down the diffusion of the liposomes, and thus, ultimately prolong the retention of the injected Gd compound in the tumors. This is based on data in the literature and from our own studies.

Previously, we have developed a Gd-DTPA (diethylenetriamine pentaacetic acid gadolinium (III)) carrier by encapsulating the Gd-DTPA into liposomes (Le and Cui, 2006a). The Gd-DTPA was complexed with a cationic polymer, poly L-lysine (pLL), to prevent or slow down the diffusion of the Gd-DTPA out of the liposomes. Data from our *in vitro* release study clearly showed that the encapsulation of the Gd-DTPA into the liposomes significantly slowed down the diffusion of the Gd-DTPA. Only less than 5% of the Gd-DTPA diffused out of the liposomes within 24 h (Le and Cui, 2006b). Similarly, it was reported that when certain tumor chemotherapy agents (i.e., doxorubicin or cisplatin) were dosed intratumorally, they stayed in the tumors much longer when given as a liposome formulation than when as a free drug (Harasym et al., 1997; Hwang et al., 2007). Also, it was shown that when mice were injected (i.t.) with anticancer chemicals in injectable gels or in solutions, sustained drug retention was observed only in tumors injected with the gels (Okino et al., 2003; Ruel-Gariepy et al., 2004; Smith et al., 1995). Finally, there were multiple previous reports of the preparation of liposomal gel formulations (liposomes in gel) (Alamelu and Rao, 1991; Bochot et al., 1998; Boulmedarat et al., 2005; Dai et al., 2006; DiTizio et al., 2000; Dragicevic-Curic et al., 2005; Glavas-Dodov et al., 2003; Glavas-Dodov et al., 2002; Gong et al., 2006; Langer et al., 2006; Mourtas et al., 2007; Ning et al., 2005; Paavola et al., 2000; Pavelic et al., 2005a; Pavelic et al., 2004; Pavelic et al., 2005b; Pavelic et al., 2001; Ruel-Gariepy et al., 2002; Takagi et al., 1996; Weiner et al., 1985). Generally, it was shown that the incorporation of small molecules

into the liposomal gel formulations reduced the release or diffusion of the molecules. However, successful *in vivo* applications of those liposomal gels were rare, if any, especially for local intratumor delivery.

To test this hypothesis, we chose to use the commercially available BD Matrigel™ Matrix (Matrigel). It is a solubilized basement membrane preparation extracted from the Engelbreth-Holm-Swarm mouse sarcoma (Kleinman, 1982). Its major component is laminin, followed by collagen IV, heparan sulfate proteoglycans, entactin, and nidogen (Kleinman, 1982). Below 22^{o}C, the Matrigel is in a liquid state. Above 22^{o}C, it rapidly transforms to a semi-solid matrix gel, resembling the mammalian cellular basement membrane. Its rapid gelation to form a semi-solid gel above 22^{o}C makes it ideal to disperse our Gd-DTPA-encapsulated liposomes in. It was expected that this liposome-in-Matrigel formulation would rapidly gel upon injection into tumors, and thus, prevent or slow down the diffusion of the liposomes and the Gd-DTPA out of the tumors. In the present study, we have shown that this thermo-sensitive Matrigel with Gd-encapsulated liposomes dispersed inside significantly enhanced the retention of the Gd in tumors established in mouse models. A similar liposomal gel system may be used to intratumorally deliver other cytotoxic chemotherapy agents to improve the resultant anti-tumor effect.

4.3 Materials and Methods

4.3.1 Materials

Soy hydrogenated phosphatidylcholine (Soy HPC), 1, 2-distearoyl-Sn-glycero-3-phosphoethanolamine-N-[methoxy (polyethylene glycol)-2000] (PEG 2000), and polycarbonate membranes were purchased from Avanti Polar Lipids, Inc (Alabaster, AL). Cholesterol (Chol), Gd-DTPA, phosphate buffered saline (PBS, pH 7.4), chloroform, and poly-L-lysine (pLL) (MW 5,600) were purchased from Sigma-Aldrich (St. Louis, MO). Nitric acid was from Fischer Scientific, Inc. (Fair Lawn, NJ). Cellulose dialysis tubes (MWC 10,000) and cellulose dialysis membranes (MWC 50,000) were from the Spectrum Laboratories, Inc. (New Brunswick, NJ). BD Matrigel^{TM} matrix (Matrigel) was purchased from BD Biosciences (San Jose, CA). The PC-3 cells were from the ATCC (Manassas, VA). They were a human prostate cancer cell line initiated from a bone metastasis of a grade IV prostatic adenocarcinoma. The cells were grown in F-12K medium (ATCC) supplemented with 10% fetal bovine serum (FBS) (Invitrogen, Carlsbad, CA). TC-1 cells were engineered by Dr. T. C. Wu's group at the Johns Hopkins University by transforming the primary lung cells from C57BL/6 mice with the human papillomavirus (HPV) type 16 E6 and E7 oncogenes and an activated H-*ras* (Lin et al., 1996). They were grown in RPMI1640 medium supplemented with 10% FBS, 100 U/mL of penicillin (Sigma), and 100 μg/mL of streptomycin (Sigma). EL4/PSA cells were kindly provided by Dr. Pavel Pisa in the Karolinska Hospital/Institute (Stockholm). This is a clonally-derived cell line stably

transfected with the plasmid pCDNA3-PSA to express human PSA. The cells were grown in RPMI1640 medium in the presence of a selective antibiotic, G418 (500 μg/mL, Invitrogen).

4.3.2 Methods

4.3.2.1 Preparation of Gd-DTPA-encapsulated liposomes (Gd-liposome or Gd-LP)

Gd-liposomes were prepared by the thin film hydration method with subsequent repeated freezing-and-thawing (Le and Cui, 2006a). Briefly, a thin film of soy HPC:Chol:PEG 2000 (50:35:5, molar ratio) was formed in the bottom of a glass tube. The lipid thin film was suspended with an aqueous solution of Gd-DTPA, complexed with pLL (1:0.25, w/w). The suspension was frozen-and-thawed for 6 cycles, sonicated for 15 min, and then extruded 11 times sequentially through a 1,000 nm and a 400 nm-polycarbonate membrane. Free unencapsulated Gd-DTPA was removed by dialyzing against 0.9% NaCl solution through a cellulose dialysis membrane (MWC 50,000) for 15 h. The amount of Gd-DTPA encapsulated into the liposomes was determined using an Inductively Coupled Plasma Optical Emission Spectrometer (ICP-OES, Teledyne Leeman Prodigy, Teledyne Technologies Company, New Hampshire) at 342.247 nm.

4.3.2.2 Dispersing Gd-DTPA or Gd-liposomes into Matrigel

Matrigel was thawed on ice overnight and then gently pipetted using pre-cooled pipette tips to ensure homogeneity. Pure Gd-DTPA solution or Gd-liposome suspension was mixed with the Matrigel at a volume ratio of 1:2 to

prepare the Gd in gel formulation (Gd-Gel) or the Gd-liposomes in gel formulation (Gd-LP-Gel), respectively. The entire process was completed on ice to avoid gelling, and the final products were kept on ice prior to further use. At this ratio, the mixture rapidly gelled when placed into a 37^{o}C water bath (data not shown).

4.3.2.3 *In vitro* release of gadolinium

Pure Gd-DTPA, Gd-Gel, Gd-LP, or Gd-LP-Gel, all containing ~ 574 μg of Gd-DTPA, was placed into a 1 mL cellulose ester dialysis tube. The tube was placed into a tube containing 12 mL of PBS (10 mM, pH 7.4) and incubated in a 37^{o}C shaker incubator (VWR International). At predetermined time points, the dialysis tube was taken out and re-placed into another tube containing 12 mL of fresh PBS. The amount of Gd in the PBS was determined using ICP-OES.

4.3.2.4 Animal studies

Female C57BL/6 mice (6-8 weeks) and male Nu/Nu mice (6 weeks) were from the Charles River Laboratories (Wilmington, MA). To establish tumors in nude mice, PC-3 cells in suspension were mixed (1:1 ratio, v/v) with the Matrigel, and a 0.1 mL of the mixture (1 x 10^{6} cells) was subcutaneously (s.c.) injected in both the left and the right sides in the mouse flank on day 0. On day 27, mice (n = 3, with a total of 5-6 tumors) were intratumorally (i.t.) injected with a single dose of pure Gd-DTPA, Gd-Gel, Gd-LP, or Gd-LP-Gel. Mice were euthanized 10 min or 4 h after the injection. Tumors were collected, weighed, desiccated at 60^{o}C for

12 h, and incinerated with nitric acid (6.6 N) at 60^{o}C for 15 h (Le and Cui, 2006a). The concentration of the Gd in the samples was determined using ICP-OES.

To establish tumors in C57BL/6 mice, TC-1 cells or EL4/PSA cells (5 x 10^5) were s.c. injected in the flank of mice on day 0 (one tumor per mouse). In the case of TC-1 cells, on day 14, mice (n = 3-4) were i.t. injected with a single dose of pure Gd-DTPA, Gd-Gel, Gd-LP, or Gd-LP-Gel, and euthanized 4 h after the injection. Tumor, liver, spleen, and blood in the mice were collected to quantify the content of the Gd in them. The total blood volume of a mouse was assumed to be 7.5% (v/w) of its total body weight (Le and Cui, 2006a). In the case of the EL4/PSA tumors, on day 25, mice (n = 3-5) were i.t. injected with a single dose of the Gd-Gel or the Gd-LP-Gel, and the Gd content in the tumors was measured 4 h after the injection.

4.3.2.5 Statistical analysis

The student t-test assuming equal variances was used if two groups were compared. If more than two groups were involved, the one way analysis of variance (ANOVA) followed by pair-wise comparisons with Fisher's protected least significant difference procedure was used. A p value of ≤ 0.05 (two-tail) was considered to be statistically significant.

4.4 Results and Discussions

4.4.1 *In vitro* release of Gd-DTPA

To maintain the Gd-DTPA inside tumors after it is directly injected into tumors, the release of the Gd-DTPA from the Gd carrier needs to be controlled or prevented first. As shown in Fig. 1, when placed into a dialysis tube, all free Gd-DTPA rapidly diffused out of the tube within 30 min. The incorporation of Gd-DTPA into the Matrigel significantly slowed down the diffusion of the Gd-DTPA as compared to the free Gd-DTPA. However, up to 20% of the Gd-DTPA still diffused out the gel within 24 h (Fig. 4.1), indicating that the incorporation of the Gd-DTPA into the Matrigel alone may not be sufficient to prevent the diffusion of the Gd-DTPA out of tumors when directly injected into tumors. As expected, the release of the Gd-DTPA from the liposomes (Gd-LP) was very limited (Le and Cui, 2006a), less than 3% within 24 h. Dispersing the Gd-liposomes into the Matrigel did not further slowed down the diffusion of the Gd (Fig. 4.1). Apparently, the diffusion of the Gd-DTPA out of the liposomes was the rate-limiting step. Our previous data have shown that the complexation of the Gd-DTPA with the cationic polymer, pLL (MW 5600), helped to prevent or slow down the diffusion of the Gd-DTPA out of the liposomes (Le and Cui, 2006a). Although the *in vitro* release rate of the Gd-DTPA was not further decreased when the Gd-liposomes were dispersed into the Matrigel, it did not necessarily suggest that the Matrigel would be irrelevant in preventing the outflow of the Gd from tumors *in vivo*. Liposomes cannot diffuse out of the dialysis tube used in the

present *in vitro* release study, but can directly diffuse out tumors *in vivo*. Therefore, the Matrigel may slow down the diffusion of the liposomes, and thus, the outflow of the Gd-DTPA *in vivo*.

4.4.2 The retention of the Gd-DTPA in PC-3 prostate tumors in nude mice

To evaluate the ability of the Gd-LP-Gel to prolong the retention of the Gd inside tumors, a single dose of Gd-LP-Gel containing 60 μg of Gd was injected i.t. into the PC-3 prostate tumors established in nude mice. Ten min after the injection, a Gd concentration as high as 3,794 ± 490 (μg per gram of tumor per mg of Gd injected) was recovered from the tumors (Fig. 4.2). This corresponded to 64.5% of the injected Gd dose. As controls, tumors were also injected with the free Gd-DTPA, the Gd-Gel, or the Gd-liposome. After 10 min, a significant amount of the Gd was also recovered from all the tumors, but much less than from tumors injected with the Gd-LP-Gel (Fig. 4.2).

Since the Matrigel is a thermo-sensitive gel, which very rapidly transforms to a semi-solid matrix gel at above 22^{o}C, we speculated that when the Gd-LP-Gel was injected into tumors *in vivo*, the Matrigel might have immediately gelated into a semi-solid state, and thus, prevented the significant outflow of the Gd-liposomes from the tumors. However, in the absence of the Matrigel, a significant fraction of the Gd-liposomes injected into the tumors might have been forced out of the tumors because of the increased intratumor pressure generated by the injection. Thus, it was likely that the Matrigel have prevented or decreased the outflow of the

liposomes immediately after the injection. If the injected was not forced out of the tumors immediately after the injection, the liposomes alone were sufficient to prevent or slow down the diffusion of the Gd-DTPA out of the tumors. For example, 4 h after the injection, the Gd-DTPA content in tumors injected with the Gd-liposomes did not significantly decrease, regardless of the presence or absence of the Matrigel (Fig. 4.2). However, when the Gd-DTPA was not encapsulated into the liposomes, almost all of the Gd-DTPA injected into the tumors diffused out of the tumors within those 4 h, regardless of whether it was incorporated into the Matrigel or not (Fig. 4.2). Apparently, in order to maintain a larger fraction of the injected Gd-DTPA inside tumors, it was the best to combine the encapsulation of the Gd-DTPA into liposomes and the dispersion of the liposomes into the thermo-sensitive Matrigel together.

4.4.3 The retention of the Gd-DTPA in TC-1 and EL4/PSA tumors in C57BL/6 mice

To further confirm the ability of the Gd-LP-Gel to retain the Gd-DTPA in tumors, two other tumor models, TC-1 and EL4/PSA in C57BL/6 mice, were used. Again, as shown in Fig. 4.3A and 4.4, the Gd-LP-Gel significantly extended the retention of the Gd in both tumors. The average content of the Gd in tumors in the C57BL/6 mice was lower than that in the nude mice (Fig. 4.2) simply because the tumors in the C57BL/6 mice were significantly larger than in the nude mice (0.82 ± 0.64 vs. 0.13 ± 0.04, $p << 0.05$). For the TC-1 tumors in C57BL/6 mice, we have also quantified the amount of the Gd recovered from the blood, spleen, and liver to

examine the re-distribution of the Gd-DTPA 4 h after the i.t. injection. The free Gd-DTPA was rapidly eliminated from the mice (Fig. 4.3B), in agreement with what was observed when the free Gd-DTPA was injected intravenously (Le and Cui, 2006b). However, when the Gd-liposomes (Gd-LP and Gd-LP-Gel) were injected directly into tumors, a significant fraction of the injected Gd was recovered from the blood, liver, and spleen 4 h after the injection (Fig. 4.3B), in agreement with our previous finding that the liposomes had a long half-life in blood (Le and Cui, 2006a). When the Gd-liposomes in Matrigel (Gd-LP-Gel) were injected into tumors, the Gd was also recovered from the blood, liver, and spleen 4 h after the injection, but all significantly less than when the Gd-liposomes were injected into tumors in the absence of the Matrigel (Fig. 4.3B). This is likely because the Matrigel limited the diffusion of the Gd-liposomes from the tumors. Therefore, a lower percent of the i.t. injected Gd-liposomes was diffused out the tumor and into the blood circulation for re-distribution.

Previously, liposomes in polymeric hydrogels, such as the thermo-sensitive chitosan-based gel (Ruel-Gariepy et el. 2002) and the poloxamer-based gel (Fattal et al, 2004), have been developed, aimed at enhancing the retention of drugs when delivered locally (e.g., topical, vaginal, or intravitreal) (Alamelu and Rao, 1991; Bochot et al., 1998; Boulmedarat et al., 2005; Dai et al., 2006; DiTizio et al., 2000; Dragicevic-Curic et al., 2005; Glavas-Dodov et al., 2003; Glavas-Dodov et al., 2002; Gong et al., 2006; Langer et al., 2006; Mourtas et al., 2007; Ning et al., 2005; Paavola et al., 2000; Pavelic et al., 2005a; Pavelic et al., 2004;

Pavelic et al., 2005b; Pavelic et al., 2001; Ruel-Gariepy et al., 2002; Takagi et al., 1996; Weiner et al., 1985). However, most of the studies were limited to *in vitro* characterization and release studies, and there rarely were any data showing the *in vivo* performance of these systems. In one study, Ning *et al*. (2005) evaluated the efficacy of using a clotrimazole-in-liposomes-in-carbopol gel system to deliver the clotrimazole vaginally and found that the liposomal gel system was more effective in treating yeast in rat vagina, compared to a commercial clotrimazole ointment (Ning et al., 2005). However, the activity of the clotrimazole-in-liposomes without the carbopol gel was not reported, making it impossible to know whether the liposomal gel system had prolonged the retention of the clotrimazole locally. In another study, Fattal *et al*. (2004) tested the feasibility of intravitreal delivery of oligonucleotides using liposomes in a thermo-sensitive poloxmer gel. Unfortunately, it was found that the oligos were cleared from the vitreous humor significantly faster when they were in the liposomal gel system than when they were in the liposomes alone without the gel (Fattal et al., 2004). The authors attributed the short residence time of the oligos within the vitreous obtained with the liposomal gel system to the slightly increased release of the oligos from the liposomes in the presence of the polymers (poloxamer). In our study, the dispersion of the Gd-liposomes into the Matrigel did not affect the release of the Gd-DTPA from the liposomes (Fig. 4.1), which might partially explain the prolonged retention of the Gd in the tumors when delivered intratumorally using the Gd-liposomes-in-Matrigel formulation.

In conclusion, we have shown that dispersing the Gd-DTPA-liposomes into a thermo-sensitive polymeric gel helped to prolong the retention of the Gd-DTPA in the tumors. This was confirmed in three different solid tumor models. Similar systems may be used in future Gd-NCT trials to improve the efficacy of NCT. Moreover, other cytotoxic chemotherapeutic agents may also be locally delivered into tumors using similar liposomes-in-thermo-sensitive gel systems to prolong the residence time of the chemotherapeutic agents in the tumors, and thus, to improve their anti-tumor efficacy and decrease their non-targeted toxicity.

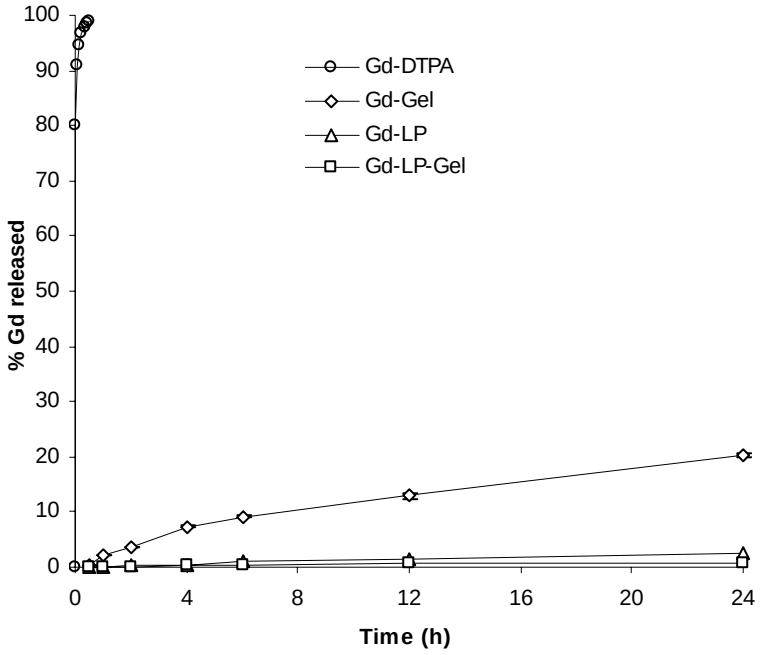

Figure 4.1 *In vitro* release of Gd-DTPA. Pure Gd-DTPA, Gd-Gel, Gd-LP, or Gd-LP-Gel was placed into a dialysis tube. The tube was placed into PBS, and the amount of Gd released as a function of time was monitored. Data shown are mean ± S.D. (n = 3).

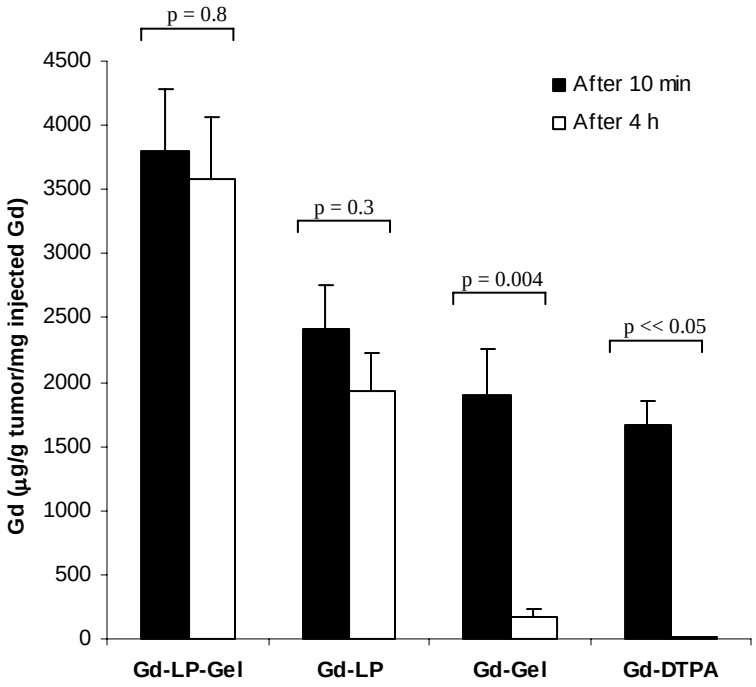

Figure 4.2 The retention of the Gd in PC-3 tumors. PC-3 cells were s.c. injected into mice to create tumors. Twenty-seven days later, Gd-LP-Gel, Gd-LP, Gd-Gel, or free Gd-DTPA was injected into the tumors. Ten min or 4 h later, the tumors were collected and weighed, and the content of Gd inside them was determined. Ten min after the injection, the value of the Gd-LP-Gel was significantly higher than that of the others ($p = 0.003$). Four h after the injection, the values of all four treatments were significantly different from one another ($p << 0.05$).

(A)

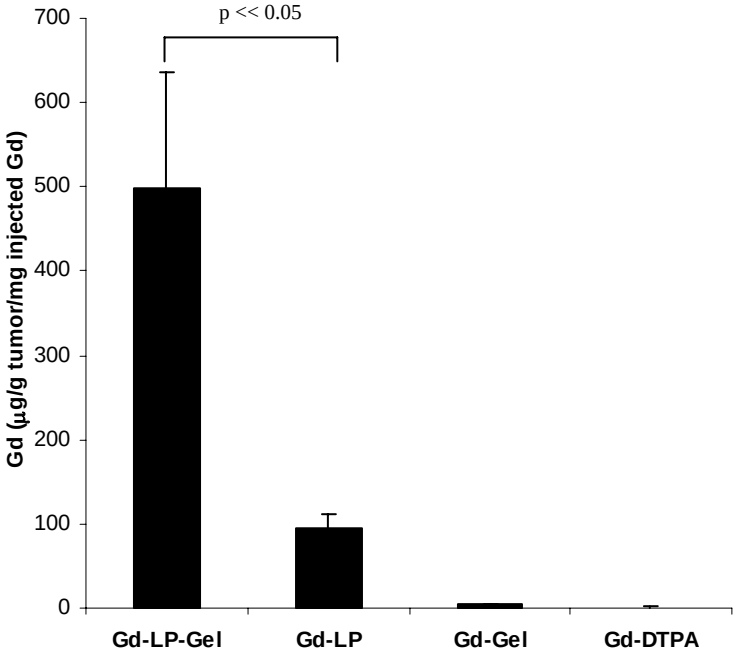
p << 0.05
700
600
500
400
300
200
100
0
Gd (µg/g tumor/mg injected Gd)
Gd-LP-Gel
Gd-LP
Gd-Gel
Gd-DTPA

(B)

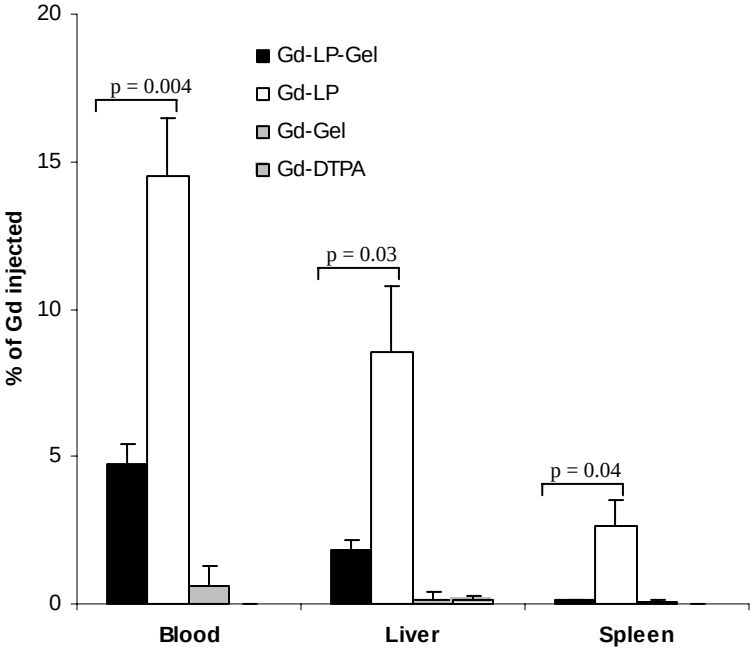
20
15
10
5
0
% of Gd injected
Gd-LP-Gel
Gd-LP
Gd-Gel
Gd-DTPA
p = 0.004
p = 0.03
p = 0.04
Blood
Liver
Spleen

Figure 4.3

Figure 4.3 The retention of the Gd in TC-1 tumors. A single dose of Gd-LP-Gel, Gd-LP, Gd-Gel, or Gd-DTPA was injected into TC-1 tumors (120 μg of Gd/mouse). Four h later, mice were sacrificed. Their tumor, blood, liver, and spleen were harvested to quantify Gd content. (**A**). Gd-DTPA recovered from tumors. Data shown are mean ± S.E.M. (n = 4-6). The levels of Gd in tumors of the four different groups were significantly different among one another ($p << 0.05$). (**B**). The content of Gd in blood and other organs. The values of the Gd-LP and the Gd-LP-Gel were different from each other in the blood, liver, and spleen.

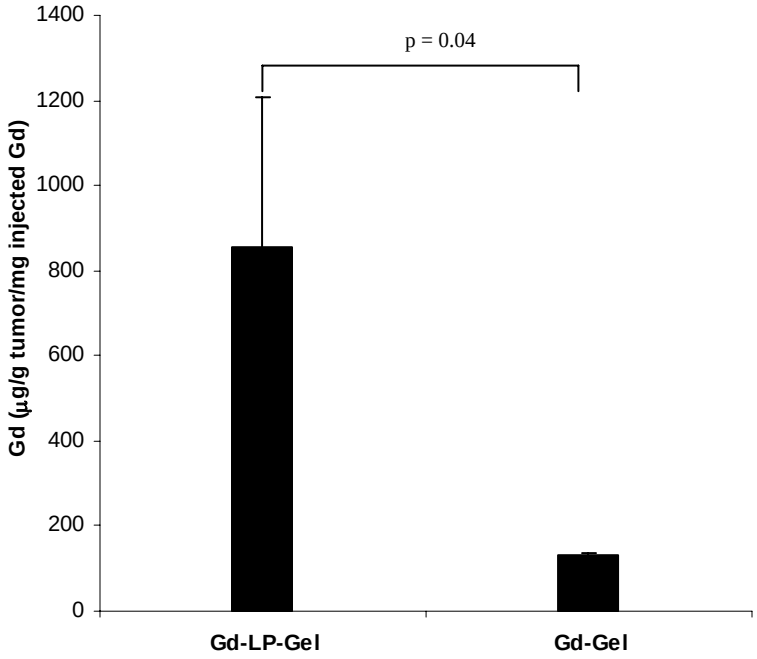

Figure 4.4 The retention of the Gd in EL4/PSA tumors. The Gd-LP-Gel or Gd-Gel was directly injected into EL4/PSA tumors. After 4 h, tumors were collected and weighed, and the Gd content was determined. Data shown are mean ± S.E.M. (n = 3-5). The levels of Gd in tumors in the two groups were significantly different from each other (p = 0.04).

Chapter 5

TUMOR CHEMO-IMMUNOTHERAPY USING GEMCITABINE AND A SYNTHETIC dsRNA

Uyen M. Le, Nijaporn Yanasarn, Christiane V. Löhr,
Kay A. Fischer, and Zhengrong Cui

Cancer Biology & Therapy, 2008; 7(3): 440-7.

5.1 Abstract

Both gemcitabine and synthetic double-stranded RNA (dsRNA) are known to be pro-apoptotic and immuno-stimulatory (-modulatory). We sought to evaluate the extent to which a combination therapy using gemcitabine and a synthetic dsRNA, polyinosine-cytosine (poly(I:C)), would improve the resultant anti-tumor activity. Using model lung and breast cancers in mice, we demonstrated that combination treatment of tumor-bearing mice with the poly(I:C) and gemcitabine synergistically delayed the tumor growth and prolonged the survival of the mice. The combination treatment also synergistically inhibited tumor cell growth *in vitro* and promoted more tumor cells to undergo apoptosis *in vivo*. Finally, the combination therapy generated a strong and durable specific anti-tumor immune response, although the immune response alone was unable to control the tumor growth after the termination of the therapy. This approach represents a promising therapy to improve the clinical outcomes for tumors sensitive to both dsRNA and gemcitabine.

5.2 Introduction

Cancer is one of the leading causes of death in the U.S. Chemotherapy remains an important cancer treatment modality. Traditionally, small cytotoxic molecules that activate only a single killing mechanism are used. Combination therapy involves treating patients with a number of different drugs simultaneously. The drugs differ in their killing mechanisms. Gemcitabine is a nucleoside analog used as chemotherapy in various carcinomas: non-small cell lung cancers,

pancreatic cancers, breast cancers, and bladder cancers. However, the clinical outcome of the current gemcitabine formulation (Gemzar®) is rather limited. For example, although being the drug of choice for pancreatic cancer, gemcitabine shows only slightly increased response rate and median survival of patients. This weak systemic activity was partially attributed to the very short half-life of the gemcitabine in the plasma (8-17 min) (Abbruzzese et al., 1991), because recent data from animal studies indicated that the encapsulation of gemcitabine into a simple liposome formulation significantly improved its *in vivo* anti-tumor activity (Bornmann et al., 2008; Moog et al., 2002). Another approach to improve the outcome of gemcitabine therapy is to utilize the commonly practiced combination chemotherapy.

A recent development is the use of synthetic dsRNA (e.g., polyinosine-cytosine, poly(I:C)) as a tumor chemotherapy agent. Certain dsRNA molecules are potent inducer of type I interferons (IFNs), which are anti-proliferative, pro-apoptotic, and anti-angiogenic (Balkwill and Taylor-Papadimitriou, 1978; Chawla-Sarkar et al., 2003). The IFN-inducing activity of dsRNA has been exploited in numerous pre-clinical and clinical tumor therapy trials. More importantly, dsRNA can also directly promote apoptosis through mechanisms such as the intracellular dsRNA-dependent protein kinase (PKR) and the 2,5-oligo A synthetase pathways (Chawla-Sarkar et al., 2003), or by directly interacting with the Toll-like receptor-3 (TLR3) on certain tumor cell surface (Salaun et al., 2006). Recently, it becomes evident that besides the indirect anti-tumor activity of the dsRNA-induced IFNs,

the dsRNA itself can also be utilized to directly kill tumor cells (Hirabayashi et al., 1999; Shir et al., 2006). Thus, we hypothesized that a combination therapy using gemcitabine and a synthetic dsRNA, especially when delivered inside tumor cells, will synergistically improve the resultant anti-tumor activity, as compared to using either of them alone.

Moreover, dsRNA is also known to activate both innate and adaptive immune responses by interacting with TLR3 and the retinoic acid-inducible gene-1 protein (RIG1) (Alexopoulou et al., 2001; Yoneyama et al., 2004). The type I IFNs induced by dsRNA are immunostimulatory too (Chawla-Sarkar et al., 2003; Le Bon et al., 2003; Liu et al., 2001). In addition, the effects of the gemcitabine on the immune system are well-documented (Nowak et al., 2002; Plate et al., 2005; Suzuki et al., 2005; Suzuki et al., 2007). The apoptotic bodies generated by gemcitabine are a good source of tumor antigens (Nowak et al., 2003b). It was shown that gemcitabine selectively eliminated splenic myeloid suppressor cells in tumor-bearing animals, but increased the activity of tumor-specific $CD8^+$ T cells and natural killer (NK) cells (Suzuki et al., 2005). Also, gemcitabine selectively depleted B cells and was > 2-fold more potent in inhibiting B-lymphocyte proliferation than T-lymphocyte proliferation (Nowak et al., 2002). Data generated in patients with pancreatic cancers also suggested that gemcitabine may promote the activation of naïve T cells (Plate et al., 2005). A very recent article reported that gemcitabine has a significant immuno-modulatory activity in murine tumor models, independent of its cytotoxic effects (Suzuki et al., 2007). Thus, we further

hypothesized that a combination therapy using gemcitabine and a synthetic dsRNA will not only synergistically inhibit the tumor growth, but also induce innate and specific tumor-killing CTL immune responses.

In the present study, we first demonstrated that a synthetic dsRNA poly(I:C) in the form of poly(I:C)-cationic liposome lipoplexes was cytotoxic in a model mouse lung tumor cell line and significantly inhibited the growth of model lung and pancreatic tumors *in vivo*. The lipoplexes were used to improve the delivery of the poly(I:C) into tumor cells. We then showed that the combined anti-tumor activity of the poly(I:C)-lipoplexes and the gemcitabine was synergistic both *in vitro* and *in vivo* in the model mouse lung tumor cells. The combination therapy also generated a strong and long-lasting tumor-specific CTL response, although the CTL response alone did not control the tumor growth after the combination treatment was terminated. Finally, we showed that the same combination therapy also synergistically inhibited the growth of a model breast tumor in mice.

5.3 Materials and methods

5.3.1 Materials and cell lines

MTT (3-(4,5-dimethylthiazol-2-yl)-2,5-diphenyltetrazolium bromide), concanavalin A, and mouse IL-2 were from Sigma-Aldrich (St. Louis, MO). Poly(I:C) (or pI:C) was from GE Healthcare (Piscataway, NJ). It was a duplex polymer composed of a poly(I) strand (152-539 b) annealed to a poly(C) strand (319-1,305 b). GEMZAR® (gemcitabine hydrochloride) was purchased from Eli

Lilly (Indianapolis, IN). The $E7_{49-57}$ peptide (RAHYNIVTF) was synthesized by the GenScript Corp. (Piscataway, NJ). TC-1 cells (ATCC # CRL-2785™) were engineered by Dr. T. C. Wu's group in the Johns Hopkins University by transforming primary lung cells from C57BL/6 mice with human papillomavirus (HPV) type 16 E6 and E7 oncogenes and an activated H-*ras* (Lin et al., 1996). The TC-1 cells are also used by many researchers as model cervical cancer cells. The Panc-02 cell line and the 410.4 cell line were kindly provided by Dr. Joyce Solheim from the University of Nebraska and Dr. Fred Miller in the Karmanos Cancer Institute (Detroit, MI), respectively. The TC-1 and the Panc-02 cells were grown in RPMI1640 medium (Invitrogen, Carlsbad, CA). The 410.4 cells were grown in a folic acid-deficient RPMI1640 medium. All media were supplemented with 10% fetal bovine serum (FBS, Sigma), 100 U/mL of penicillin (Sigma), and 100 μg/mL of streptomycin (Sigma).

5.3.2 Preparation of poly(I:C)-liposome lipoplexes (poly(I:C)-lipoplexes or pI:C/LP)

Cationic liposomes comprised of cholesterol, egg phosphatidylcholine, and 1,2-dioleoyl-3-trimethylamonium-propane (DOTAP) (all from Avanti Polar Lipids, Alabaster, AL) at a molar ratio of 4.6:10.8:12.9 were prepared by the thin film hydration method (Le and Cui, 2006a). The final concentration of the DOTAP in the liposomes was 10 mg/mL. The poly(I:C)-liposome lipoplexes were prepared by mixing equal volumes of a poly(I:C) (50 μg) solution and a liposome suspension containing 8 μg of DOTAP, followed by gentle pipetting. The resultant

lipoplexes were net negatively charged. The final poly(I:C) concentration in the lipoplexes was 250 μg/mL. Dextrose was used to adjust the tonicity of the lipoplexes.

5.3.3 *In vitro* cytotoxicity assays

To evaluate the combined effect of the gemcitabine and the pI:C/LP, TC-1 cells (3,000/well) were incubated in the presence of various amounts of gemcitabine, pI:C/LP, or their mixture at a molar ratio of 3290:1 (pI:C vs. gemcitabine) for 48 h at 37^{o}C, 5% CO_2. Fresh serum-free RPMI 1640 medium alone was added in the control samples. The number of cells alive was quantified using an MTT assay. The fraction of affected/killed cells (Fa) and the fraction of unaffected/live cells (Fu) at every dose (D) were calculated and plotted following the equation of Log(Fa/Fu) = m*Log(D)-m*Log(Dm) (Chou and Talalay, 1984). Dm is the dose required to produce the median effect (analogous to the IC_{50} value), and the m is a coefficient (Chou and Talalay, 1984). The combination index (CI) was calculated using the m and Dm values of the gemcitabine, pI:C/LP, or their mixture as previously described (Chou and Talalay, 1984). A CI value of 1, > 1, and < 1 indicates additive, antagonism, and synergism, respectively.

The 'by-stander' cytotoxic effect of the poly(I:C) was evaluated using TC-1 cells as previously described (Shir et al., 2006). Briefly, cells (5 x 10^5) were cultured in complete RPMI medium in the presence or absence of the pI:C/LP (1 μg/mL of pI:C) for 24 h, and the culture supernatant was collected. Fresh TC-1

cells (5,000 cells/well) were cultured for 48 h in the presence of the supernatant collected above (ratio of supernatant to fresh medium, 2:1, v/v). As a control, the TC-1 cells were also cultured in fresh RPMI medium.

5.3.4 Animal studies

Female C57BL/6 and Balb/C mice (6-8 weeks) were from the Simonsen Labs (Gilroy, CA, USA). TC-1 tumors were established in the flank of mice by subcutaneous (s.c.) injection of 5 x 10^5 cells. Starting on day 3 after the tumor cell implantation, the tumors became visible (~3 mm), and the mice were injected peritumorally (p.t.) with the liposomes alone or the pI:C/LP (25 μg of pI:C per day, 80-100 μL) for 5 consecutive days. The tumor size was measured and calculated based on the following equation: Tumor volume (mm^3) = ½ [length x $(width)^2$].

To evaluate the anti-tumor activity when mice were treated with the pI:C/LP and gemcitabine, starting on day 3 after the tumor cell injection, mice were pertitumorally (p.t.) injected with the pI:C/LP (50 μg of pI:C per day) for 5 consecutive days and intraperitoneally (i.p.) injected with the gemcitabine in PBS (10 mM, pH 7.4) (100 mg per kg of body weight, twice a week). After a two-day break, the injections were repeated once. On day 17, three mice in each group were euthanized to collect tumor samples and spleens. The tumor samples were used for histological evaluations, and the spleens were used to prepare splenocytes to carry out *in vitro* CTL assays. The CTL assay was completed as previously described,

and the target cells used were the TC-1 cells (Ren et al., 2004). The 24JK cells, another C57BL/6 mouse lung cell line that does not express the HPV 16 E6 and E7 oncogene proteins (Hwu et al., 1995), were used as the non-target control cells. To evaluate the kinetics of the CTL response, a group of TC-1 tumor-bearing mice were treated as above. On days 10, 20, 30, and 40 after the tumor injection, mice (n = 4) were sacrificed to collect their splenocytes for CTL assay. Negative control mice were tumor-free and left untreated. Positive control mice were tumor-free, but immunized with the complexes of poly(I:C) with an MHC class I-restricted epitope derived from the HPV 16 E7 protein (pI:C/E7$_{49-57}$) on days 0 and 14 (Cui and Qiu, 2006), and their spleens were collected on day 40.

Balb/C mice with the breast cancer (410.4 cells, 1 x 10^6) were also treated similarly. The 410.4 cells were originally isolated from a single spontaneous mammary tumor. The cells are highly metastatic and weakly immunogenic. They grew very slowly in the injection site.

5.3.5 Histology

To detect apoptosis, the immunohistochemistry was performed using the cleaved caspase-3 (Asp175) (5A1) rabbit mAb (Cell Signaling Technology, Danvers, MA) following a protocol provided by the manufacturer. Assessment of the apoptosis was performed at 400 x magnification using a counting grid eyepiece graticule. A minimum of 1,000 cells per section within ten random fields were scored for cleaved caspase-3 positivity. The apoptotic index was defined as the %

of the cleaved caspase-3^{+} cells among the total counted cells. For haematoxylin and eosin (H & E) staining, tumor tissues were fixed in 10% neutral buffered formalin, processed on a Tissue-Tek VIP5 Tissue Processor (Sakura), and then embedded in Paraffin Type 9 (Richard-Allen Scientific, Kalamazoo, MI). The tissues were sectioned at 4-5 microns and then stained with Gill-3 Haematoxylin (Fisher Scientific) followed by Eosin Y Alcoholic (Fisher). The slides were observed under a light microscope.

5.3.6 Calculation of combination index in *in vivo* studies

The combination effect was evaluated as previously described (Dings et al., 2003). An index of greater than 1 indicates the presence of a synergistic effect whereas an index of 1 or less than 1 indicates an additive effect or less than additive effect, respectively.

5.3.7 Statistical analysis

Except that the survival curves were compared using the Kaplan-Meier method (GraphPad Prism 5), other statistical analyses were completed using ANOVA followed by pair-wise comparisons using the Fisher's protected least significant different procedure. A *p*-value of < 0.05 was considered to be statistically significant.

5.4 Results

5.4.1 Poly(I:C) inhibited tumor growth *in vitro* and *in vivo*

First, we confirmed the anti-tumor activity of the poly(I:C) using the TC-1 tumor cells in culture. Although 'naked' poly(I:C) did not inhibit the TC-1 cell growth at a concentration as high as 300 nM (data not shown), the poly(I:C) in the form of the poly(I:C)-lipoplexes was apparently cytotoxic, with an IC_{50} value of 1.42 nM (Fig. 5.1A). The supernatant of the TC-1 cells cultured in the presence of the poly(I:C)-lipoplexes also significantly inhibited the growth of fresh TC-1 cells (Fig. 5.1B).

We then evaluated the poly(I:C)'s ability to inhibit the growth of the TC-1 tumors in mice. Data in Fig. 5.1C showed that tumors in mice injected with the liposomes alone grew uncontrolled, and the mice died ~20 days after the tumor implantation. The poly(I:C)-lipoplexes significantly delayed the tumor growth (Fig. 5.1C). However, the tumor growth was delayed for only 7 days, thereby indicating that the poly(I:C)-lipoplexes alone were not sufficiently effective. Finally, when a similar experiment was carried out using a model pancreatic tumor cells (Panc-02) in mice, the poly(I:C)-lipoplexes also significantly extended the survival of the Panc-02 tumor-bearing mice (Fig. 5.1D), and 2 of the 7 mice became tumor-free in the end. The following combination therapy experiments were mainly carried out using the TC-1 lung cancer model because the TC-1 cells grew much faster in mice than the Panc-02 cells. Also, the poly(I:C)-lipoplexes alone tended to be less effective in the TC-1 tumor model.

5.4.2 Combination therapy using the poly(I:C)-liposome lipoplexes and gemcitabine synergistically further inhibited tumor growth *in vitro* and *in vivo*

Shown in Fig. 5.2A are the dose-effect plots when the TC-1 cells in culture were treated with the poly(I:C)-lipoplexes, gemcitabine, or their mixture. The IC_{50} values for the gemcitabine, the pI:C/LP, and their mixture were 0.04 nM, 1.42 nM, and 0.60 nM, respectively. Because the dose-effect plots in Fig. 5.2A did not indicate whether the activities of the gemcitabine and the poly(I:C)-lipoplexes were mutually exclusive or non-exclusive, the combination index (CI) was calculated on the basis of both mutually exclusive and non-exclusive assumptions. When assumed mutually exclusive, at high fraction affected (Fa) values, there was a marked synergism for their combined effect (CI < 1) (Fig. 5.2B). When assumed mutually non-exclusive, the combined effect was also synergistic, except that an antagonism was likely at very high Fa values (Fig. 5.2B). Thus, the combined tumor-inhibitory effect of the gemcitabine and the poly(I:C)-lipoplexes was generally synergistic in cell culture.

In vivo, combination treatment with gemcitabine and poly(I:C)-lipoplexes, dosing schedule shown in Fig. 5.2C, significantly further delayed the tumor growth (Fig. 5.2D) and prolonged the survival of the mice (Fig. 5.2E), as compared to treatment with the poly(I:C)-lipoplexes alone or the gemcitabine alone. In fact, the time it took for the tumors in mice treated with PBS, poly(I:C)-lipoplexes, gemcitabine, or the combination of poly(I:C)-lipoplexes and gemcitabine to reach 800 mm^3 (or 11.5-12.5 mm in diameter) was 15.7 ± 0.7, 18.6

± 1.7, 35.4 ± 0.9, and 43.2 ± 4.3 days, respectively, and the combination treatment significantly delayed the tumor growth as compared to the gemcitabine single treatment ($p = 0.003$). Interestingly, the tumors in mice received the combination treatment were suppressed for more than 30 days, and for unknown reasons started to grow about 30 days after the tumor cell injection (or 16 days after the last dosing). Also, the combined anti-tumor activity was synergistic. For example, on days 7 and 19 after the tumor cell injection, the tumor volume synergistic indexes were 1.63 and 2.06, respectively. Shown in Fig. 5.2F are typical photographs of the tumors 17 days after the TC-1 cell injection.

5.4.3 The combination therapy enhanced the proportion of the tumor cells undergoing apoptosis

Very few apoptotic cells were detected in the tumors in mice left untreated (Fig. 5.3Aa). Apoptosis was apparent in the tumors in mice received the poly(I:C)-lipoplexes (Fig. 5.3Ab) or the gemcitabine alone (Fig. 5.3Ac). The combination treatment generated significantly more positive staining than each of the single treatment alone (Fig. 5.3Ad). In fact, the apoptotic index of the combination therapy was more than 3-fold higher than any of the single treatments alone (Fig. 5.3B).

5.4.4 Histology

Significant areas of necrosis (20-60%) were detected in the large tumors (central or disseminated) in mice injected with the sterile PBS. Infiltration of the tumors by mononuclear cells and polymorphonuclear cells was rare and

peritumoral (Fig. 5.4A, B). Necrosis was also extensive (40-60%) in the tumors in mice received the poly(I:C)-lipoplexes alone but mainly in the center of the tumors. There was severe infiltration of mononuclear and polymorphonuclear cells in the periphery of the tumors. Moreover, severe edema was also apparent in these tumors (Fig. 5.4C, D). Necrosis was rare in the tumors in mice received the gemcitabine alone. Cellular infiltration and edema were rare to moderate in these tumors (Fig. 5.4E, F). Finally, necrosis was random but extensive (60-80%) in tumors in mice received the combination therapy. Cellular infiltration of the tumors was rare, but located inside the tumors (Fig. 5.4G, H).

5.4.5 The combination therapy generated a specific tumor lytic immune response, which alone was unable to control the tumor growth

Data in Fig. 5.5A showed that a TC-1 specific CTL response was induced in tumor-bearing mice received the combination treatment. At the effector to target ratio of 50:1, a weak target cell lysis was also detectable in mice injected with the poly(I:C)-lipoplexes alone (data not shown). However, there was not any detectable CTL activity in mice injected with the gemcitabine alone, nor in mice injected with sterile PBS. In addition, when the 24JK cells were used as the target, no significant CTL activity was detected in any of the mice (data not shown), indicating that the tumor cell lytic activity was specific against the TC-1 tumor cells.

To understand why the specific CTL activity in tumor-bearing mice received the combination therapy failed to control the tumor growth after the

termination of the treatment (Fig. 5.2D), we evaluated the durability of the CTL activity. As shown in Fig. 5.5B, although a TC-1 specific CTL activity was not detectable in mice 10 days after the beginning of the combination therapy, a CTL response became apparent 20 days after the beginning of the therapy, and was still strong on days 30 and 40 (Fig. 5.5B). Thus, the combination therapy had induced a relatively strong and long-last specific tumor lytic immune response, but the response alone failed to effectively control the tumor growth after the combination therapy was terminated.

5.4.6 The combination therapy synergistically inhibited the growth of breast cancer cells in a mouse model

The 410.1 breast cancer cells were shown to be sensitive to both poly(I:C)-lipoplexes and the gemcitabine, and the combination of them significantly further inhibited the growth of the 410.4 breast cancer cells in culture (data not shown). *In vivo,* a combination therapy using the poly(I:C)-lipoplexes and the gemcitabine also synergistically delayed the growth of the 410.4 tumors (Fig. 5.6). On days 10, 19, and 35 after the tumor cell injection, the synergistic indexes for the tumor volume were 1.68, 3.87, and 4.63, respectively.

5.5 Discussion

In the present study, we showed that the treatment of model solid tumors in mice with the poly(I:C)-lipoplexes and gemcitabine synergistically inhibited the tumor growth and prolonged the survival of the mice. The combination therapy also induced a strong and durable tumor-specific CTL response, although the CTL

response alone was unable to effectively control the tumor growth after the termination of the treatment. When fully optimized, this approach may represent a promising modality to improve the clinical outcomes of the therapy of cancers sensitive to both gemcitabine and synthetic dsRNA. For example, a dsRNA therapy may be integrated into the standard gemcitabine therapy to improve the resultant therapeutic outcome.

The anti-tumor activity of the poly(I:C) was known for decades. It is known that dsRNA activates a number of pro-apoptotic processes, including the PKR and the 2,5-oligo A pathways, both of which turn off protein synthesis and ultimately lead to cell death (Farrell et al., 1978). More recent data also showed that the direct binding of the TLR3 on the surface of certain human breast cancer cells with poly(I:C) also triggered apoptosis (Salaun et al., 2006). In addition, dsRNA has indirect anti-tumor activities. Poly(I:C) is a very potent inducer of type I IFN-α/β (Absher and Stinebring, 1969), which are known to have multiple anti-tumor mechanisms (see review (Chawla-Sarkar et al., 2003)). Firstly, they are anti-proliferative and can affect all phases of the mitotic cell cycling, most commonly with a blockade of the G1 phase (Balkwill and Taylor-Papadimitriou, 1978). Secondly, type I IFNs are pro-apoptotic and were shown to be cytotoxic to malignant cells (Chawla-Sarkar et al., 2001). In general IFN-induced cell death occurs > 48 hours after treatment and can be prevented by inhibitors of caspase-8 or caspase-3 (Chawla-Sarkar et al., 2001). Finally, type I IFNs also inhibit tumor

angiogenesis. Following treatment with IFNs, tumor endothelial cells exhibit microvascular injury and necrosis (Sidky and Borden, 1987).

Starting from the end of 1960, there had been numerous studies using synthetic dsRNA to inhibit tumors in experimental animal models and in clinical trials. The poly(I:C) was generally dosed systemically, and the anti-tumor activity of the poly(I:C) was mainly attributed to its ability to induce the production of type I IFNs, which then either kill tumor cells or enhance the host immune response. However, the effects of the systemic poly(I:C) on tumors are not consistent, and higher doses of systemic poly(I:C) may generate unwanted effects (Anderson et al., 1972; Larson et al., 1970; Meier et al., 1970; Pimm et al., 1976; Sakurai et al., 1990; Weinstein et al., 1971). In contrast, the local administration of poly(I:C) has been shown to be rather more effective in suppressing tumor growth (DuBuy, 1972; Pimm et al., 1976; Shir et al., 2006). For example, it was shown that the growth of transplanted rat tumors was retarded and in some cases completely suppressed when the tumor cells were injected s.c. in admixture with poly(I:C). Systemic treatment of the same tumor with the poly(I:C) failed to prevent the progressive growth of a range of rat tumors (Pimm et al., 1976). The total tumor regression observed by Shir et al. after direct intratumoral injection of tumor cell-targeting poly(I:C) is another example (Shir et al., 2006). Thus, the direct cytotoxic effects of the poly(I:C) seemed to be more effective in suppressing tumor growth than the indirect effects from the IFNs induced by the poly(I:C), which prompted us to inject the poly(I:C) locally in the present study. The cationic

liposomes were used as a carrier for the poly(I:C) to improve the uptake of the poly(I:C) by the tumor cells. Only when delivered inside tumor cells, can the poly(I:C) cause cell death directly by interacting with the intracellular proteins such as the PKR and the 2,5-oligo A synthetase (Farrell et al., 1978). It needs to be emphasized that the peritumoral route was chosen in the present study simply to prove the feasibility of this combination therapy. This local injection is feasible for a few tumors such as melanoma and certain head and neck cancers, but may be clinically difficult to practice for other tumors. Therefore, we are currently focused on developing a delivery system to target dsRNA into tumor cells after intravenous injection.

It was interesting that a relatively strong and durable tumor-specific CTL immune response was induced by the combination therapy (Fig. 5.5). The immunostimulatory activity of the poly(I:C) was originally established in the 1960-1970's (Park and Baron, 1968). However, it was not until recently that the TLR3 was identified as a receptor of dsRNA (Alexopoulou et al., 2001), and interest in studying its immunostimulatory activity was revived again. To summarize, dsRNA was shown to induce the maturation of human DCs (Verdijk et al., 1999), to augment NK cell-mediated cytotoxicity (Schmidt et al., 2004; Sivori et al., 2004), to promote the survival of T cells (Cui and Qiu, 2006; Gelman et al., 2004; Salem et al., 2005). Moreover, the cellular protein RIG-1 also senses intracellular dsRNA and stimulate dsRNA-induced innate immune responses (Schulz et al., 2005; Yoneyama et al., 2004). Recently, it was shown that mouse

$CD8a^+$ DCs were activated by virus-infected cells, but not by uninfected cells (Schulz et al., 2005). Similarly, the $CD8\alpha^+$ DCs were activated by irradiated epithelial Vero cells pre-loaded with poly(I:C), but not by irradiated Vero cells in the absence of poly(I:C). The activation of DCs required the phagocytosis of infected cells (or the irradiated cells) by the DCs, followed by TLR3 signaling (Schulz et al., 2005). Immunization of mice with dead tumor cells with poly(I:C) transfected inside also led to a stronger anti-tumor immune responses than with the same dead tumor cells admixed with poly(I:C) (Cui et al., 2007). Moreover, the type I IFNs induced by dsRNA are also immunostimulatory. Type I IFNs were shown to augment cytotoxic T cells, NK cells, and DCs and promote the cross-priming of $CD8^+$ T cells by stimulating the maturation of DCs (Le Bon et al., 2003). All these direct and indirect immuno-stimulatory activities of the dsRNA, as well as the immuno-modulatory effects of the gemcitabine mentioned early (Nowak et al., 2002; Suzuki et al., 2005; Suzuki et al., 2007), may explain the induction of the tumor-specific CTL response after the combination therapy. We speculate that the poly(I:C) and the type I IFNs induced by the poly(I:C) have likely promoted the dead or dying tumor cells generated by the gemcitabine and the poly(I:C) to cross-prime tumor cell-specific $CD8^+$ T cells. The tumor cell apoptotic bodies generated by gemcitabine were shown to be a good source of tumor antigens (Nowak et al., 2003a), and intratumoral or p.t. injection of poly(I:C) was also shown to generate some weak specific $CD8^+$ T cell responses (Fujimura et al., 2006). However, a more interesting finding in this study is that

the specific tumor-killing immune response, being strong and durable when assayed *in vitro* (Fig. 5.5), evidently failed to control the tumor cell growth after the combination treatment was terminated (Fig. 5.2D). Although it is unknown whether the tumor cell-specific T cells have reached the tumor tissues or not, the H & E micrographs shown in Fig. 5.4 indicated that there was infiltration of the immune cells into the center of the tumor tissues. Thus, it is possible that these tumor cells that escaped the action of the poly(I:C) and the gemcitabine were also resistant or became insensitive to the killing by the specific immune cells. Detailed mechanisms to explain the lack of effectiveness of the specific immune responses induced by the combination treatment will be further elucidated in future experiments. However, the data in Fig. 5.2D and Fig. 5.5 did suggest that more efforts may need to be directed towards “persuading” more tumor cells to die from the direct cytotoxic effects of the poly(I:C) and the gemcitabine. This may be achieved by actively targeting the chemicals into tumor cells. On the other hand, the tumor-specific immune responses induced by the combination of the poly(I:C)-lipoplexes and the gemcitabine may have partially contributed to the observed synergism of the *in vivo* anti-tumor activity. Another possible explanation to the observed synergism, both *in vivo* and *in vitro* (Figs. 5.2, 5.6), could be that the gemcitabine rendered the tumor cells more sensitive to the killing by the poly(I:C) or vice versa. We will further elucidate the mechanisms responsible for the observed synergism in future studies.

Finally, we speculate that the anti-tumor activity of the combination therapy using the poly(I:C) and the gemcitabine may be further improved by optimizing the dosing schedule. In the present study, we dosed the poly(I:C) and the gemcitabine concurrently to the tumor-bearing mice, reasoning that this schedule will expose the tumor cells to both poly(I:C) and gemcitabine simultaneously. Since the cytotoxic mechanisms of the poly(I:C) and gemcitabine differ from each other, simultaneous exposure of the same cell to both chemicals may result in a faster and more effective killing of the tumor cell. In addition, the concurrent dosing of the gemcitabine and the poly(I:C) may also allow the poly(I:C) to more effectively promote the dead or dying tumor cells generated by the gemcitabine to prime the induction of specific immune responses. However, this concurrent dosing schedule may not be optimal. In previous studies where the therapy involved the gemcitabine and other immunostimulatory molecules, the gemcitabine was dosed first, and the immunostimulatory molecules (e.g., CpG oligos or the anti-CD40 antibody FGK45) were dosed after the gemcitabine application was completed (Nowak et al., 2003a; Pratesi et al., 2005). It was shown that this sequential dosing schedule was much more effective than when they were dosed concurrently (Pratesi et al., 2005). It is possible that if the tumor-bearing mice in our study were dosed with the gemcitabine first followed by the poly(I:C)-lipoplexes, the resultant anti-tumor activity would be stronger. More experiments will have to be carried out to identify the more effective dosing schedule. Finally, we completed only two cycles of combination dosing in the

present study (1 cycle per week). We expect that the anti-tumor activity of the combination therapy can be further improved by increasing the number of dosing cycles and/or by allowing more appropriate time between each dosing cycle to allow the small fraction of unaffected tumor cells to enter into an active growth stage and be more effectively killed in the following dosing cycle.

Finally, the combination therapy also synergistically inhibited the growth of a model breast tumor in mice, suggesting that this approach is applicable for many tumors. Also, we would like to point out that compared to the TC-1 cells, the 410.4 breast cancer cells grew much slower in mice and tended to metastasize. Moreover, the 410.4 cells are weakly immunogenic, while the TC-1 cells are strongly immunogenic. Thus, more experiments need to be carried out to evaluate the extent to which the adaptive immune response induced by the combination therapy was responsible to the tumor growth delay observed in Figs. 5.2D and 5.6.

In conclusion, we reported a novel combination tumor chemotherapy approach that synergistically improved the resultant anti-tumor activity. The combination therapy increased the percent of tumor cells undergoing apoptosis and promoted the induction of a strong and durable tumor-specific immune response. After further optimization, this approach may improve the clinical outcomes for the therapy of the cancers sensitive to both gemcitabine and dsRNA. A similar strategy may also be adopted to combine synthetic dsRNA and other chemotherapy agents to more effectively fight other cancers.

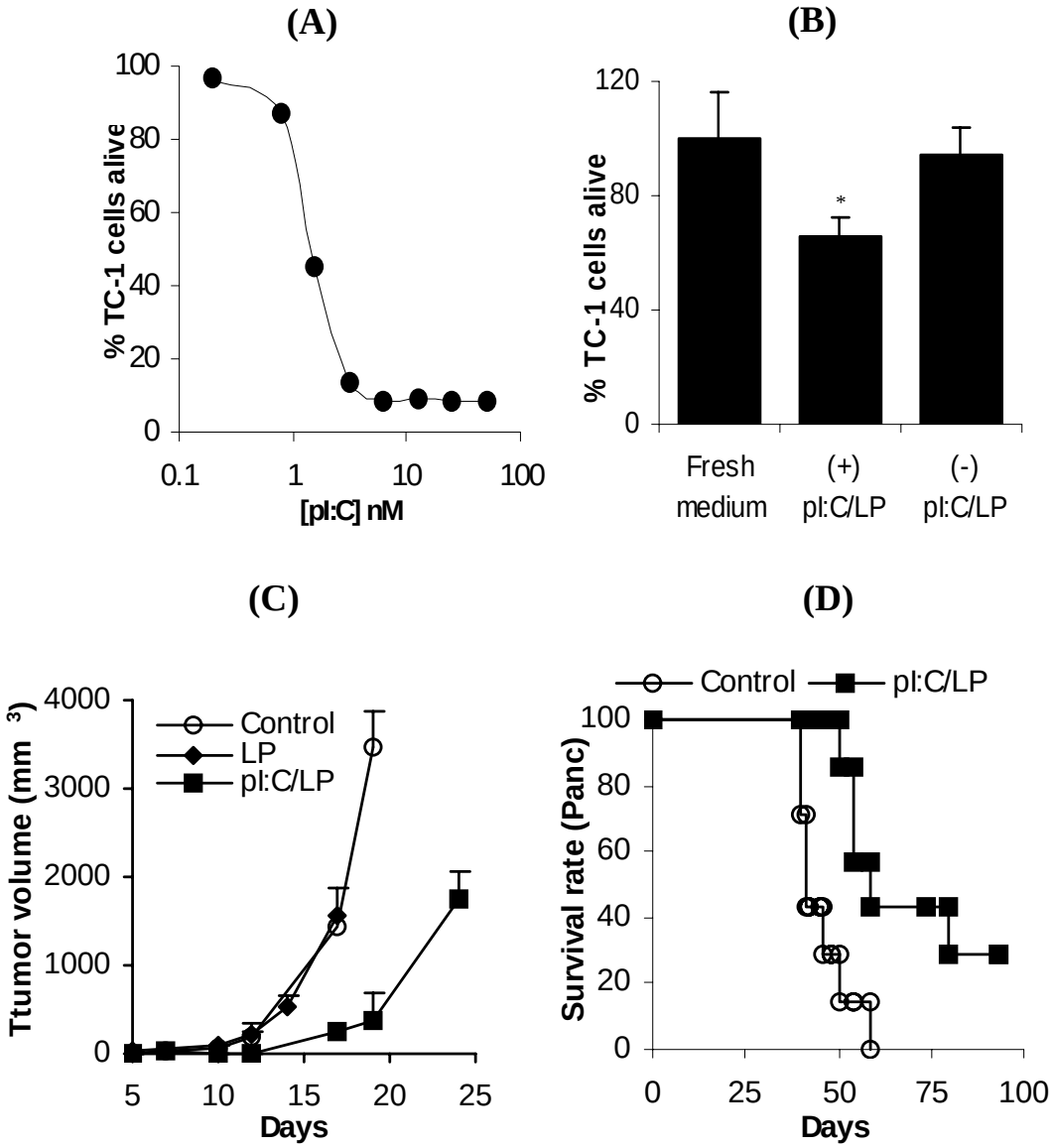

Figure 5.1 Poly(I:C)-in-lipoplexes inhibited tumor growth *in vitro* and *in vivo*. (**A**). Dose-effect plot of the % TC-1 cells alive as a function of the concentration of the pI:C in pI:C/LP (n = 3). (**B**). Indirect killing effect of the pI:C. The supernatant of TC-1 cells incubated with the pI:C/LP inhibited the growth of fresh TC-1 cells (n = 3). The (*) indicates that the value of the (+) pI:C/LP differs from that of the other two. (**C**). pI:C/LP delayed the growth of TC-1 tumors in mice (n = 7). (**D**). pI:C/LP prolonged the survival of Panc-02 tumor-bearing mice (p = 0.02, n = 7). Two of the 7 mice became tumor-free.

(A)

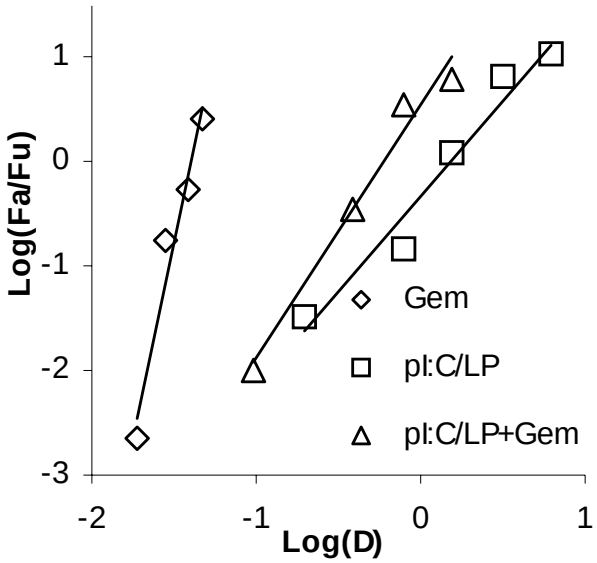
Log(Fa/Fu)
Log(D)
Gem
pl:C/LP
pl:C/LP+Gem

(B)

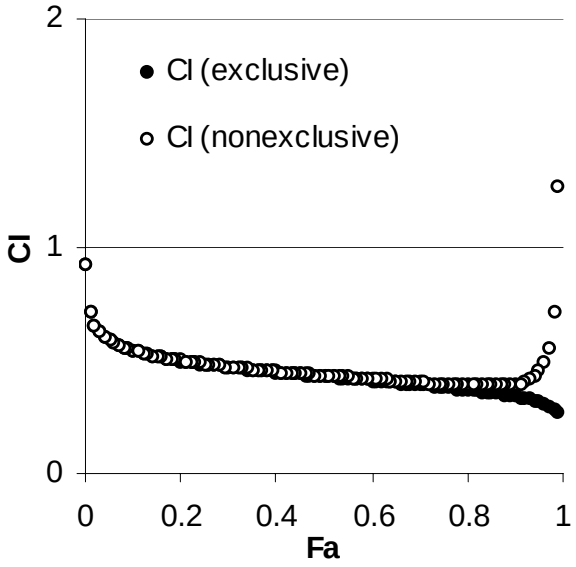
CI
Fa
CI (exclusive)
CI (nonexclusive)

Figure 5.2

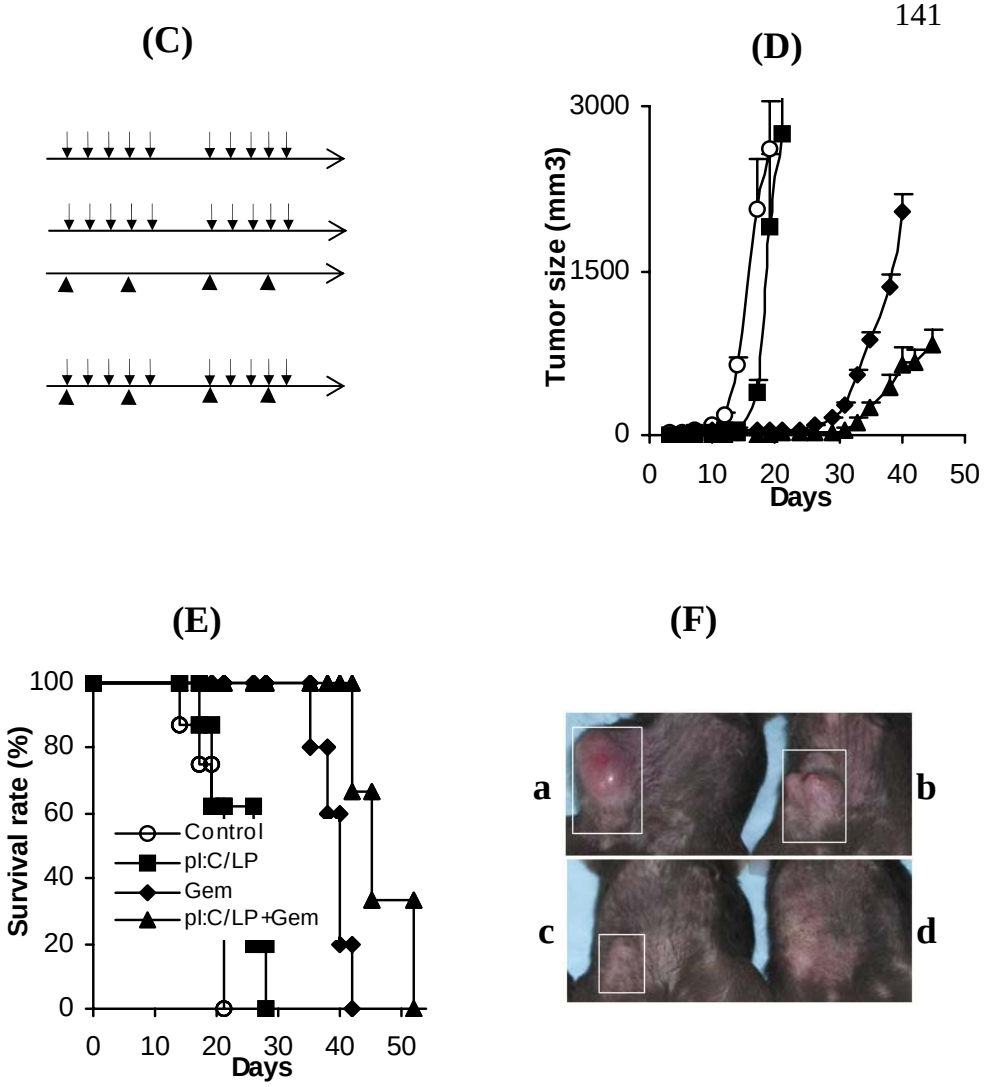

Figure 5.2 The combination of poly(I:C)-in-lipoplexes and gemcitabine synergistically inhibited tumor growth *in vitro* and *in vivo*. (**A**). Dose-effect plots showing the killing of TC-1 cells by gemcitabine, pI:C/LP, or their mixture (3290:1, pI:C/Gem). Fa is the fraction of cells affected/killed. Fu is the fraction of cells un-effected. D is the dose in nM. (**B**). Combination index (CI) with respect to the Fa. (**C**). *In vivo* dosing schedule. (**D**). TC-1 tumor growth kinetics. The values of the Gem and pI:C/LP+Gem differed starting from day 5. Data reported are mean ± S.E.M. (n = 6-7). (**E**). Survival of mice with TC-1 tumors (p = 0.003, Gem *vs*. pI:C/LP+Gem). (**F**). Photographs of typical tumors in mice 17 days after tumor cell injection. (a) PBS, (b) pI:C/LP, (c) Gem, (d) pI:C/LP+Gem.

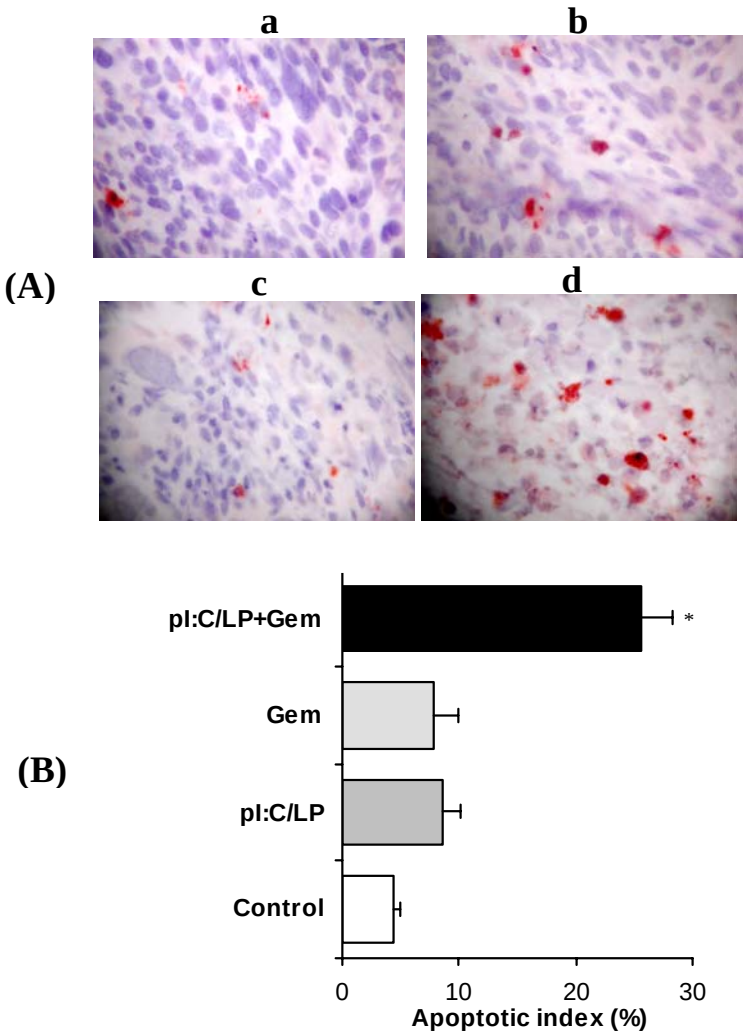

Figure 5.3 The combination therapy promoted more tumor cells to undergo apoptosis *in vivo*. (**A**). Micrographs of tumors stained against activated Caspase-3 into red. (a). PBS, (b). pI:C/LP, (c). Gem, (d). pI:C/LP+Gem, (**B**)**.** Apoptotic index. Data reported are mean ± S.D. (n = 3). (*) indicates that the value of the pI:C/LP+Gem differs from that of the others. The values of the Gem and the pI:C/LP alone were comparable.

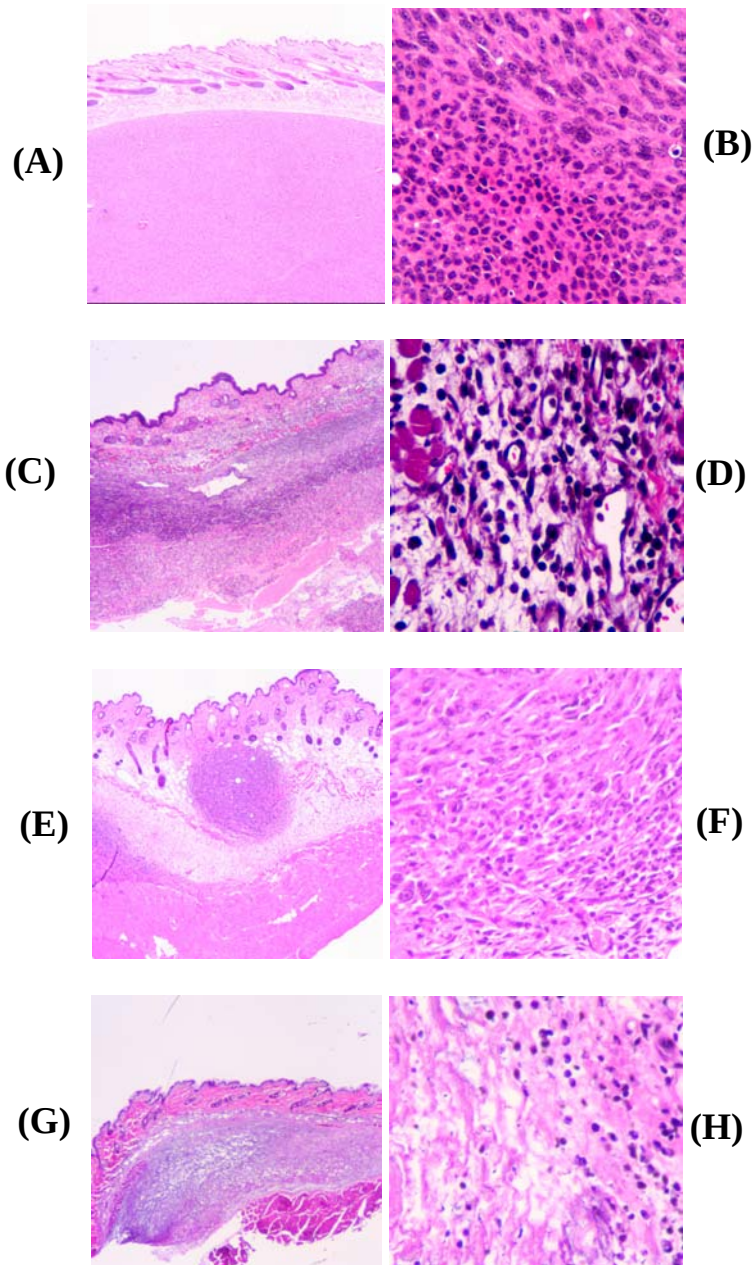

Figure 5.4 H & E micrographs. (**A**, **B**) PBS, (**C**, **D**) pI:C/LP, (**E**, **F**) Gem, (**G**, **H**) pI:C/LP+Gem. A, C, E, and G, 4 x magnification; B, D, F, and H, 40 x magnification.

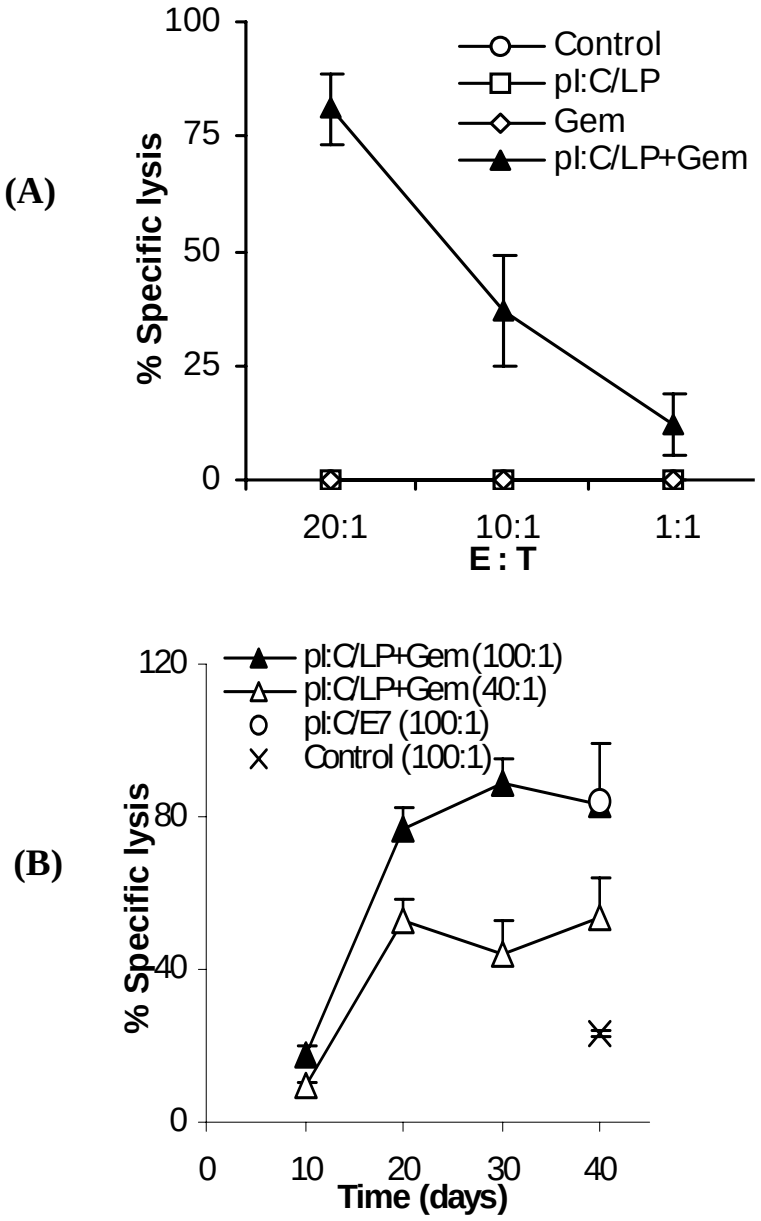

Figure 5.5 Combination therapy using pI:C/LP and gemcitabine induce tumor-specific CTL responses (**A**), and the CTL response was still strong 40 days after the tumor cell implantation (**B**). Data in A and B were from two separate experiments. In B, the (x) and (O) were the values of the negative and positive controls, respectively. The numbers in the parentheses (100:1 or 40:1) are the E to T ratios.

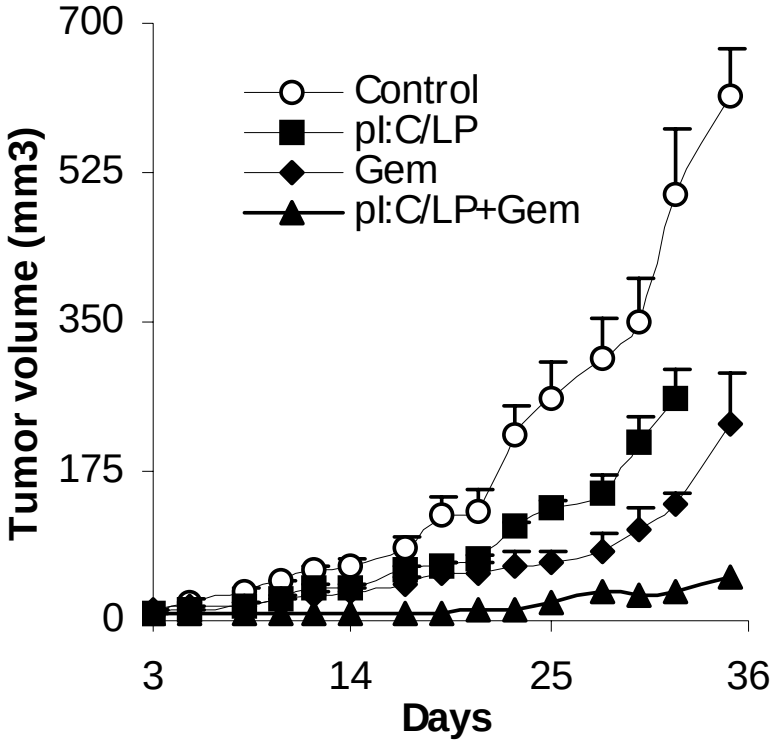

Figure 5.6 The combination therapy also synergistically inhibited the growth of a model breast cancer (410.4) *in vivo*. Data reported are mean ± S.E.M. (n = 7-8). The values of the Gem and the pI:C/LP+Gem differ from each other starting from day 5. The 410.4 cells in the injection site grew very slowly and tended to metastasize spontaneously.

Chapter 6

LOCALIZED IRRADIATION OF TUMORS PRIOR TO SYNTHETIC dsRNA THERAPY ENHANCED THE RESULTANT ANTI-TUMOR ACTIVITY

Uyen M. Le , Darryl G. L. Kaurin , Brian R. Sloat , Nijaporn Yanasarn , and Zhengrong Cui

Manucsript Submitted for Publication

6.1 Abstract

Despite of the potent tumoricidal activity of the synthetic dsRNA in culture, its *in vivo* anti-tumor activity has proven to be limited. We sought to devise and validate a new strategy to improve the *in vivo* anti-tumor activity by integrating localized irradiation into the dsRNA therapy. Using a mouse lung cancer model and a mouse melanoma model in immuno-competent mice or athymic nude mice, we evaluated the combined anti-tumor activity using a synthetic dsRNA, polyinosine-cytosine (poly(I:C)). Localized irradiation of tumors prior to the poly(I:C) therapy significantly delayed the tumor growth as compared to monotherapies using the radiation or poly(I:C) alone. The combined effect was synergistic only in immuno-competent mice with highly immunogenic tumors, but was simply additive in immuno-competent mice with poorly immunogenic tumors and in nude mice with highly immunogenic tumors. The anti-tumor activity of the combination therapy was significantly impaired when the type I interferons in the mice were neutralized. This combination modality may represent a promising approach to exploit synthetic dsRNA in cancer therapy. T cell-mediated immunity was likely responsible for the combined synergistic effect. Type I interferons contributed significantly to the resultant anti-tumor activity.

6.2 Introduction

Cancer is one of the leading causes of death in the U.S. New or improved approaches to control cancers are constantly sought. Double-stranded RNA can

activate multiple pro-apoptotic mechanisms simultaneously (Chawla-Sarkar et al., 2003). It also induces apoptosis in certain tumor cells by interacting with the Toll-like receptor 3 (TLR3) (Salaun et al., 2006). Moreover, dsRNA is a potent inducer of type I interferons (IFNs) (Absher and Stinebring, 1969), which are pro-apoptotic, anti-proliferative, and anti-angiogenic (Balkwill and Taylor-Papadimitriou, 1978; Chawla-Sarkar et al., 2001; Chawla-Sarkar et al., 2003; Sidky and Borden, 1987). Finally, both dsRNA and the type I IFNs induced by it are strongly immunostimulatory (Le Bon et al., 2003; Schulz et al., 2005; Sivori et al., 2004; Yoneyama et al., 2004). Previously, there had been numerous studies utilizing the poly(I:C) to control tumors in experimental animal models and clinical trials, and the anti-tumor activity was attributed to a large extent to the poly(I:C)'s ability to induce the production of type I IFNs. Overall, the anti-tumor activity of the poly(I:C) was limited and inconsistent *in vivo* (Gazdar, 1972; Sakurai et al., 1990; Weinstein et al., 1971), and higher doses of poly(I:C) were reported to be associated with adverse effects (De Clercq et al., 1972; Freeman et al., 1977; Okada et al., 2005).

Recently, efforts to exploit the anti-tumor activities of synthetic dsRNA to kill tumor cells were revived again (Fujimura et al., 2006; Le et al., 2007; Shir et al., 2006). *In vitro*, when delivered into tumor cells using cationic liposomes, poly(I:C) inhibited the growth of a variety of tumor cells with IC_{50} values in the nM range (Hirabayashi et al., 1999; Le et al., 2007). In a nude mouse model, Shir et al. (2006) reported that targeting the poly(I:C) into human glioblastoma cells or

breast cancer cells over-expressing epidermal growth factor receptors by direct intratumoral injection led to the regression of pre-established tumors (Shir et al., 2006). In a more recent study, we reported an alternative approach to improve the anti-tumor activity of the poly(I:C) by combining the dsRNA therapy with a chemotherapy agent, gemcitabine (Le et al., 2007). Our data showed that the poly(I:C) and gemcitabine synergistically delayed the tumor growth and prolonged the survival of the tumor-bearing mice (Le et al., 2007). The combination therapy also generated a strong and durable tumor-specific immune response (Le et al., 2007). This combination approach may help decrease the dose of the poly(I:C), and thus, minimize its adverse effects.

In the present study, we evaluated the feasibility of integrating radiotherapy into the poly(I:C) therapy to improve the anti-tumor activity of the poly(I:C). Ionizing radiation has a well-established ability to kill tumor cells (Watters, 1999). We hypothesized that localized irradiation of the tumors prior to the poly(I:C) therapy will improve the resultant anti-tumor activity. Moreover, being a ligand to the TLR3, poly(I:C) is strongly immunostimulatory and can activate both innate and adaptive immune responses (Alexopoulou et al., 2001; Le Bon et al., 2003; Schulz et al., 2005). The tumor cells killed by the radiation are a good source of tumor antigens, and the dead tumor cells may be taken up by antigen-presenting cells, such as the dendritic cells, to induce T-cell mediated immunity (Demaria et al., 2004; Salio and Cerundolo, 2005). Therefore, we further hypothesized that T

cell-mediated immunity will contribute to the anti-tumor activity generated by the combination therapy.

Using a highly immunogenic lung tumor model in immuno-competent mice, we demonstrated that localized irradiation of the tumors prior to the poly(I:C) therapy synergistically improved the resultant anti-tumor activity as compared to monotherapies using the poly(I:C) or the radiation alone. However, the combined effect was only additive when the combination therapy was applied to the same tumors in athymic nude mice or to immuno-competent mice with a poorly immunogenic model tumor, indicating that the T cell-mediated immunity was responsible for the synergistic effect from the combination therapy. Finally, our data showed that the type I IFNs induced by the poly(I:C) contributed significantly to the anti-tumor activity from the combination therapy. When fully developed, it is expected that this combination therapy will represent a promising approach to more effectively take advantage of the anti-tumor activity of the synthetic dsRNA and to further improve the efficacy of the current radiotherapy.

6.3 Materials and Methods

6.3.1 Mice and cell lines

Female C57BL/6 mice, 6-8 weeks of age, were from Simonsen Laboratories, Inc. (Gilroy, CA). The Nu/Nu female nude mice (6-8 weeks) were from Charles River Laboratories, Inc. (Wilmington, MA). The TC-1 cells (ATCC #, CRL-2785), a highly immunogenic lung cancer cell line, were engineered by transforming primary C57BL/6 lung cells with human papillomavirus (HPV) type

16 E6 and E7 oncogenes and an activated H-*ras* (Lin et al., 1996). They were grown in RPMI 1640 medium (Invitrogen). The poorly or non-immunogenic B16-F10 mouse melanoma cells were from ATCC and grown in DMEM medium. All media were supplemented with 10% FBS, 100 U/mL of penicillin, and 100 μg/mL of streptomycin.

6.3.2 Preparation of poly(I:C)-liposome lipoplexes (pI:C/LP)

Cationic liposomes comprised of cholesterol, egg L-α-phosphatidylcholine, and 1, 2-dioleoyl-3-trimethylamonium-propane (DOTAP) (4.6:10.8:12.9, m/m/m, all from Avanti Polar Lipids) were prepared by the thin film hydration method. The final concentration of the DOTAP in the liposomes was 10 mg/mL. The pI:C/LP lipoplexes were prepared by mixing equal volumes of pI:C solution (50 μg, Amersham Biosciences, Piscataway, NJ) and the liposome suspension (8 μg of DOTAP) followed by gentle pipetting (Le et al., 2007).

6.3.3 Animal studies

NIH guidelines for animal use and care were followed. The animal protocol was approved by our institutional IACUC. To establish tumor models in mice, tumor cells (TC-1 or B16-F10, 5 x 10^5 cells/mouse) were subcutaneously (s.c.) injected in the right hind upper leg of mice. The hair, if any, in the injection site was carefully trimmed before the injection. The size of the tumors and the values of tumor growth delay were calculated as previously described (Milas et al., 2004). Tumor therapy was started when the diameters of the tumors reached 6-8

mm. To irradiate the tumors, anesthetized mice were restrained into a jig, while their right hind legs with tumors were exposed outside of the jig in a row. The tumors were irradiated with a desired dose of X-ray using a Varian 6/100 Accelerator (serial # 103). The X-ray field was 4.0 cm x 15.0 cm, and only the tumor-bearing legs were placed in the field. The dose of the X-ray was verified using thermoluminescent dosimetry. Mice were allowed to rest for one day before the start of the dosing of the pI:C/LP, which were injected peritumorally (p.t.) (or subcutaneously in a site distal to the tumors as where mentioned). The combined anti-tumor activity was evaluated as previously described (Dings et al., 2003). A combination index of greater than 1 indicates the presence of a synergistic effect; an index of ≤ 1 indicates an additive or less than additive effect.

6.3.4 *In vivo* IFN-α/β blockade

The *in vivo* IFN-α/β blockade was completed as previously described with slight modifications (Currie et al., 2008). Sheep antiserum to murine C-Cell IFNs (NR-3087) and sheep antiserum control for the NR-3087 were from the BEI Resources (Manassas, MD). Mice were intraperitoneally injected with 0.18 mL of the antiserum on days –1, +2, and +4 with respect to the first pI:C/LP administration (Currie et al., 2008).

6.3.5 Quantification of IFN-α in tumors and blood

Tumor samples were homogenized in a microtube using a mini beadbeater (BioSpec Products, Inc., Bartlesville, OK) and then centrifuged for 10 min. The

supernatant was collected. The concentration of IFN-α was determined using a mouse IFN alpha (Mu-IFN-α) ELISA kit (PBL Biomedical Laboratories, Piscataway, NJ).

6.3.6 Statistical analysis

Except that the survival curves were compared using the Kaplan-Meier method (GraphPad Prism 5), other statistical analyses were completed using ANOVA followed by pair-wise comparisons using the Fisher's PLSD procedure. A *p*-value of < 0.05 was considered statistically significant.

6.4 Results

6.4.1 Localized irradiation prior to the poly(I:C) therapy significantly delayed the growth of the highly immunogenic TC-1 tumors in immuno-competent mice

First, we confirmed that the poly(I:C) in the form of pI:C-liposome lipoplexes (pI:C/LP) significantly delayed the growth of the TC-1 tumors in mice, and that the poly(I:C) was more effective when injected peritumorally than when injected in a site distal to tumors (data not shown). Overall, the anti-tumor activity of the pI:C/LP lipoplexes was very limited. Localized irradiation of the TC-1 tumors significantly inhibited the tumor growth (Fig. 6.1A), and increasing the dose of the X-ray further prolonged the tumor growth delay (Fig. 6.1A). However, 40 Gy, the highest dose of X-ray we used, generated some observable side-effects, such as hair loss on the right hind leg and a relatively shorter mouse survival time (Fig. 6.1B). Thus, the dose of 20 Gy or less was used for further studies.

Data in Fig. 6.1C showed that localized irradiation prior to the start of the injection of the pI:C/LP significantly further delayed the tumor growth as compared to monotherapies using the radiation or the pI:C/LP alone. The mean time it took for the tumors to reach 12-13 mm after the first dose of pI:C/LP was 4.0, 5.3 ± 1.0, 4.8 ± 1.0, and 21.0 ± 4.6 days for the control, pI:C/LP, irradiation (IR), and the combination (IR+pI:C/LP) groups, respectively (Fig. 6.1C). The value of the tumor growth delay caused by the combination therapy was larger than that of the monotherapies ($p < 0.05$).

Finally, data in Fig. 6.1D showed that increasing the dose of the X-ray from 5 to 20 Gy enhanced the resultant anti-tumor activity by the combination therapy.

6.4.2 The combination therapy was more effective than the monotherapies in athymic nude mice with highly immunogenic tumors and in immuno-competent mice with poorly or non-immunogenic tumors

To understand whether the combination therapy was still effective in immuno-compromised mice or with poorly immunogenic tumors, we evaluated the anti-tumor activities in nude mice with the TC-1 tumors and in C57BL/6 mice with the poorly immunogenic B16-F10 melanoma. As shown in Fig. 6.2A, the combination therapy was still more effective than the monotherapies in delaying the growth of the TC-1 tumors in nude mice. The mean time it took for the tumors to reach 7-8 mm was 3.3 ± 2.4, 4.7 ± 1.4, 9.4 ± 6.0, and 19.1 ± 4.9 days for the control, pI:C/LP, IR, and IR+pI:C/LP groups, respectively (Fig. 2A, $p = 0.002$,

IR+pI:C/LP vs. IR, $p = 3 \times 10^{-6}$, IR+pI:C/LP vs. pI:C/LP). Similarly, in the B16-F10 mouse melanoma model, the combination therapy also significantly delayed the tumor growth (Fig. 6.2B). The diameters of the tumors in mice that received the combination therapy were significantly smaller than in mice received the monotherapies, starting 8 days after the first dose of pI:C/LP (e.g., on day 8, $p = 0.002$ vs. pI:C/LP, $p = 0.02$ vs. IR).

6.4.3 The immunogenicity of the tumors and the immuno-competency of the mice determined whether the combined activity was synergistic or additive

We calculated the combination index (CI) based on the diameter of the tumors after the combination therapy. As shown in Table 6.1, the combined effect was synergistic ($CI > 1.0$) only in the C57BL/6 mice with TC-1 tumors, but was additive or less than additive ($CI \leq 1.0$) in athymic nude mice with the TC-1 tumors and in the C57BL/6 mice with the poorly immunogenic B16-F10 melanoma.

6.4.4 The type I IFNs induced by the poly(I:C) contributed significantly to the anti-tumor activity of the combination therapy

Data in Fig. 6.3A showed that when the pI:C/LP was injected into a site distal to the tumors, the combination therapy significantly improved the resultant anti-tumor activity as well, although not as effective as when the pI:C/LP was injected close to the tumors.

As shown in Fig. 6.3B, peritumoral injection of the pI:C/LP induced a higher level of IFN-α in the tumor tissues than when the pI:C/LP was injected

distal to the tumors, whereas the levels of the IFN-α in the serum samples were comparable regardless of whether the pI:C/LP was injected close or distal to the tumors (Fig. 6.3C). The serum IFN-α level was measured 24 h after the injection of the pI:C/LP because the mouse serum IFN-α level peaked about 24 h after the pI:C/LP was subcutaneously injected into mice (Fig. 6.3D).

Finally, our data shown in Fig. 6.3E demonstrated that neutralization of the type I IFNs in the tumor-bearing mice significantly impaired the ability of the combination therapy to delay the tumor growth.

6.5 Discussions

Synthetic dsRNA has multiple anti-tumor mechanisms that may be exploited to control tumor growth. It is pro-apoptotic and immunostimulatory (Alexopoulou et al., 2001; Chawla-Sarkar et al., 2003; Le Bon et al., 2003; Meurs et al., 1993; Salaun et al., 2006; Schulz et al., 2005). It is a potent inducer of type I IFNs, which are known to be pro-apoptotic, immunostimulatory, and anti-angiogenic (Absher and Stinebring, 1969; Balkwill and Taylor-Papadimitriou, 1978; Chawla-Sarkar et al., 2001; Chawla-Sarkar et al., 2003; Sidky and Borden, 1987). Thus, it is not surprising that numerous studies have been carried out since the 1960's to materialize the tumor therapeutic potentials of the poly(I:C). Unfortunately, the results from previous studies including clinical trials have not been encouraging. In general, treatment with the poly(I:C) only slightly delayed the tumor growth, and the anti-tumor activity was inconsistent. Increasing the dose

of the poly(I:C) is not a practical option to improve the efficacy of the poly(I:C) because the poly(I:C) has serious dose-limiting adverse effects (De Clercq et al., 1972; Freeman et al., 1977; Okada et al., 2005). Nevertheless, data from some recent studies indicated that alternative approaches may be devised to improve the efficacy of the dsRNA therapy (Le et al., 2007; Shir et al., 2006).

In the present study, we designed and validated an approach that can potentially improve the clinical efficacy of dsRNA therapy. Ionizing irradiation is tumoricidal, which prompted us to locally irradiate the tumors prior to the dsRNA therapy. We hypothesized that the combination therapy will enhance the resultant anti-tumor activity, which was strongly supported by our data in Figs. 6.1C and 6.2A, B. In all these experiments, monotherapies using the poly(I:C) lipoplexes or the localized irradiation alone only slightly delayed the growth of the tumors. However, the tumor growth delay caused by the combination therapy was significantly longer (Figs. 6.1C, 6.2A, and 6.2B). Just one round of therapy using a single dose of X-ray followed by a few doses of the poly(I:C) significantly delayed the growth of the two different and very aggressive tumors. For example, the growth of the TC-1 cells was delayed by 17 days (Fig. 6.1C), which is significant considering that the TC-1 tumor-bearing mice can survive for only about 20 days if left untreated (Cui and Qiu, 2006). The B16-F10 melanoma cells grew even more aggressively. When 5×10^5 of B16-F10 cells were injected into the C57BL/6 mice, mouse death was observed as early as 12 days later. If more than one round of the combination therapy is to be applied, it is very likely that the tumor growth

delay will be more extensive. A fractionized radiation followed by poly(I:C) therapy is also expected to be more effective. In fact, tumor combination therapy using the poly(I:C) and localized radiation has been tested before (Leonidze et al., 1986; Lvovsky et al., 1988; Lvovsky et al., 1985), and the poly(I:C) was used as a radio-sensitizing agent and was given prior to the radiation. For example, it was shown that when Lewis lung carcinoma-bearing mice were dosed with poly(I:C) in the form of pI:C-poly-L-Lysine complexes 6 h before radiation (4 Gy), three times in 1.5 weeks, the combination treatment significantly delayed the tumor growth, although mechanistic studies were not reported (Lvovsky et al., 1985). However, the regimen of radiation followed by poly(I:C) therapy is likely preferred because a proper dose of localized radiation is expected to significantly decrease the tumor load so that the follow-up poly(I:C) therapy will become more effective. Moreover, our unpublished data suggested that radiation followed by the poly(I:C) therapy seemed to be more effective than when the radiation was administered after the completion of the poly(I:C) therapy.

Evidently the direct tumoricidal activity of the localized irradiation have contributed significantly to the anti-tumor activity from the combination therapy because a decreased dose of X-ray generated a decreased anti-tumor activity when the dose and dosing schedule of the poly(I:C) remained unchanged (Fig. 6.1D). Poly(I:C) is multi-functional, and we expected that multiple anti-tumor mechanisms have contributed to the improvement of the anti-tumor activity. Poly(I:C) has direct tumor-killing activity, especially when delivered inside tumor

cells (Chawla-Sarkar et al., 2003; Meurs et al., 1993; Salaun et al., 2006). Immunohistology data from our previous study showed that the peritumorally injected poly(I:C)-lipoplexes induced significant tumor cell apoptosis (Le et al., 2007). Thus, it is very likely that the direct pro-apoptotic activity of the poly(I:C) has contributed to some extent to the anti-tumor activity from the present combination therapy. The involvement of the poly(I:C) in the direct killing of the tumor cells was also partially supported by our data in Fig. 6.3A, which showed that the poly(I:C) was more effective in controlling the tumor growth when injected peritumorally than when injected in a site distal to the tumors. However, the stronger anti-tumor activity generated by the peritumorally injected poly(I:C) may be attributed to other reasons too. In the present study, we primarily examined whether the T cell-mediated immunity and the type I IFNs induced by the poly(I:C) have contributed to the resultant anti-tumor activity.

Our data in Fig. 6.2A showed that the combination therapy was still more effective than the monotherapies in delaying the growth of the TC-1 tumors in the athymic nude mice (Fig. 6.2A). This finding is interesting because data from recent studies indicated that functional T cells were indispensible in the anti-tumor activity generated by combination therapy using localized radiation and CpG oligos, because the combinational CpG-irradiation therapy was no more effective than the irradiation alone in delaying the tumor growth in athymic nude mice or in whole-body irradiated mice (Mason et al., 2005; Meng et al., 2005; Milas et al., 2004). CpG motifs are a ligand to TLR9 (Hemmi et al., 2000), and the poly(I:C) is

a ligand to TLR3 (Alexopoulou et al., 2001). Both CpG motifs and poly(I:C) are immunostimulatory. Thus, we expected that the combinational poly(I:C)-localized irradiation therapy would not be more effective than the radiation alone in the athymic nude mice. However, a more careful evaluation of the tumor growth revealed that while the combined effect from the localized irradiation followed by the poly(I:C) therapy was synergistic in the TC-1 tumors in immuno-competent C57BL/6 mice, it was only additive in athymic nude mice with the TC-1 tumors (Table 6.1). Therefore, it is likely that the T cell-mediated immunity contributed to the combined anti-tumor activity by rendering it synergistic. Interestingly, we have also shown that the combined effect from the localized irradiation and the poly(I:C) was only additive in the immuno-competent C57BL/6 mice when the highly immunogenic TC-1 tumors were replaced by the poorly immunogenic B16-F10 tumors (Fig. 6.2B and Table 6.1), again suggesting that the T-cell mediated immunity was responsible for the synergistic effect observed in immuno-competent mice with highly immunogenic tumors. More experiments will be carried out in the future to further identify the extent to which the T cells and natural killer (NK) cells have contributed to the anti-tumor activity from the combination therapy. Poly(I:C) can activate NK cells, which are tumoricidal as well. Nevertheless, this finding may also point out one of the advantages for using the poly(I:C) instead of the CpG oligos in the combination therapy. The TC-1 tumors in nude mice and the B16-F10 tumors in C57BL/6 mice resemble the real clinical situations. Many human tumors are poorly or non-immunogenic, and the

immune system of patients with advanced cancers is generally compromised to some extent.

The poly(I:C) is a potent inducer of type I IFNs, and the type I IFNs are pro-apoptotic, anti-proliferative, and anti-angiogenic (Balkwill and Taylor-Papadimitriou, 1978; Chawla-Sarkar et al., 2001; Chawla-Sarkar et al., 2003; Sidky and Borden, 1987). Thus, it is very likely that the type I IFNs have contributed significantly to the anti-tumor activity of the combination therapy. For example, it was found that the concentration of the type I IFN-α in the tumor tissues was much higher when the poly(I:C) were injected locally than when injected into a site distal to the tumors (Fig. 6.3B,C). This finding may explain the stronger anti-tumor activity observed when the poly(I:C)-lipoplexes were peritumorally injected in the combination therapy than when they were injected into a site distal to the tumors (Fig. 6.3A), in agreement with a previous finding that the poly(I:C) was more efficacious when given locally (DuBuy, 1972; Le et al., 2007; Pimm et al., 1976). However, more convincing evidence supporting that the type I IFNs contributed significantly to the anti-tumor activity of the combination therapy was shown in Fig. 6.3E, in which the type I IFNs were neutralized in mice using antiserum against IFN-α,β. The neutralization of the type I IFNs significantly compromised the anti-tumor activity of the combination therapy (Fig. 6.3E). The importance of type I IFNs in the anti-tumor activity of the poly(I:C) has been reported before. For example, Currie et al. (2008) showed that when AB1-HA tumor-bearing mice were treated with poly(I:C) in the presence of

the polyclonal IFN-α,β-neutralizing antiserum, the neutralization completely inhibited the poly(I:C)-driven tumor resolution (Currie et al., 2008). However, there were cases where the anti-tumor activity of the poly(I:C) was found to be de-coupled from its ability to induce the production of type I IFNs (Sakurai et al., 1990; Weinstein et al., 1971). We suspect that how effectively the poly(I:C) is delivered into the tumor cells determines the extent to which the type I IFNs contribute to the resultant anti-tumor activity. When the poly(I:C) was given by systemic injection, the anti-tumor activity of the poly(I:C) was thought to be related to its ability to induce type I IFNs. In contrast, consistent with our data in figure 6.3A, locally dosed poly(I:C) has been shown to be more effective in suppressing tumor growth (DuBuy, 1972; Pimm et al., 1976; Shir et al., 2006). For example, it was shown that the growth of transplanted rat tumors was retarded when the cells were injected subcutaneously in admixture with poly(I:C), while systemic treatment of the same tumors with poly(I:C) failed to prevent the growth of a range of rat tumors (Pimm et al., 1976). The tumor regression observed by Shir et al. (2006) after the intratumoral injection of tumor cell-targeting poly(I:C) is another example (Shir et al., 2006). Therefore, our future work should be directed towards improving the delivery of the poly(I:C) into tumors to further improve the anti-tumor activity from the combination therapy. Our data in Fig. 6.3A showed that subcutaneous injection of the poly(I:C) into a site distal to the tumors was still effective, although less effective than when the poly(I:C) was given by peritumoral injection. Therefore, the peritumoral route was used in this

study. Peritumoral injection is clinically feasible for some cancers, such as melanoma and certain head and neck cancers. It would be clinically difficult to inject other tumors peritumorally, however. We are currently investigating the feasibility of targeting the poly(I:C) into tumors after systemic injections.

Finally, data from some previous studies indicated that the poly(I:C) caused dose-limiting adverse effects, especially to the liver (De Clercq et al., 1972; Freeman et al., 1977; Okada et al., 2005), which significantly restricted its potential in cancer therapy. Our data in this study suggested that the combination approach may help overcome or minimize this issue because the integration of the localized irradiation into the poly(I:C) therapy makes it possible to use less poly(I:C) and to dose it less frequently. Moreover, our unpublished data also suggested that the potential liver toxicity issue of the poly(I:C) may be addressed using PEGylated poly(I:C)-liposome lipoplexes.

In conclusion, we reported that localized irradiation of tumors prior to synthetic dsRNA therapy significantly enhanced the resultant anti-tumor activity. The combination therapy was effective regardless of the immunogenicity of the tumors or the immuno-competency of the host, although a synergistic effect was observed only in immuno-competent mice with highly immunogenic tumors. Finally, the type I IFNs induced by the dsRNA contributed significantly to the anti-tumor activity from the combination therapy. Improved targeting of the synthetic dsRNA into tumor cells is expected to further improve the efficacy of this novel tumor therapeutic modality.

Table 6.1 Fractional tumor diameter (FTD[a]) relative to control mice in combination therapy using localized irradiation and poly(I:C).

			IR+pI:C/LP		Combination index[d]
Day[b]	**pI:C/LP**	**IR**	**Observed**	**Expected[c]**	
TC-1 cells in C57BL/6 mice					
13	0.85	0.79	0.56	0.68	1.2
14	0.91	0.81	0.59	074	1.3
TC-1 cells in nude mice[e]					
8	0.93	0.92	0.93	0.86	0.9
11	0.88	0.86	0.78	0.75	1.0
13	0.99	0.71	0.66	0.71	1.1
15	0.82	0.67	0.54	0.55	1.0
B16F10 cells in C57BL/6 mice					
10	1.03	0.94	0.94	0.97	1.0
12	0.92	0.85	0.80	0.78	1.0
14	0.91	0.81	0.75	0.73	1.0
17	0.79	0.71	0.62	0.56	0.9

Table 6.1

[a] FTD, fractional tumor diameter (mean tumor diameter experimental)/(mean tumor diameter of control). Values were calculated only after the start of the combination therapy and when tumor diameter values for the control group are available.

[b] Day after tumor seeding.

[c] (Mean FTD of pI:C/LP) x (mean FTD of IR).

[d] Combination index (CI) = expected FTD / observed FTD.

[e] CI was not calculated for day 17 because some mice were preemptively euthanized.

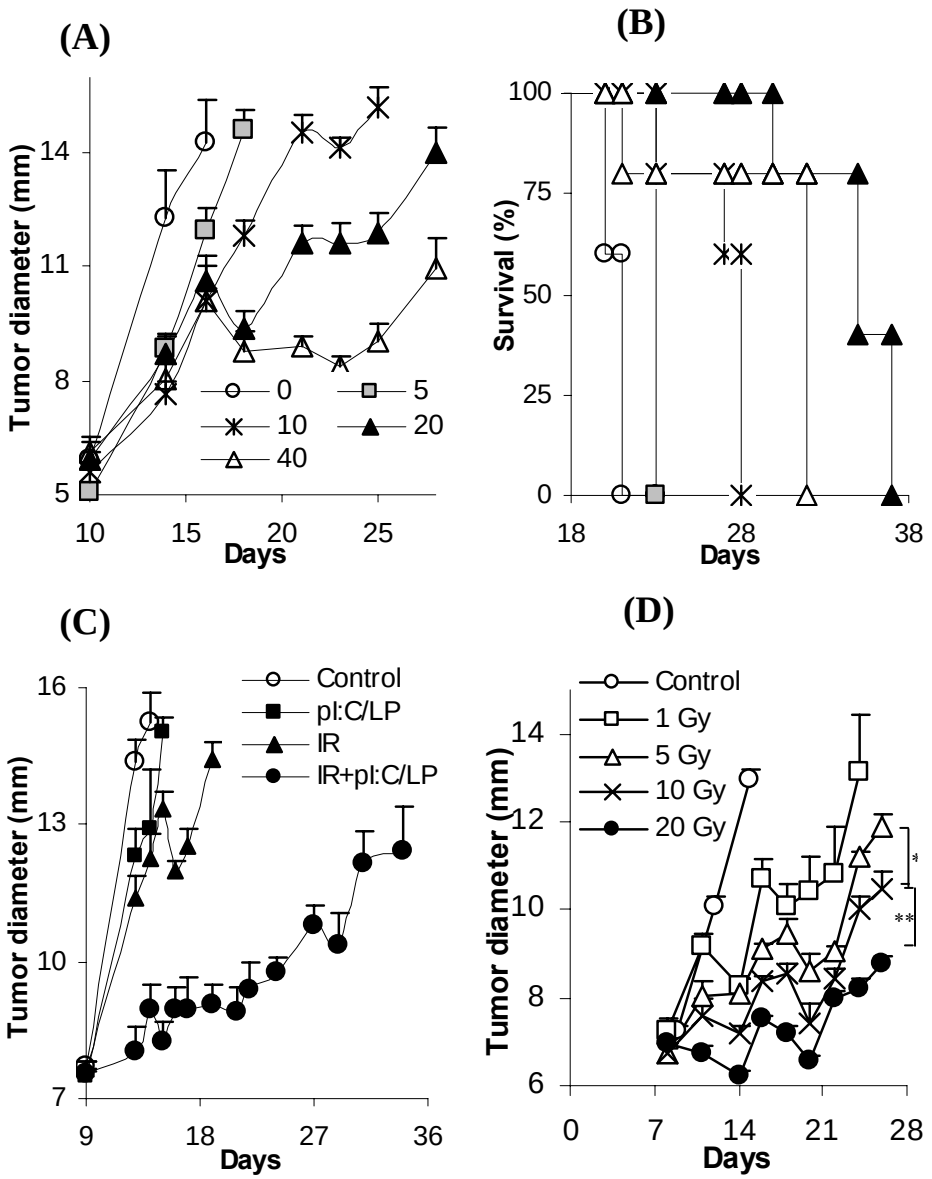
(A)
Tumor diameter (mm)
14
11
8
5
10
15
20
25
Days
0
5
10
20
40
(B)
Survival (%)
100
75
50
25
0
18
28
38
Days
(C)
Tumor diameter (mm)
16
13
10
7
9
18
27
36
Days
Control
pI:C/LP
IR
IR+pI:C/LP
(D)
Tumor diameter (mm)
14
12
10
8
6
0
7
14
21
28
Days
Control
1 Gy
5 Gy
10 Gy
20 Gy
*
**

Figure 6.1

Figure. 6.1 Localized irradiation of tumors prior to the pI:C/LP therapy significantly inhibited the growth of TC-1 tumors in C57BL/6 mice. (**A**). The effect of the dose of the localized X-ray on the growth of TC-1 tumors in mice. TC-1 cells were s.c. seeded in mice on day 0. On day 10, mice (n = 5) were locally irradiated. (**B**). The effect of the dose of the localized X-ray on the survival of TC-1 tumor-bearing mice. Mice were treated as in 1A. (**C**). Combination therapy using radiation followed by pI:C/LP significantly inhibited the growth of TC-1 tumors in a mouse model. Ten days after tumor seeding (tumor diameter = 7.6 ± 0.3 mm), mice (n = 9-10) were locally irradiated with a single dose of X-ray (20 Gy). Starting on day 12, mice were dosed with pI:C/LP (50 μg of pI:C per mouse) for 5 consecutive days. (**D**). Effect of the dose of the X-ray on the anti-tumor activity of the combination therapy. Eight days after tumor seeding, the tumors were locally irradiated (1 to 20 Gy). Starting on day 10, mice (n = 5-6) were dosed with pI:C/LP (50 μg pI:C) 3 times a week for two consecutive weeks. ANOVA revealed differences among 4 groups received X-ray ($p = 0.003$ on day 26). (*), $p = 0.02$ on day 26. (**) $p = 0.007$ on day 26. All data were reported as mean ± SEM.

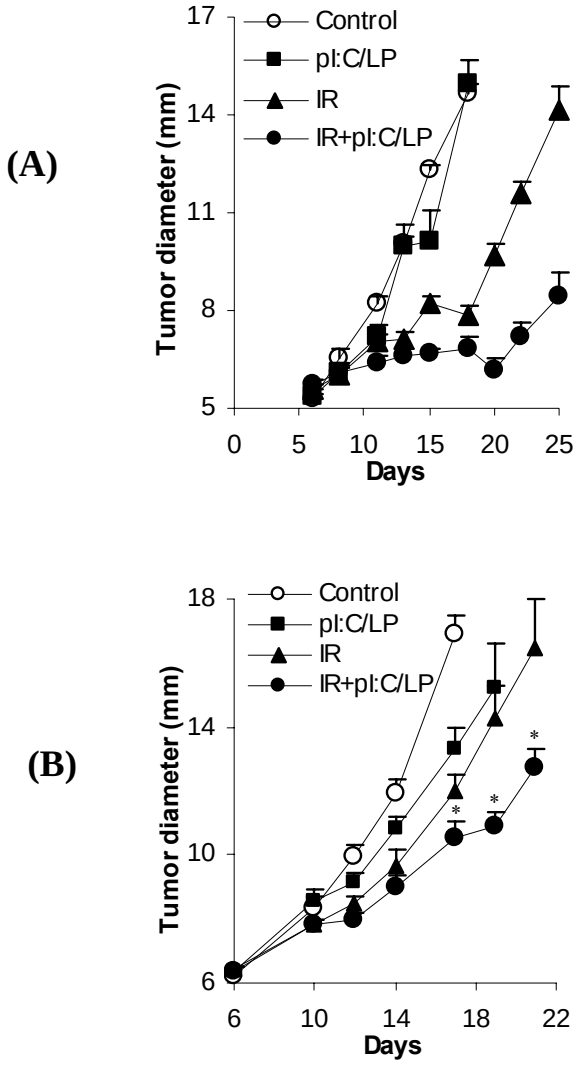

Figure 6.2 The combination therapy was more effective than the monotherapies in athymic nude mice with highly immunogenic tumors and in immuno-competent mice with poorly or non-immunogenic tumors. (**A**). Athymic nude mice with TC-1 tumors. TC-1 cells were seeded in mice on day 0. On day 6, mice (n = 7-10) were locally irradiated with (20 Gy). Starting on day 8, mice were dosed with pI:C/LP (37.5 μg of pI:C) 3 times a week for 2 consecutive weeks. (**B**). C57BL/6 mice with B16-F10 tumors. Tumor cells were seeded in mice on day 0. On day 7, mice were locally irradiated (15 Gy). Starting on day 9, mice (n = 8-10) were dosed with pI:C/LP (50 μg of pI:C) 3 times a week for 2 consecutive weeks. (*) The values of the IR+pI:C/LP were significantly smaller than that of the others. Data reported are mean ± SEM.

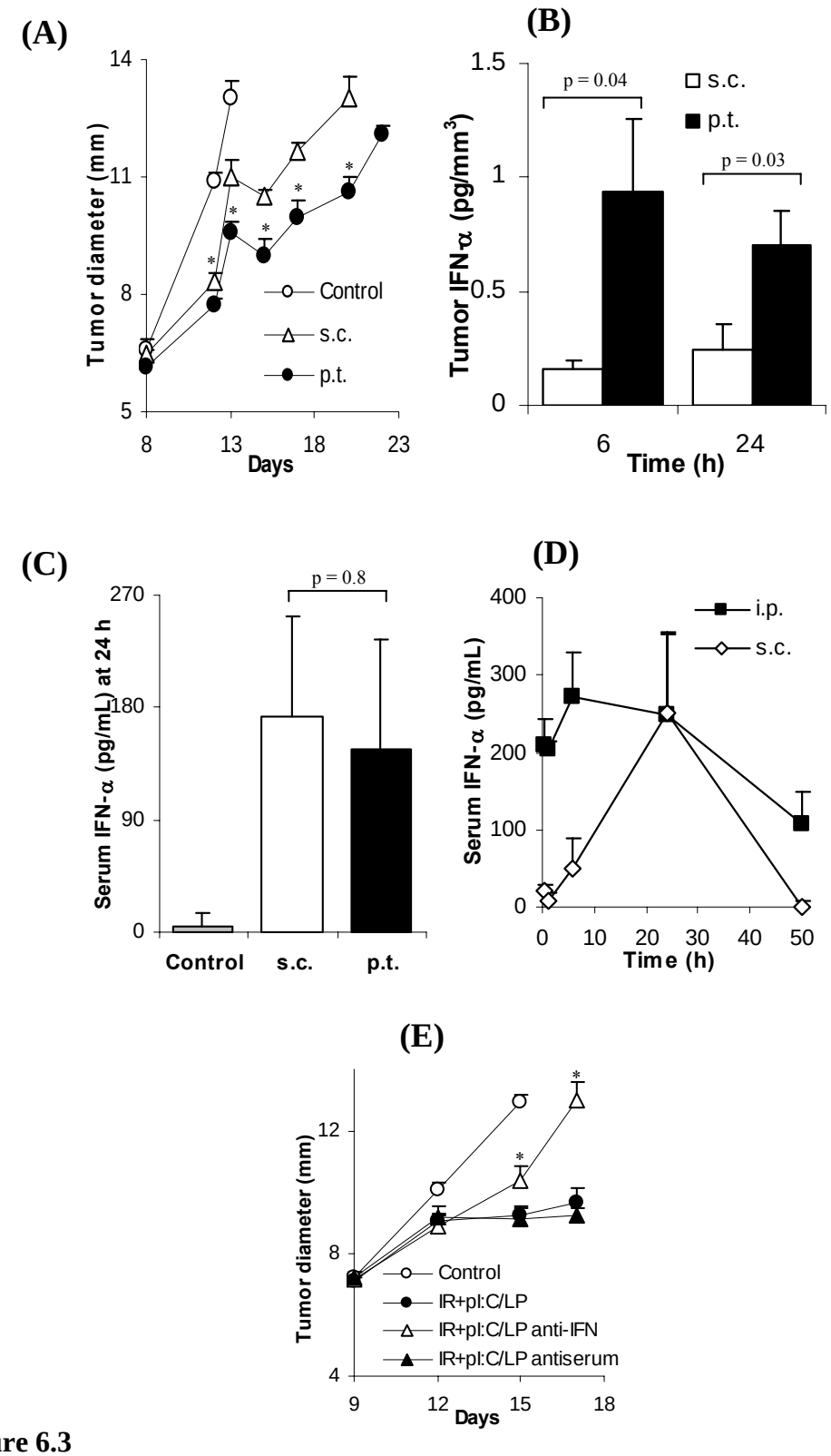
(A)
Tumor diameter (mm)
14
11
8
5
8
13
18
23
Days
Control
s.c.
p.t.
(B)
Tumor IFN-α (pg/mm3)
1.5
1
0.5
0
p = 0.04
p = 0.03
s.c.
p.t.
6
24
Time (h)
(C)
Serum IFN-α (pg/mL) at 24 h
270
180
90
0
p = 0.8
Control
s.c.
p.t.
(D)
Serum IFN-α (pg/mL)
400
300
200
100
0
i.p.
s.c.
0
10
20
30
40
50
Time (h)
(E)
Tumor diameter (mm)
12
8
4
9
12
15
18
Days
Control
IR+pI:C/LP
IR+pI:C/LP anti-IFN
IR+pI:C/LP antiserum

Figure 6.3

Figure. 6.3 The type I IFNs induced by the poly(I:C) contributed significantly to the anti-tumor activity generated by the combination therapy. (**A**). In the combination therapy, the injection of the pI:C/LP closely to the tumors was more effective in inhibiting the tumor growth. TC-1 tumors in C57BL/6 mice were irradiated (20 Gy) 9 days after tumor seeding. Starting on day 11, mice (n = 6-7) were injected with pI:C/LP (37.5 μg of pI:C) peritumorally (p.t.) or distal to the tumors (s.c.) 3 times a week for 2 consecutive weeks. (*) Starting from day 12, the values of the p.t. and s.c. were different from each other ($p < 0.05$). (**B)**, (**C**). Peritumoral injection of the pI:C/LP induced a higher level of IFN-α in tumor tissues. TC-1 tumor-bearing mice were injected with pI:C/LP (37.5 μg of pI:C) p.t. or in a site distal to the tumor (s.c.). The IFN-α level in the tumor (B) and blood (C) samples was measured 6 or 24 h later (n = 3). (**D**). Kinetics of IFN-α in the blood when tumor-free mice (n =3) were injected once with the pI:C/LP (pI:C = 50 μg) subcutaneously (s.c.) or intraperitoneally (i.p.). (**E**). Neutralization of the type I IFNs decreased the anti-tumor activity of the combination therapy. TC-1 tumors were irradiated (15 Gy) 9 days after tumor seeding. Mice (n = 5-6) were injected (p.t.) with pI:C/LP (50 μg) starting on day 11, three times a week for one week. One group of mice was injected i.p. with antiserum against type I IFN-α,β, another group with control anti-serum. (*) The values in mice injected with the anti-type I IFN anti-serum were different from that in mice received the control anti-serum or received no anti-serum. Data reported are mean ± SEM.

Chapter 7

GENERAL CONCLUSIONS

In the Gd delivery studies, we engineered a Gd-DTPA-encapsulated liposome formulation that encapsulated an average of 6.8 mg of pure Gd per mL of liposomes. The unique characteristic of our formulation is the complexing of Gd-DTPA and poly-L-lysine before loading them into liposomes that helped increase the encapsulation efficiency of Gd-DTPA in liposomes and reduce the release of Gd-DTPA from the liposomes *in vitro* and *in vivo*. Approximately 12 h after being intravenously injected into mice with pre-established tumors, our Gd-DTPA-encapsulated liposomes delivered as high as 159 μg of Gd per g of wet tumor tissue, which fulfilled one of the requirements for a successful Gd-NCT (e.g. 50-200 μg of Gd/ g tumor). Increasing the doses of Gd by injecting the formulation multiple times was associated with enhanced uptake of Gd by the tumors. The ratio of Gd uptake by tumors to that by normal tissues (e.g. based on blood, liver, spleen, heart, lung, and kidney) was mostly greater than 1, except the spleen, which suggested that the formulation is safe to normal tissues. However, the spleen may need to be properly avoided when neutrons are applied in NCT. There was a strong inverse correlation between tumor size and the amount of Gd taken up by the tumors. Finally, we also found that dispersing the Gd-DTPA-encapsulated liposomes into a thermo-sensitive polymeric gel further extended the

retention of the Gd in murine tumors. In short, our Gd-DTPA-encapsulated liposomes may hold great potential to systemically deliver Gd into solid tumors for Gd-NCT. Furthermore, the alternative approach using a thermo-sensitive gel to disperse the Gd-encapsulated liposome formulation can be used to prolong the retention of Gd in localized delivery of Gd for NCT. The feasibility of our Gd-liposome formulation for Gd-NCT will be validated in future studies.

In the studies of using combination therapy to improve the anti-tumor activity of poly(I:C), we found that combining gemcitabine with poly(I:C) (e.g. chemo^2-immuno therapy) synergistically inhibited the tumor growth. The combination therapy synergistically induced more tumor cells to undergo apoptosis *in vivo* as compared to monotherapies. It also generated a strong and long-lasting specific anti-tumor immune response although the immune response alone was unable to control the tumor growth after the termination of the therapy. Similarly, localized x-ray irradiation prior to the administration of poly(I:C) (e.g. chemo-immuno-radiotherapy) also significantly delayed the tumor growth, as compared to monotherapies. However, a synergistic effect was observed only in immuno-competent mice with highly immunogenic tumors, not in immuno-competent mice with weakly immunogenic tumors or in athymic nude mice with highly immunogenic tumors, suggesting that the T cell-mediated immunity was responsible for the synergy. We also found that the type I IFNs induced by the poly(I:C) contributed significantly to the anti-tumor activity. Finally, poly(I:C) delivered close to tumors was more effective in inhibiting tumor growth and

inducing type I IFNs in the tumors than when delivered distal to the tumor sites. These combination therapies may represent a promising approach to improve the clinical outcomes of the dsRNA therapy.

BIBLIOGRAPHY

Abbruzzese, J.L., Grunewald, R., Weeks, E.A., Gravel, D., Adams, T., Nowak, B., Mineishi, S., Tarassoff, P., Satterlee, W., Raber, M.N. and et al., 1991. A phase I clinical, plasma, and cellular pharmacology study of gemcitabine. J Clin Oncol 9, 491-8.

Absher, M. and Stinebring, W.R., 1969. Toxic properties of a synthetic double-stranded RNA. Endotoxin-like properties of poly I. poly C, an interferon stimulator. Nature 223, 715-7.

Acker, J.C., Dewhirst, M.W., Honore, G.M., Samulski, T.V., Tucker, J.A. and Oleson, J.R., 1990. Blood perfusion measurements in human tumours: evaluation of laser Doppler methods. Int J Hyperthermia 6, 287-304.

Akine, Y., Tokita, N., Tokuuye, K., Satoh, M., Churei, H., Le Pechoux, C., Kobayashi, T. and Kanda, K., 1993. Suppression of rabbit VX-2 subcutaneous tumor growth by gadolinium neutron capture therapy. Jpn J Cancer Res 84, 841-3.

Akine, Y., Tokita, N., Tokuuye, K., Satoh, M., Fukumori, Y., Tokumitsu, H., Kanamori, R., Kobayashi, T. and Kanda, K., 1992. Neutron-capture therapy of murine ascites tumor with gadolinium-containing microcapsules. J Cancer Res Clin Oncol 119, 71-3.

Alamelu, S. and Rao, K.P., 1991. Studies on the carboxymethyl chitosan-containing liposomes for their stability and controlled release of dapsone. J Microencapsul 8, 505-19.

Alexopoulou, L., Holt, A.C., Medzhitov, R. and Flavell, R.A., 2001. Recognition of double-stranded RNA and activation of NF-kappaB by Toll-like receptor 3. Nature 413, 732-8.

Allen, T.M., 1994. Long-circulating (sterically stabilized) liposomes for targeted drug delivery. Trends Pharmacol Sci 15, 215-20.

Anderson, K.M., Evans, A. and Kellen, J.A., 1972. Unimpaired development of DMBA-induced mammary tumors in rats treated with poly(I)-poly(C). Res Commun Chem Pathol Pharmacol 4, 193-202.

Andresen, T.L., Jensen, S.S. and Jorgensen, K., 2005. Advanced strategies in liposomal cancer therapy: problems and prospects of active and tumor specific drug release. Prog Lipid Res 44, 68-97.

Bakouche, O. and Gerlier, D., 1985. Localization of an entrapped item within unilamellar vesicle compartments: use of ultrasound disruption as a procedure to separate aqueous phase and lipidic lamellae. J Microencapsul 2, 39-43.

Balkwill, F. and Taylor-Papadimitriou, J., 1978. Interferon affects both G1 and S+G2 in cells stimulated from quiescence to growth. Nature 274, 798-800.

Bandak, S., Goren, D., Horowitz, A., Tzemach, D. and Gabizon, A., 1999. Pharmacological studies of cisplatin encapsulated in long-circulating liposomes in mouse tumor models. Anticancer Drugs 10, 911-20.

Bangham, A.D., Standish, M.M. and Watkins, J.C., 1965. Diffusion of univalent ions across the lamellae of swollen phospholipids. J Mol Biol 13, 238-52.

Barnhart, J.L., Kuhnert, N., Bakan, D.A. and Berk, R.N., 1987. Biodistribution of GdCl3 and Gd-DTPA and their influence on proton magnetic relaxation in rat tissues. Magn Reson Imaging 5, 221-31.

Barth, R.F., Coderre, J.A., Vicente, M.G. and Blue, T.E., 2005. Boron neutron capture therapy of cancer: current status and future prospects. Clin Cancer Res 11, 3987-4002.

Barth, R.F. and Soloway, A.H., 1994a. Boron neutron capture therapy of primary and metastatic brain tumors. Mol Chem Neuropathol 21, 139-54.

Barth, R.F. and Soloway, A.H., 1994b. Perspective on boron neutron capture therapy. Int J Radiat Oncol Biol Phys 28, 1059-60.

Bertini, I., Bianchini, F., Calorini, L., Colagrande, S., Fragai, M., Franchi, A., Gallo, O., Gavazzi, C. and Luchinat, C., 2004. Persistent contrast enhancement by sterically stabilized paramagnetic liposomes in murine melanoma. Magn Reson Med 52, 669-72.

Blanco, D.R., Champion, C.I., Dooley, A., Cox, D.L., Whitelegge, J.P., Faull, K. and Lovett, M.A., 2005. A monoclonal antibody that conveys *in vitro* killing and partial protection in experimental syphilis binds a phosphorylcholine surface epitope of Treponema pallidum. Infect Immun 73, 3083-95.

Bochot, A., Fattal, E., Gulik, A., Couarraze, G. and Couvreur, P., 1998. Liposomes dispersed within a thermosensitive gel: a new dosage form for ocular delivery of oligonucleotides. Pharm Res 15, 1364-9.

Bock, J.C., Pison, U., Wlodarczyk, W., Kaufmann, F., Lehmann, J., Saupe, M. and Felix, R., 1997. [Magnetic resonance imaging of the degree of pulmonary edema using a macromolecular contrast medium]. Rofo 167, 509-15.

Bornmann, C., Graeser, R., Esser, N., Ziroli, V., Jantscheff, P., Keck, T., Unger, C., Hopt, U.T., Adam, U., Schaechtele, C., Massing, U. and von Dobschuetz, E., 2008. A new liposomal formulation of Gemcitabine is active in an orthotopic mouse model of pancreatic cancer accessible to bioluminescence imaging. Cancer Chemother Pharmacol 61, 395-405.

Boulmedarat, L., Piel, G., Bochot, A., Lesieur, S., Delattre, L. and Fattal, E., 2005. Cyclodextrin-mediated drug release from liposomes dispersed within a bioadhesive gel. Pharm Res 22, 962-71.

Brown, J.M., 2007. Tumor hypoxia in cancer therapy. Methods Enzymol 435, 297-321.

Brugger, R.M. and Shih, J.A., 1989. Evaluation of gadolinium-157 as a neutron capture therapy agent. Strahlenther Onkol 165, 153-6.

Brusa, P., Immordino, M.L., Rocco, F. and Cattel, L., 2007. Antitumor activity and pharmacokinetics of liposomes containing lipophilic gemcitabine prodrugs. Anticancer Res 27, 195-9.

Cagnoni, P.J., 2002. Liposomal amphotericin B versus conventional amphotericin B in the empirical treatment of persistently febrile neutropenic patients. J Antimicrob Chemother 49 Suppl 1, 81-6.

Caliceti, P. and Veronese, F.M., 2003. Pharmacokinetic and biodistribution properties of poly(ethylene glycol)-protein conjugates. Adv Drug Deliv Rev 55, 1261-77.

Campos, S.M., Penson, R.T., Mays, A.R., Berkowitz, R.S., Fuller, A.F., Goodman, A., Matulonis, U.A., Muzikansky, A. and Seiden, M.V., 2001. The clinical utility of liposomal doxorubicin in recurrent ovarian cancer. Gynecol Oncol 81, 206-12.

Caravan, P., Ellison, J.J., McMurry, T.J. and Lauffer, R.B., 1999. Gadolinium(III) Chelates as MRI Contrast Agents: Structure, Dynamics, and Applications. Chem Rev 99, 2293-352.

Carlsson, J., Forssell-Aronsson, E. and Glimelius, B., 2002. Radiation therapy through activation of stable nuclides. Acta Oncol 41, 629-34.

Castelli, F., Sarpietro, M.G., Rocco, F., Ceruti, M. and Cattel, L., 2007. Interaction of lipophilic gemcitabine prodrugs with biomembrane models studied by Langmuir-Blodgett technique. J Colloid Interface Sci 313, 363-8.

Chawla-Sarkar, M., Leaman, D.W. and Borden, E.C., 2001. Preferential induction of apoptosis by interferon (IFN)-beta compared with IFN-alpha2: correlation with TRAIL/Apo2L induction in melanoma cell lines. Clin Cancer Res 7, 1821-31.

Chawla-Sarkar, M., Lindner, D.J., Liu, Y.F., Williams, B.R., Sen, G.C., Silverman, R.H. and Borden, E.C., 2003. Apoptosis and interferons: role of interferon-stimulated genes as mediators of apoptosis. Apoptosis 8, 237-49.

Chou, T.C. and Talalay, P., 1984. Quantitative analysis of dose-effect relationships: the combined effects of multiple drugs or enzyme inhibitors. Adv Enzyme Regul 22, 27-55.

Coley, W.B., 1991. The treatment of malignant tumors by repeated inoculations of erysipelas. With a report of ten original cases. 1893. Clin Orthop Relat Res, 3-11.

Collins, K., Jacks, T. and Pavletich, N. P., 1997. The cell cycle and cancer. Proc. Natl. Acad. Sci. USA 94, 2776-2778.

Cui, Z., Han, S.J. and Huang, L., 2004. Coating of mannan on LPD particles containing HPV E7 peptide significantly enhances immunity against HPV-positive tumor. Pharm Res 21, 1018-25.

Cui, Z. and Huang, L., 2005. Liposome-polycation-DNA (LPD) particle as a carrier and adjuvant for protein-based vaccines: Therapeutic effect against cervical cancer. Cancer Immunol Immunother 54, 1180-90.

Cui, Z., Le, U.M., Qiu, F. and Shaker, D.S., 2007. Learning from viruses: the necrotic bodies of tumor cells with intracellular synthetic dsRNA induced strong anti-tumor immune responses. Pharm Res 24, 1645-52.

Cui, Z. and Qiu, F., 2006. Synthetic double-stranded RNA poly(I:C) as a potent peptide vaccine adjuvant: therapeutic activity against human cervical cancer in a rodent model. Cancer Immunol Immunother 55, 1267-79.

Cullis, P.R., Chonn, A. and Semple, S.C., 1998. Interactions of liposomes and lipid-based carrier systems with blood proteins: Relation to clearance behaviour *in vivo*. Adv Drug Deliv Rev 32, 3-17.

Currie, A.J., van der Most, R.G., Broomfield, S.A., Prosser, A.C., Tovey, M.G. and Robinson, B.W., 2008. Targeting the effector site with IFN-alphabeta-inducing TLR ligands reactivates tumor-resident CD8 T cell responses to eradicate established solid tumors. J Immunol 180, 1535-44.

Curtet, C., Maton, F., Havet, T., Slinkin, M., Mishra, A., Chatal, J.F. and Muller, R.N., 1998. Polylysine-Gd-DTPAn and polylysine-Gd-DOTAn coupled to anti-CEA F(ab')2 fragments as potential immunocontrast agents. Relaxometry, biodistribution, and magnetic resonance imaging in nude mice grafted with human colorectal carcinoma. Invest Radiol 33, 752-61.

Dai, C., Wang, B., Zhao, H., Li, B. and Wang, J., 2006. Preparation and characterization of liposomes-in-alginate (LIA) for protein delivery system. Colloids Surf B Biointerfaces 47, 205-10.

Damen, J., Regts, J. and Scherphof, G., 1981. Transfer and exchange of phospholipid between small unilamellar liposomes and rat plasma high density lipoproteins. Dependence on cholesterol content and phospholipid composition. Biochim Biophys Acta 665, 538-45.

Dass, C.R., 2002. Biochemical and biophysical characteristics of lipoplexes pertinent to solid tumour gene therapy. Int J Pharm 241, 1-25.

Davies, B. and Morris, T., 1993. Physiological parameters in laboratory animals and humans. Pharm Res 10, 1093-5.

De Clercq, E., Stewart, W.E., 2nd and De Somer, P., 1972. Interferon production linked to toxicity of polyriboinosinic acid-polyribocytidylic acid. Infect Immun 6, 344-7.

De Stasio, G., Casalbore, P., Pallini, R., Gilbert, B., Sanita, F., Ciotti, M.T., Rosi, G., Festinesi, A., Larocca, L.M., Rinelli, A., Perret, D., Mogk, D.W., Perfetti, P., Mehta, M.P. and Mercanti, D., 2001. Gadolinium in human glioblastoma cells for gadolinium neutron capture therapy. Cancer Res 61, 4272-7.

Degre, M. and Elgjo, K., 1971. Methylcholanthrene-induced skin carcinogenesis modified by treatment with polyinosinic:polycytidylic acid (poly I:C). Acta Pathol Microbiol Scand [A] 79, 687-8.

Demaria, S., Ng, B., Devitt, M.L., Babb, J.S., Kawashima, N., Liebes, L. and Formenti, S.C., 2004. Ionizing radiation inhibition of distant untreated tumors (abscopal effect) is immune mediated. Int J Radiat Oncol Biol Phys 58, 862-70.

Desai, M.P., Labhasetwar, V., Walter, E., Levy, R.J. and Amidon, G.L., 1997. The mechanism of uptake of biodegradable microparticles in Caco-2 cells is size dependent. Pharm Res 14, 1568-73.

Desormeaux, A. and Bergeron, M.G., 2005. Lymphoid tissue targeting of anti-HIV drugs using liposomes. Methods Enzymol 391, 330-51.

Devoisselle, J.M., Vion-Dury, J., Galons, J.P., Confort-Gouny, S., Coustaut, D., Canioni, P. and Cozzone, P.J., 1988. Entrapment of gadolinium-DTPA in liposomes. Characterization of vesicles by P-31 NMR spectroscopy. Invest Radiol 23, 719-24.

Dierling, A.M., Sloat, B.R. and Cui, Z., 2005. Gadolinium incorporated reconstituted chylomicron emulsion for potential application in tumor neutron capture therapy. Eur J Pharm Biopharm.

Dings, R.P., Yokoyama, Y., Ramakrishnan, S., Griffioen, A.W. and Mayo, K.H., 2003. The designed angiostatic peptide anginex synergistically improves chemotherapy and antiangiogenesis therapy with angiostatin. Cancer Res 63, 382-5.

DiTizio, V., Karlgard, C., Lilge, L., Khoury, A.E., Mittelman, M.W. and DiCosmo, F., 2000. Localized drug delivery using crosslinked gelatin gels containing liposomes: factors influencing liposome stability and drug release. J Biomed Mater Res 51, 96-106.

Dohlsten, M., Lando, P.A., Bjork, P., Abrahmsen, L., Ohlsson, L., Lind, P. and Kalland, T., 1995. Immunotherapy of human colon cancer by antibody-targeted superantigens. Cancer Immunol Immunother 41, 162-8.

Dragicevic-Curic, N., Stupar, M., Milic, J., Zoric, T., Krajisnik, D. and Vasiljevic, D., 2005. Hydrophilic gels containing chlorophyllin-loaded liposomes: development and stability evaluation. Pharmazie 60, 588-92.

Drummond, D.C., Meyer, O., Hong, K., Kirpotin, D.B. and Papahadjopoulos, D., 1999. Optimizing liposomes for delivery of chemotherapeutic agents to solid tumors. Pharmacol Rev 51, 691-743.

DuBuy, H.G., 1972. Effect of local or distal therapeutic treatment with polyinosinic-polycytidylic acid on survival of mice with Ehrlich carcinoma. J Natl Cancer Inst 48, 1525-7.

Ewel, C.H., Urba, W.J., Kopp, W.C., Smith, J.W., 2nd, Steis, R.G., Rossio, J.L., Longo, D.L., Jones, M.J., Alvord, W.G., Pinsky, C.M. and et al., 1992. Polyinosinic-polycytidylic acid complexed with poly-L-lysine and carboxymethylcellulose in combination with interleukin 2 in patients with cancer: clinical and immunological effects. Cancer Res 52, 3005-10.

Farrell, P.J., Sen, G.C., Dubois, M.F., Ratner, L., Slattery, E. and Lengyel, P., 1978. Interferon action: two distinct pathways for inhibition of protein synthesis by double-stranded RNA. Proc Natl Acad Sci U S A 75, 5893-7.

Fattal, E., De Rosa, G. and Bochot, A., 2004. Gel and solid matrix systems for the controlled delivery of drug carrier-associated nucleic acids. Int J Pharm 277, 25-30.

FDA, 1996. FDA approves DaunoXome as first-line therapy for Kaposi's sarcoma. Food and Drug Administration. J Int Assoc Physicians AIDS Care 2, 50-1.

FDA, 2008. Drug Information. FDA approval for gemcitabine hydrochloride, http://www.cancer.gov/cancertopics/druginfo/fda-gemcitabine-hydrochloride. Acess on 08/05/08.

Fisher, J.C., Cooperband, S.R. and Mannick, J.A., 1970. Inhibition of tumor growth with a new synthetic ribonucleic acid. Surg Forum 21, 122-4.

Freeman, A.I., Al-Bussam, N., O'Malley, J.A., Stutzman, L., Bjornsson, S. and Carter, W.A., 1977. Pharmacologic effects of polyinosinic-polycytidylic acid in man. J Med Virol 1, 79-93.

Fujimura, T., Nakagawa, S., Ohtani, T., Ito, Y. and Aiba, S., 2006. Inhibitory effect of the polyinosinic-polycytidylic acid/cationic liposome on the progression of murine B16F10 melanoma. Eur J Immunol 36, 3371-80.

Gabizon, A., Goren, D., Fuks, Z., Meshorer, A. and Barenholz, Y., 1985. Superior therapeutic activity of liposome-associated adriamycin in a murine metastatic tumour model. Br J Cancer 51, 681-9.

Gabizon, A., Isacson, R., Libson, E., Kaufman, B., Uziely, B., Catane, R., Ben-Dor, C.G., Rabello, E., Cass, Y., Peretz, T. and et al., 1994. Clinical studies of liposome-encapsulated doxorubicin. Acta Oncol 33, 779-86.

Gabizon, A. and Papahadjopoulos, D., 1988. Liposome formulations with prolonged circulation time in blood and enhanced uptake by tumors. Proc Natl Acad Sci U S A 85, 6949-53.

Gabizon, A., Price, D.C., Huberty, J., Bresalier, R.S. and Papahadjopoulos, D., 1990. Effect of liposome composition and other factors on the targeting of liposomes to experimental tumors: biodistribution and imaging studies. Cancer Res 50, 6371-8.

Gabizon, A.A., 2001. Stealth liposomes and tumor targeting: one step further in the quest for the magic bullet. Clin Cancer Res 7, 223-5.

Gazdar, A.F., 1972. Enhancement of tumor growth rate by interferon inducers. J Natl Cancer Inst 49, 1435-8.

Gelman, A.E., Zhang, J., Choi, Y. and Turka, L.A., 2004. Toll-like receptor ligands directly promote activated CD4+ T cell survival. J Immunol 172, 6065-73.

Gillies, R.J., Schornack, P.A., Secomb, T.W. and Raghunand, N., 1999. Causes and effects of heterogeneous perfusion in tumors. Neoplasia 1, 197-207.

Glavas-Dodov, M., Fredro-Kumbaradzi, E., Goracinova, K., Calis, S., Simonoska, M. and Hincal, A.A., 2003. 5-Fluorouracil in topical liposome gels for anticancer treatment--formulation and evaluation. Acta Pharm 53, 241-50.

Glavas-Dodov, M., Goracinova, K., Mladenovska, K. and Fredro-Kumbaradzi, E., 2002. Release profile of lidocaine HCl from topical liposomal gel formulation. Int J Pharm 242, 381-4.

Gong, J.H., Liu, Y., Tang, L.H., Xu, X.J. and Zhang, X.N., 2006. An alternative lidocaine hydrochloride liposomal gel formulation: preparation, percutaneous permeation, and release kinetics. PDA J Pharm Sci Technol 60, 259-63.

Grunder, W., Biesold, M., Wagner, M. and Werner, A., 1998. Improved nuclear magnetic resonance microscopic visualization of joint cartilage using liposome entrapped contrast agents. Invest Radiol 33, 193-202.

Halford, S., Yip, D., Karapetis, C.S., Strickland, A.H., Steger, A., Khawaja, H.T. and Harper, P.G., 2001. A phase II study evaluating the tolerability and efficacy of CAELYX (liposomal doxorubicin, Doxil) in the treatment of unresectable pancreatic carcinoma. Ann Oncol 12, 1399-402.

Harashima, H., Hiraiwa, T., Ochi, Y. and Kiwada, H., 1995. Size dependent liposome degradation in blood: *in vivo*/*in vitro* correlation by kinetic modeling. J Drug Target 3, 253-61.

Harasym, T.O., Cullis, P.R. and Bally, M.B., 1997. Intratumor distribution of doxorubicin following i.v. administration of drug encapsulated in egg phosphatidylcholine/cholesterol liposomes. Cancer Chemother Pharmacol 40, 309-17.

Harrington, K.J., Lewanski, C.R., Northcote, A.D., Whittaker, J., Wellbank, H., Vile, R.G., Peters, A.M. and Stewart, J.S., 2001a. Phase I-II study of pegylated liposomal cisplatin (SPI-077) in patients with inoperable head and neck cancer. Ann Oncol 12, 493-6.

Harrington, K.J., Mohammadtaghi, S., Uster, P.S., Glass, D., Peters, A.M., Vile, R.G. and Stewart, J.S., 2001b. Effective targeting of solid tumors in patients with locally advanced cancers by radiolabeled pegylated liposomes. Clin Cancer Res 7, 243-54.

Harrington, K.J., Rowlinson-Busza, G., Syrigos, K.N., Abra, R.M., Uster, P.S., Peters, A.M. and Stewart, J.S., 2000. Influence of tumour size on uptake of(111)ln-DTPA-labelled pegylated liposomes in a human tumour xenograft model. Br J Cancer 83, 684-8.

Harris, T.J., Hipkiss, E.L., Borzillary, S., Wada, S., Grosso, J.F., Yen, H.R., Getnet, D., Bruno, T.C., Goldberg, M.V., Pardoll, D.M., Deweese, T.L. and Drake, C.G., 2008. Radiotherapy augments the immune response to prostate cancer in a time-dependent manner. Prostate 68, 1319-29.

Hemmi, H., Takeuchi, O., Kawai, T., Kaisho, T., Sato, S., Sanjo, H., Matsumoto, M., Hoshino, K., Wagner, H., Takeda, K. and Akira, S., 2000. A Toll-like receptor recognizes bacterial DNA. Nature 408, 740-5.

Hirabayashi, K., Yano, J., Inoue, T., Yamaguchi, T., Tanigawara, K., Smyth, G.E., Ishiyama, K., Ohgi, T., Kimura, K. and Irimura, T., 1999. Inhibition of cancer cell growth by polyinosinic-polycytidylic acid/cationic liposome complex: a new biological activity. Cancer Res 59, 4325-33.

Hobbs, S.K., Monsky, W.L., Yuan, F., Roberts, W.G., Griffith, L., Torchilin, V.P. and Jain, R.K., 1998. Regulation of transport pathways in tumor vessels: role of tumor type and microenvironment. Proc Natl Acad Sci U S A 95, 4607-12.

Hofmann, B., Fischer, C.O., Lawaczeck, R., Platzek, J. and Semmler, W., 1999. Gadolinium neutron capture therapy (GdNCT) of melanoma cells and solid tumors with the magnetic resonance imaging contrast agent Gadobutrol. Invest Radiol 34, 126-33.

Hwang, T.L., Lee, W.R., Hua, S.C. and Fang, J.Y., 2007. Cisplatin encapsulated in phosphatidylethanolamine liposomes enhances the *in vitro* cytotoxicity and *in vivo* intratumor drug accumulation against melanomas. J Dermatol Sci 46, 11-20.

Hwu, P., Yang, J.C., Cowherd, R., Treisman, J., Shafer, G.E., Eshhar, Z. and Rosenberg, S.A., 1995. *In vivo* antitumor activity of T cells redirected with chimeric antibody/T-cell receptor genes. Cancer Res 55, 3369-73.

Immordino, M.L., Brusa, P., Rocco, F., Arpicco, S., Ceruti, M. and Cattel, L., 2004. Preparation, characterization, cytotoxicity and pharmacokinetics of liposomes containing lipophilic gemcitabine prodrugs. J Control Release 100, 331-46.

Immordino, M.L., Dosio, F. and Cattel, L., 2006. Stealth liposomes: review of the basic science, rationale, and clinical applications, existing and potential. Int J Nanomedicine 1, 297-315.

Jain, R.K., 1996. Delivery of molecular medicine to solid tumors. Science 271, 1079-80.

James, J.S., 1995. DOXIL approved for KS. AIDS Treat News, 6.

Janeway, C.A., Travers, P., Walport, M., Shlomchik, M.J, 2005. Immunobiology 6, 3-11.

Jono, K., Ichikawa, H., Fujioka, K., Fukumori, Y., Akine, Y. and Tokuuye, K., 1999. Preparation of lecithin microcapsules by a dilution method using the Wurster process for intraarterial administration in gadolinium neutron capture therapy. Chem Pharm Bull (Tokyo) 47, 54-63.

Kerr, J.F., Wyllie, A.H. and Currie, A.R., 1972. Apoptosis: a basic biological phenomenon with wide-ranging implications in tissue kinetics. Br J Cancer 26, 239-57.

Khokhlov, V.F., Yashkin, P.N., Silin, D.I., Djorova, E.S. and Lawaczeck, R., 1995. Neutron capture therapy with gadopentetate dimeglumine: experiments on tumor-bearing rats. Acad Radiol 2, 392-8.

Kleinman, H.K., et. al., 1982. Biochem. 21, 6188.

Kojima, N., Ueno, N., Takano, M., Yabushita, H., Noguchi, M., Ishihara, M. and Yagi, K., 1986. Effect of adriamycin entrapped by sulfatide-containing liposomes on ovarian tumor-bearing nude mice. Biotechnol Appl Biochem 8, 471-8.

Kong, G., Anyarambhatla, G., Petros, W.P., Braun, R.D., Colvin, O.M., Needham, D. and Dewhirst, M.W., 2000. Efficacy of liposomes and hyperthermia in a human tumor xenograft model: importance of triggered drug release. Cancer Res 60, 6950-7.

Koski, G.K. and Czerniecki, B.J., 2005. Combining innate immunity with radiation therapy for cancer treatment. Clin Cancer Res 11, 7-11.

Kreuter, J., 1995. Nanoparticles as adjuvants for vaccines. Pharm Biotechnol 6, 463-72.

Laginha, K., Mumbengegwi, D. and Allen, T., 2005. Liposomes targeted via two different antibodies: assay, B-cell binding and cytotoxicity. Biochim Biophys Acta 1711, 25-32.

Lake, R.A. and Robinson, B.W., 2005. Immunotherapy and chemotherapy--a practical partnership. Nat Rev Cancer 5, 397-405.

Landberg, T.G., 1995. Progress in radiotherapy. Acta Oncol 34, 1023-9.

Langer, S., Botteck, N.M., Bosse, B., Reimer, K., Vogt, P.M., Steinau, H.U. and Mueller, S., 2006. Effect of polyvinylpyrrolidone-iodine liposomal hydrogel on wound microcirculation in SKH1-hr hairless mice. Eur Surg Res 38, 27-34.

Larson, V.M., Clark, W.R., Dagle, G.E. and Hilleman, M.R., 1969. Influence of synthetic double-stranded ribonucleic acid, poly I:C, on Friend leukemia in mice. Proc Soc Exp Biol Med 132, 602-7.

Larson, V.M., Panteleakis, P.N. and Hilleman, M.R., 1970. Influence of synthetic double-stranded ribonucleic acid (poly I:C) on SV40 viral oncogenesis and transplant tumor in hamsters. Proc Soc Exp Biol Med 133, 14-9.

Lasic, D.D., Ceh, B., Stuart, M.C., Guo, L., Frederik, P.M. and Barenholz, Y., 1995. Transmembrane gradient driven phase transitions within vesicles: lessons for drug delivery. Biochim Biophys Acta 1239, 145-56.

Lasic, D.D., Frederik, P.M., Stuart, M.C., Barenholz, Y. and McIntosh, T.J., 1992. Gelation of liposome interior. A novel method for drug encapsulation. FEBS Lett 312, 255-8.

Le Bon, A., Etchart, N., Rossmann, C., Ashton, M., Hou, S., Gewert, D., Borrow, P. and Tough, D.F., 2003. Cross-priming of CD8+ T cells stimulated by virus-induced type I interferon. Nat Immunol 4, 1009-15.

Le, U.M. and Cui, Z., 2006a. Long-circulating gadolinium-encapsulated liposomes for potential application in tumor neutron capture therapy. Int J Pharm 312, 105-12.

Le, U.M. and Cui, Z., 2006b. Biodistribution and tumor-accumulation of gadolinium (Gd) encapsulated in long-circulating liposomes in tumor-bearing mice for potential neutron capture therapy. Int J Pharm 320, 96-103.

Le, U.M., Yanasarn, N., Lohr, C.V., Fischer, K.A. and Cui, Z., 2007. Tumor chemo-immunotherapy using gemcitabine and a synthetic dsRNA. Cancer Biol Ther 7, 440-7.

Leonidze, D.L., Afanas'ev, G.G., Poverennyi, A.M. and Pelevina, II, 1986. [Radiosensitizing effect of interferon synthesis inducers]. Radiobiologiia 26, 227-31.

Li, S., Rizzo, M.A., Bhattacharya, S. and Huang, L., 1998. Characterization of cationic lipid-protamine-DNA (LPD) complexes for intravenous gene delivery. Gene Ther 5, 930-7.

Liang, W., Levchenko, T.S. and Torchilin, V.P., 2004. Encapsulation of ATP into liposomes by different methods: optimization of the procedure. J Microencapsul 21, 251-61.

Lin, K.Y., Guarnieri, F.G., Staveley-O'Carroll, K.F., Levitsky, H.I., August, J.T., Pardoll, D.M. and Wu, T.C., 1996. Treatment of established tumors with a novel vaccine that enhances major histocompatibility class II presentation of tumor antigen. Cancer Res 56, 21-6.

Litzinger, D.C., Buiting, A.M., van Rooijen, N. and Huang, L., 1994. Effect of liposome size on the circulation time and intraorgan distribution of amphipathic poly(ethylene glycol)-containing liposomes. Biochim Biophys Acta 1190, 99-107.

Liu, S., Yu, Y., Zhang, M., Wang, W. and Cao, X., 2001. The involvement of TNF-alpha-related apoptosis-inducing ligand in the enhanced cytotoxicity of IFN-beta-stimulated human dendritic cells to tumor cells. J Immunol 166, 5407-15.

Lvovsky, E.A., D'Souza, J., Eng, D., D'Souza, D., Lvovsky, B., Hetland, R., Craver, W.L. and Sobel, S.H., 1988. Tumor response to interferon inducer and radiation effect of serum interferon levels. J Biol Regul Homeost Agents 2, 1-6.

Lvovsky, E.A., Mossman, K.L., Levy, H.B. and Dritschilo, A., 1985. Response of mouse tumor to interferon inducer and radiation. Int J Radiat Oncol Biol Phys 11, 1721-5.

Manojlovic, V., Winkler, K., Bunjes, V., Neub, A., Schubert, R., Bugarski, B. and Leneweit, G., 2008. Membrane interactions of ternary

phospholipid/cholesterol bilayers and encapsulation efficiencies of a RIP II protein. Colloids Surf B Biointerfaces 64, 284-96.

Martin, R.F., D'Cunha, G., Pardee, M. and Allen, B.J., 1988. Induction of double-strand breaks following neutron capture by DNA-bound 157Gd. Int J Radiat Biol 54, 205-8.

Maruyama, K., Ishida, O., Takizawa, T. and Moribe, K., 1999. Possibility of active targeting to tumor tissues with liposomes. Adv Drug Deliv Rev 40, 89-102.

Mason, K.A., Ariga, H., Neal, R., Valdecanas, D., Hunter, N., Krieg, A.M., Whisnant, J.K. and Milas, L., 2005. Targeting toll-like receptor 9 with CpG oligodeoxynucleotides enhances tumor response to fractionated radiotherapy. Clin Cancer Res 11, 361-9.

Massing, U. and Fuxius, S., 2000. Liposomal formulations of anticancer drugs: selectivity and effectiveness. Drug Resist Updat 3, 171-177.

Matsumura, A., Zhang, T., Yamamoto, T., Yoshida, F., Sakurai, Y., Shimojo, N. and Nose, T., 2003. *In vivo* gadolinium neutron capture therapy using a potentially effective compound (Gd-BOPTA). Anticancer Res 23, 2451-6.

McDannold, N., Fossheim, S.L., Rasmussen, H., Martin, H., Vykhodtseva, N. and Hynynen, K., 2004. Heat-activated liposomal MR contrast agent: initial *in vivo* results in rabbit liver and kidney. Radiology 230, 743-52.

Meier, H., Myers, D.D. and Huebner, R.J., 1970. Ineffectiveness of poly rI:rC on transplanted tumors induced by methylcholanthrene. Naturwissenschaften 57, 248-9.

Meng, Y., Carpentier, A.F., Chen, L., Boisserie, G., Simon, J.M., Mazeron, J.J. and Delattre, J.Y., 2005. Successful combination of local CpG-ODN and radiotherapy in malignant glioma. Int J Cancer 116, 992-7.

Meurs, E.F., Galabru, J., Barber, G.N., Katze, M.G. and Hovanessian, A.G., 1993. Tumor suppressor function of the interferon-induced double-stranded RNA-activated protein kinase. Proc Natl Acad Sci U S A 90, 232-6.

Milas, L., Mason, K.A., Ariga, H., Hunter, N., Neal, R., Valdecanas, D., Krieg, A.M. and Whisnant, J.K., 2004. CpG oligodeoxynucleotide enhances tumor response to radiation. Cancer Res 64, 5074-7.

Miyamoto, M., Hirano, K., Ichikawa, H., Fukumori, Y., Akine, Y. and Tokuuye, K., 1999. Biodistribution of gadolinium incorporated in lipid emulsions intraperitoneally administered for neutron-capture therapy with tumor-bearing hamsters. Biol Pharm Bull 22, 1331-40.

Miyamoto, M., Ichikawa, H., Fukumori, Y., Akine, Y. and Tokuuye, K., 1997. Design and preparation of gadolinium-reservoir microcapsules for neutron-capture therapy by means of the Wurster process. Chem Pharm Bull (Tokyo) 45, 2043-50.

Moog, R., Burger, A.M., Brandl, M., Schuler, J., Schubert, R., Unger, C., Fiebig, H.H. and Massing, U., 2002. Change in pharmacokinetic and pharmacodynamic behavior of gemcitabine in human tumor xenografts upon entrapment in vesicular phospholipid gels. Cancer Chemother Pharmacol 49, 356-66.

Mosqueira, V.C., Legrand, P., Morgat, J.L., Vert, M., Mysiakine, E., Gref, R., Devissaguet, J.P. and Barratt, G., 2001. Biodistribution of long-circulating PEG-grafted nanocapsules in mice: effects of PEG chain length and density. Pharm Res 18, 1411-9.

Mourtas, S., Fotopoulou, S., Duraj, S., Sfika, V., Tsakiroglou, C. and Antimisiaris, S.G., 2007. Liposomal drugs dispersed in hydrogels. Effect of liposome, drug and gel properties on drug release kinetics. Colloids Surf B Biointerfaces 55, 212-21.

Muggia, F. and Hamilton, A., 2001. Phase III data on Caelyx in ovarian cancer. Eur J Cancer 37 Suppl 9, S15-8.

Nakamura, O., Shitara, N., Matsutani, M., Takakura, K. and Machida, H., 1982. Phase I-II trials of poly(ICLC) in malignant brain tumor patients. J Interferon Res 2, 1-4.

NCI, 2008. Radiation Therapy for Cancer: Questions and Answers. U.S. National Institute of Health's website. Acess on 08/05/08.

Needham, D., Anyarambhatla, G., Kong, G. and Dewhirst, M.W., 2000. A new temperature-sensitive liposome for use with mild hyperthermia: characterization and testing in a human tumor xenograft model. Cancer Res 60, 1197-201.

Needham, D., McIntosh, T.J. and Lasic, D.D., 1992. Repulsive interactions and mechanical stability of polymer-grafted lipid membranes. Biochim Biophys Acta 1108, 40-8.

Ning, M., Guo, Y., Pan, H., Chen, X. and Gu, Z., 2005. Preparation, *in vitro* and *in vivo* evaluation of liposomal/niosomal gel delivery systems for clotrimazole. Drug Dev Ind Pharm 31, 375-83.

Nowak, A.K., Lake, R.A., Marzo, A.L., Scott, B., Heath, W.R., Collins, E.J., Frelinger, J.A. and Robinson, B.W., 2003a. Induction of tumor cell apoptosis *in vivo* increases tumor antigen cross-presentation, cross-priming rather than cross-tolerizing host tumor-specific CD8 T cells. J Immunol 170, 4905-13.

Nowak, A.K., Robinson, B.W. and Lake, R.A., 2002. Gemcitabine exerts a selective effect on the humoral immune response: implications for combination chemo-immunotherapy. Cancer Res 62, 2353-8.

Nowak, A.K., Robinson, B.W. and Lake, R.A., 2003b. Synergy between chemotherapy and immunotherapy in the treatment of established murine solid tumors. Cancer Res 63, 4490-6.

Okada, C., Akbar, S.M., Horiike, N. and Onji, M., 2005. Early development of primary biliary cirrhosis in female C57BL/6 mice because of poly I:C administration. Liver Int 25, 595-603.

Okino, H., Maeyama, R., Manabe, T., Matsuda, T. and Tanaka, M., 2003. Trans-tissue, sustained release of gemcitabine from photocured gelatin gel inhibits the growth of heterotopic human pancreatic tumor in nude mice. Clin Cancer Res 9, 5786-93.

Oyewumi, M.O. and Mumper, R.J., 2002. Engineering tumor-targeted gadolinium hexanedione nanoparticles for potential application in neutron capture therapy. Bioconjug Chem 13, 1328-35.

Oyewumi, M.O. and Mumper, R.J., 2003. Influence of formulation parameters on gadolinium entrapment and tumor cell uptake using folate-coated nanoparticles. Int J Pharm 251, 85-97.

Oyewumi, M.O., Yokel, R.A., Jay, M., Coakley, T. and Mumper, R.J., 2004. Comparison of cell uptake, biodistribution and tumor retention of folate-

coated and PEG-coated gadolinium nanoparticles in tumor-bearing mice. J Control Release 95, 613-26.

Paavola, A., Kilpelainen, I., Yliruusi, J. and Rosenberg, P., 2000. Controlled release injectable liposomal gel of ibuprofen for epidural analgesia. Int J Pharm 199, 85-93.

Pardoll, D.M., 1995. Paracrine cytokine adjuvants in cancer immunotherapy. Annu Rev Immunol 13, 399-415.

Park, J.H. and Baron, S., 1968. Herpetic keratoconjunctivitis: therapy with synthetic double-stranded RNA. Science 162, 811-3.

Patel, V.B. and Misra, A.N., 1999. Encapsulation and stability of clofazimine liposomes. J Microencapsul 16, 357-67.

Pavelic, Z., Skalko-Basnet, N., Filipovic-Grcic, J., Martinac, A. and Jalsenjak, I., 2005a. Development and *in vitro* evaluation of a liposomal vaginal delivery system for acyclovir. J Control Release 106, 34-43.

Pavelic, Z., Skalko-Basnet, N. and Jalsenjak, I., 2004. Liposomal gel with chloramphenicol: characterisation and *in vitro* release. Acta Pharm 54, 319-30.

Pavelic, Z., Skalko-Basnet, N. and Jalsenjak, I., 2005b. Characterisation and *in vitro* evaluation of bioadhesive liposome gels for local therapy of vaginitis. Int J Pharm 301, 140-8.

Pavelic, Z., Skalko-Basnet, N. and Schubert, R., 2001. Liposomal gels for vaginal drug delivery. Int J Pharm 219, 139-49.

Pimm, M.V., Embleton, M.J. and Baldwin, R.W., 1976. Treatment of transplanted rat tumours with double-stranded RNA (BRL 5907). I. Influenced of systemic and local administration. Br J Cancer 33, 154-65.

Plate, J.M., Plate, A.E., Shott, S., Bograd, S. and Harris, J.E., 2005. Effect of gemcitabine on immune cells in subjects with adenocarcinoma of the pancreas. Cancer Immunol Immunother 54, 915-25.

Pratesi, G., Petrangolini, G., Tortoreto, M., Addis, A., Belluco, S., Rossini, A., Selleri, S., Rumio, C., Menard, S. and Balsari, A., 2005. Therapeutic synergism of gemcitabine and CpG-oligodeoxynucleotides in an orthotopic human pancreatic carcinoma xenograft. Cancer Res 65, 6388-93.

Priestman, T., 2008. Cancer therapy in clinical practice. Springer-Verlag London Limited, 37-38.

Ramachandran, S., Quist, A.P., Kumar, S. and Lal, R., 2006. Cisplatin nanoliposomes for cancer therapy: AFM and fluorescence imaging of cisplatin encapsulation, stability, cellular uptake, and toxicity. Langmuir 22, 8156-62.

Ranson, M.R., Carmichael, J., O'Byrne, K., Stewart, S., Smith, D. and Howell, A., 1997. Treatment of advanced breast cancer with sterically stabilized liposomal doxorubicin: results of a multicenter phase II trial. J Clin Oncol 15, 3185-91.

Ren, J., Zheng, L., Chen, Q., Li, H., Zhang, L. and Zhu, H., 2004. Co-administration of a DNA vaccine encoding the prostate specific membrane antigen and CpG oligodeoxynucleotides suppresses tumor growth. J Transl Med 2, 29.

Rosenberg, S.A., Spiess, P. and Lafreniere, R., 1986. A new approach to the adoptive immunotherapy of cancer with tumor-infiltrating lymphocytes. Science 233, 1318-21.

Ruel-Gariepy, E., Leclair, G., Hildgen, P., Gupta, A. and Leroux, J.C., 2002. Thermosensitive chitosan-based hydrogel containing liposomes for the delivery of hydrophilic molecules. J Control Release 82, 373-83.

Ruel-Gariepy, E., Shive, M., Bichara, A., Berrada, M., Le Garrec, D., Chenite, A. and Leroux, J.-C., 2004. A thermosensitive chitosan-based hydrogel for the local delivery of paclitaxel. European Journal of Pharmaceutics and Biopharmaceutics

Sakurai, F., Nishioka, T., Saito, H., Baba, T., Okuda, A., Matsumoto, O., Taga, T., Yamashita, F., Takakura, Y. and Hashida, M., 2001. Interaction between DNA-cationic liposome complexes and erythrocytes is an important factor in systemic gene transfer via the intravenous route in mice: the role of the neutral helper lipid. Gene Ther 8, 677-86.

Sakurai, F., Terada, T., Maruyama, M., Watanabe, Y., Yamashita, F., Takakura, Y. and Hashida, M., 2003. Therapeutic effect of intravenous delivery of

lipoplexes containing the interferon-beta gene and poly I: poly C in a murine lung metastasis model. Cancer Gene Ther 10, 661-8.

Sakurai, M., Iigo, M., Sasaki, Y., Nakagawa, K., Fujiwara, Y., Tamura, T., Ohe, Y., Bungo, M. and Saijo, N., 1990. Lack of correlation between interferon levels induced by polyribonucleotides and their antimetastatic effect. Oncology 47, 251-6.

Salaun, B., Coste, I., Rissoan, M.C., Lebecque, S.J. and Renno, T., 2006. TLR3 can directly trigger apoptosis in human cancer cells. J Immunol 176, 4894-901.

Salem, M.L., Kadima, A.N., Cole, D.J. and Gillanders, W.E., 2005. Defining the antigen-specific T-cell response to vaccination and poly(I:C)/TLR3 signaling: evidence of enhanced primary and memory CD8 T-cell responses and antitumor immunity. J Immunother 28, 220-8.

Salio, M. and Cerundolo, V., 2005. Viral immunity: cross-priming with the help of TLR3. Curr Biol 15, R336-9.

Savill, J. and Fadok, V., 2000. Corpse clearance defines the meaning of cell death. Nature 407, 784-8.

Schmidt, K.N., Leung, B., Kwong, M., Zarember, K.A., Satyal, S., Navas, T.A., Wang, F. and Godowski, P.J., 2004. APC-independent activation of NK cells by the Toll-like receptor 3 agonist double-stranded RNA. J Immunol 172, 138-43.

Schulz, O., Diebold, S.S., Chen, M., Naslund, T.I., Nolte, M.A., Alexopoulou, L., Azuma, Y.T., Flavell, R.A., Liljestrom, P. and Reis e Sousa, C., 2005. Toll-like receptor 3 promotes cross-priming to virus-infected cells. Nature 433, 887-92.

Schuster, M., Nechansky, A. and Kircheis, R., 2006. Cancer immunotherapy. Biotechnol J 1, 138-47.

Senior, J. and Gregoriadis, G., 1982. Is half-life of circulating liposomes determined by changes in their permeability? FEBS Lett 145, 109-14.

Sevick, E.M. and Jain, R.K., 1989. Geometric resistance to blood flow in solid tumors perfused ex vivo: effects of tumor size and perfusion pressure. Cancer Res 49, 3506-12.

Shih, J.L. and Brugger, R.M., 1992. Gadolinium as a neutron capture therapy agent. Med Phys 19, 733-44.

Shikata, F., Tokumitsu, H., Ichikawa, H. and Fukumori, Y., 2002. *In vitro* cellular accumulation of gadolinium incorporated into chitosan nanoparticles designed for neutron-capture therapy of cancer. Eur J Pharm Biopharm 53, 57-63.

Shir, A., Ogris, M., Wagner, E. and Levitzki, A., 2006. EGF receptor-targeted synthetic double-stranded RNA eliminates glioblastoma, breast cancer, and adenocarcinoma tumors in mice. PLoS Med 3, e6.

Sidky, Y.A. and Borden, E.C., 1987. Inhibition of angiogenesis by interferons: effects on tumor- and lymphocyte-induced vascular responses. Cancer Res 47, 5155-61.

Simpson, J.K., Miller, R.F. and Spittle, M.F., 1993. Liposomal doxorubicin for treatment of AIDS-related Kaposi's sarcoma. Clin Oncol (R Coll Radiol) 5, 372-4.

Sivori, S., Falco, M., Della Chiesa, M., Carlomagno, S., Vitale, M., Moretta, L. and Moretta, A., 2004. CpG and double-stranded RNA trigger human NK cells by Toll-like receptors: induction of cytokine release and cytotoxicity against tumors and dendritic cells. Proc Natl Acad Sci U S A 101, 10116-21.

Smith, J.P., Stock, E., Orenberg, E.K., Yu, N.Y., Kanekal, S. and Brown, D.M., 1995. Intratumoral chemotherapy with a sustained-release drug delivery system inhibits growth of human pancreatic cancer xenografts. Anticancer Drugs 6, 717-26.

Sparano, J.A., Malik, U., Rajdev, L., Sarta, C., Hopkins, U. and Wolff, A.C., 2001. Phase I trial of pegylated liposomal doxorubicin and docetaxel in advanced breast cancer. J Clin Oncol 19, 3117-25.

Sparano, J.A. and Winer, E.P., 2001. Liposomal anthracyclines for breast cancer. Semin Oncol 28, 32-40.

Storrs, R.W., Tropper, F.D., Li, H.Y., Song, C.K., Sipkins, D.A., Kuniyoshi, J.K., Bednarski, M.D., Strauss, H.W. and Li, K.C., 1995. Paramagnetic polymerized liposomes as new recirculating MR contrast agents. J Magn Reson Imaging 5, 719-24.

Su, M.Y., Muhler, A., Lao, X. and Nalcioglu, O., 1998. Tumor characterization with dynamic contrast-enhanced MRI using MR contrast agents of various molecular weights. Magn Reson Med 39, 259-69.

Su, M.Y., Wang, Z., Roth, G.M., Lao, X., Samoszuk, M.K. and Nalcioglu, O., 1996. Pharmacokinetic changes induced by vasomodulators in kidneys, livers, muscles, and implanted tumors in rats as measured by dynamic Gd-DTPA-enhanced MRI. Magn Reson Med 36, 868-77.

Suzuki, E., Kapoor, V., Jassar, A.S., Kaiser, L.R. and Albelda, S.M., 2005. Gemcitabine selectively eliminates splenic Gr-1+/CD11b+ myeloid suppressor cells in tumor-bearing animals and enhances antitumor immune activity. Clin Cancer Res 11, 6713-21.

Suzuki, E., Sun, J., Kapoor, V., Jassar, A.S. and Albelda, S.M., 2007. Gemcitabine has significant immunomodulatory activity in murine tumor models independent of its cytotoxic effects. Cancer Biol Ther 6, 880-5.

Takagi, I., Shimizu, H. and Yotsuyanagi, T., 1996. Application of alginate gel as a vehicle for liposomes. I. Factors affecting the loading of drug-containing liposomes and drug release. Chem Pharm Bull (Tokyo) 44, 1941-7.

Tamat, S.R., Moore, D.E. and Allen, B.J., 1987. Determination of boron in biological tissues by inductively coupled plasma atomic emission spectrometry. Anal Chem 59, 2161-4.

Tilcock, C., Unger, E., Cullis, P. and MacDougall, P., 1989. Liposomal Gd-DTPA: preparation and characterization of relaxivity. Radiology 171, 77-80.

Tilcock, C.P., Ahkong, Q.F. and Parr, M., 1991. An improved method for the preparation of liposomal gadolinium-DTPA. Ionophore-mediated active entrapment of gadolinium. Invest Radiol 26, 242-7.

Tokumitsu, H., Hiratsuka, J., Sakurai, Y., Kobayashi, T., Ichikawa, H. and Fukumori, Y., 2000. Gadolinium neutron-capture therapy using novel gadopentetic acid-chitosan complex nanoparticles: *in vivo* growth suppression of experimental melanoma solid tumor. Cancer Lett 150, 177-82.

Tokumitsu, H., Ichikawa, H. and Fukumori, Y., 1999. Chitosan-gadopentetic acid complex nanoparticles for gadolinium neutron-capture therapy of cancer:

preparation by novel emulsion-droplet coalescence technique and characterization. Pharm Res 16, 1830-5.

Topalian, S.L., Solomon, D. and Rosenberg, S.A., 1989. Tumor-specific cytolysis by lymphocytes infiltrating human melanomas. J Immunol 142, 3714-25.

Torchilin, V.P., 2000. Polymeric contrast agents for medical imaging. Curr Pharm Biotechnol 1, 183-215.

U'Ren, L., Kedl, R. and Dow, S., 2006. Vaccination with liposome--DNA complexes elicits enhanced antitumor immunity. Cancer Gene Ther 13, 1033-44.

Unger, E., Cardenas, D., Zerella, A., Fajardo, L.L. and Tilcock, C., 1990. Biodistribution and clearance of liposomal gadolinium-DTPA. Invest Radiol 25, 638-44.

Uzgiris, E., 2004. The role of molecular conformation on tumor uptake of polymeric contrast agents. Invest Radiol 39, 131-7.

Vaage, J., Donovan, D., Mayhew, E., Uster, P. and Woodle, M., 1993. Therapy of mouse mammary carcinomas with vincristine and doxorubicin encapsulated in sterically stabilized liposomes. Int J Cancer 54, 959-64.

Verdijk, R.M., Mutis, T., Esendam, B., Kamp, J., Melief, C.J., Brand, A. and Goulmy, E., 1999. Polyriboinosinic polyribocytidylic acid (poly(I:C)) induces stable maturation of functionally active human dendritic cells. J Immunol 163, 57-61.

Vexler, V.S., Clement, O., Schmitt-Willich, H. and Brasch, R.C., 1994. Effect of varying the molecular weight of the MR contrast agent Gd-DTPA-polylysine on blood pharmacokinetics and enhancement patterns. J Magn Reson Imaging 4, 381-8.

Vodovozova, E.L., Kuznetsova, N.R., Gaenko, G.P. and Molotkovskii Iu, G., 2007. [Liposomal formulation of a methotrexate diglyceride conjugate: activity in methotrexate-resistant leukemia cultured cells]. Bioorg Khim 33, 470-3.

Wajant, H., 2002. The Fas signaling pathway: more than a paradigm. Science 296, 1635-6.

Watanabe, M., Kawano, K., Toma, K., Hattori, Y. and Maitani, Y., 2008. *In vivo* antitumor activity of camptothecin incorporated in liposomes formulated with an artificial lipid and human serum albumin. J Control Release 127, 231-8.

Watanabe, T., Ichikawa, H. and Fukumori, Y., 2002. Tumor accumulation of gadolinium in lipid-nanoparticles intravenously injected for neutron-capture therapy of cancer. Eur J Pharm Biopharm 54, 119-24.

Watters, D., 1999. Molecular mechanisms of ionizing radiation-induced apoptosis. Immunol Cell Biol 77, 263-71.

Weiner, A.L., Carpenter-Green, S.S., Soehngen, E.C., Lenk, R.P. and Popescu, M.C., 1985. Liposome-collagen gel matrix: a novel sustained drug delivery system. J Pharm Sci 74, 922-5.

Weinstein, A.J., Gazdar, A.F., Sims, H.L. and Levy, H.B., 1971. Lack of correlation between interferon induction and antitumour effect of poly I-poly C. Nat New Biol 231, 53-4.

Weissig, V.V., Babich, J. and Torchilin, V.V., 2000. Long-circulating gadolinium-loaded liposomes: potential use for magnetic resonance imaging of the blood pool. Colloids Surf B Biointerfaces 18, 293-299.

Wu, N.Z., Da, D., Rudoll, T.L., Needham, D., Whorton, A.R. and Dewhirst, M.W., 1993. Increased microvascular permeability contributes to preferential accumulation of Stealth liposomes in tumor tissue. Cancer Res 53, 3765-70.

Yanagie, H., Kobayashi, H., Takeda, Y., Yoshizaki, I., Nonaka, Y., Naka, S., Nojiri, A., Shinnkawa, H., Furuya, Y., Niwa, H., Ariki, K., Yasuhara, H. and Eriguchi, M., 2002. Inhibition of growth of human breast cancer cells in culture by neutron capture using liposomes containing 10B. Biomed Pharmacother 56, 93-9.

Yoneyama, M., Kikuchi, M., Natsukawa, T., Shinobu, N., Imaizumi, T., Miyagishi, M., Taira, K., Akira, S. and Fujita, T., 2004. The RNA helicase RIG-I has an essential function in double-stranded RNA-induced innate antiviral responses. Nat Immunol 5, 730-7.

Zamboni, W.C., Gervais, A.C., Egorin, M.J., Schellens, J.H., Zuhowski, E.G., Pluim, D., Joseph, E., Hamburger, D.R., Working, P.K., Colbern, G., Tonda, M.E., Potter, D.M. and Eiseman, J.L., 2004. Systemic and tumor disposition of

platinum after administration of cisplatin or STEALTH liposomal-cisplatin formulations (SPI-077 and SPI-077 B103) in a preclinical tumor model of melanoma. Cancer Chemother Pharmacol 53, 329-36.